Trajectories of avalanche risk resulting from socio-environmental changes in the high valleys of the French Alps

Taline Zgheib

THÈSE

Pour obtenir le grade de

DOCTEUR DE L'UNIVERSITÉ GRENOBLE ALPES

Spécialité : Sciences de la Terre et de l'Univers et de l'Environnement

Arrêté ministériel : 25 mai 2016

Présentée par

Taline ZGHEIB

Thèse dirigée par **Nicolas ECKERT**, INRAE
et codirigée par **Samuel MORIN**, CNRM
et **Anne Marie GRANET-ABISSET**, LARHRA

préparée au sein du **Laboratoire INRAE ETNA**
dans **l'École Doctorale Terre, Univers, Environnement**

Trajectoires du risque avalancheux résultant de changements sociaux-environnementaux dans les hautes vallées des Alpes françaises

Trajectories of avalanche risk resulting from socio-environmental changes in the high valleys of the French Alps

Thèse soutenue publiquement le

5 Mars 2021

devant le jury composé de :

Monsieur Christopher J. KEYLOCK
PROFESSEUR, Loughborough University, Rapporteur
Monsieur Christophe CORONA
CHARGE DE RECHERCHE, CNRS Clermont-Ferrand, Rapporteur
Madame Michaela TEICH
CHARGE DE RECHERCHE, Federal Research and Training Centre for Forests, Natural Hazards and Landscape, Examinatrice
Monsieur Vincent JOMELLI
DIRECTEUR DE RECHERCHE, CNRS Paris, Président
Monsieur Nicolas ECKERT
INGENIEUR HDR, ICPCEF/INRAE, Directeur de thèse
Monsieur Samuel MORIN
INGENIEUR HDR, ICPCEF/CNRM, Co-directeur de thèse

Acknowledgments

First and foremost I am extremely grateful to my supervisors, Dr. Nicolas Eckert, Dr. Samuel Morin and Professor Anne-Marie Granet-Abisset for their valuable guidance and patient support throughout the years of the PhD. Your insightful feedback pushed me to sharpen my thinking and brought my work to a higher level.

I would like to express my sincere gratitude to the members of the jury for the interest shown in my work as well as for the insightful discussions during the Viva.

My dear friend Florie, you have always been a major source of support when things would get a bit discouraging. Thank you for always being there for me. On a more professional level, thank you for your constant guidance and priceless help through the PhD.

A very special word of thanks goes for the members of my family Toufic, Joceline, Marie-line, Pauline and Pierre for heir wise counsel and sympathetic ear. Everytime that I complained you listened and constantly reminded me that I can do this... And I did it!

To my future in-laws Lionel and Chantal thank you for welcoming me into your family with open arms. I dedicate this work to you as a testimony of my great respect, love and appreciation.

My future husband Jocelyn, no dedication can express the depth of love and gratitude that I feel towards you. Since the day that I met you, you are by my side celebrating on the good days and supporting me on the bad days. Through your constant support and encouragement we were able to push through all obstacles. This is for US.

Trajectories of avalanche risk resulting from socio-environmental changes in the high valleys of the French Alps

Abstract: Snow avalanches are prevalent processes in mountain areas, threatening people, destroying buildings and blocking roads. Historically, approaches to reduce avalanche risk were based on the sole hazard component of risk. Recently, more comprehensive risk analyses emerged that couple hazard, exposure and vulnerability. However, existing implementations remain more often than not static, neglecting long term changes in the risk resulting from the simultaneous evolution of its three components. They also ignore the small-scale spatio-temporal patterns in the social (e.g. population dynamics, economy) and natural systems (e.g. evolution of ecosystems, climate change) as well as in their interactions (e.g. forest logging). Consequently, local variability in avalanche risk trajectories cannot be accounted for. Eventually, risk estimates generated within a quantitative risk framework generally neglect land cover changes, notably forest cover evolution, that can potentially alter avalanche activity and, hence, avalanche risk. On this basis, the aims of this PhD are to (*i*) develop an integrative qualitative approach combining knowledge from natural and social sciences to assess long term changes in avalanche risk and in all its components, hazard, vulnerability and exposure, as function of changes in their socio-economic and environmental drivers, (*ii*) investigate to which extent local socio-economic, land cover and climatic peculiarities may lead to spatial and temporal disparities in risk trajectories and (*iii*) propose quantitative avalanche risk estimates that take into account changes in forest cover within avalanche paths. Herein, the focus is on the high mountains of the French Alps for the 1860-2017 period, a highly active avalanche area that witnessed important socio-economic and environmental changes over the years.

To this end, we first propose an integrative methodology that combines land cover change detection using advanced image processing techniques, geohistorical investigations and qualitative modeling of risk changes in order to infer the evolution of avalanche risk from its socio-economic and environmental drivers. The approach is applied to the upper Maurienne valley (1860-2017) and results show that avalanche risk in that area increased locally, due to an increase in the vulnerability of exposed settlements. Second, the methodology is further developed to consider climate as a driver for risk, and it is applied to three upper valleys of the French Alps simultaneously: the upper Maurienne, the Guil valley and the Valloire municipality. Results show that, unlike in the upper Maurienne, avalanche risk in the Guil valley locally decreased following a decline in snow avalanche hazard in heavily reforested paths. In Valloire, avalanche risk remained stationary due to a low exposure to avalanches. This clearly demonstrates that, even if common large scale drivers such as climate warming and socio-economic transitions are unambiguous, local dynamics play a crucial role in avalanche risk evolution. Third, we integrate forest-cover changes within a quantitative risk assessment framework relaying on a statistical-dynamical avalanche model. We show on a typical case study on which reforestation has been intense over the 1825-2017 period that return periods of avalanches, related impact pressures and consequently risk estimates have been modified dramatically. All in all, this PhD illustrates how strongly snow avalanche risk evolves in space and time, as function of changes in its components and drivers. Ultimately, the work proposed may be of great interest for stakeholders looking to elaborate effective risk protection strategies that consider the complex dynamics of the human and natural systems.

Keywords: Snow avalanches, spatio-temporal dynamics, qualitative risk assessment, forest, quantitative risk assessment

Trajectoires du risque avalancheux résultant de changements sociaux-environnementaux dans les hautes vallées des Alpes françaises

Résumé: Les avalanches de neiges sont répandues dans les zones montagneuses. Elles menacent les personnes, détruisent les bâtiments et bloquent les routes. Historiquement, les approches visant à réduire le risque d'avalanche étaient basées seulement sur l'aléa, qui est une composante du risque. Récemment, des analyses de risques plus complètes ont émergé associant aléas, exposition et vulnérabilité. Cependant, leurs applications restent le plus souvent statiques. En effet, elles négligent les évolutions à long terme du risque résultantes des évolutions simultanées de ses trois composantes. Elles ignorent également les variations spatio-temporelles, à l'échelle locale, des systèmes sociaux et naturels (par exemple, dynamique des populations, économie, évolution des écosystèmes, changement climatique) ainsi que leurs interactions (par exemple, l'exploitation forestière). Par conséquent, la variabilité locale des trajectoires de risque d'avalanche ne peut pas être prise en compte. Enfin, les estimations de risque générées dans un cadre d'analyse quantitatives négligent généralement les changements d'occupation des sols. En particulier l'évolution du couvert forestier qui peut potentiellement modifier l'activité des avalanches et par conséquent le risque d'avalanche. Ainsi, l'objectif de cette thèse est tout d'abord de développer une approche qualitative intégrative. Cette approche combine les informations issues des sciences naturelles et sociales pour évaluer l'évolution à long terme du risque d'avalanche et de toutes ses composantes (aléa, vulnérabilité et exposition), en fonction de l'évolution des facteurs socio-économiques, environnementaux et climatiques. Ensuite le second objectif est d'étudier dans quelle mesure les particularités socio-économiques et environnementales locales peuvent entraîner des disparités spatiales et temporelles dans les trajectoires de risque. Enfin, le dernier objectif est de proposer des estimations quantitatives du risque d'avalanche qui prennent en compte les changements du couvert forestier dans les trajectoires d'avalanche. La thèse se focalise sur les Alpes Françaises, pendant la période 1860-2017, qui est une zone d'avalanche très active et qui a connu d'importants changements socio-économiques et environnementaux aux fils des années.

Pour répondre à ces objectifs, nous proposons tout d'abord une méthodologie qualitative intégrative. La méthodologie combine la détection des changements de l'occupation des sols à l'aide de techniques avancées de traitement d'image, d'enquêtes géo-historiques et de modélisation qualitative du risque pour en déduire l'évolution du risque d'avalanche et de ses facteurs socio-économiques et environnementaux. L'approche est d'abord appliquée à la haute vallée de la Maurienne (1860-2017). Les résultats montrent que le risque d'avalanche dans la Haute Maurienne a localement augmenté, en raison d'une augmentation de la vulnérabilité des bâtiments exposés. Cependant, les trajectoires d'évolution du risque peuvent varier en fonction des particularités socio-économiques et / ou environnementales locales. Ainsi, l'approche qualitative proposée est développée pour considérer le climat comme un facteur lié au risque. Ensuite, elle est appliquée à trois hautes vallées des Alpes françaises: la haute Maurienne, la vallée du Guil et Valloire. Les résultats démontrent que contrairement à la haute Maurienne, le risque d'avalanche dans la vallée du Guil a diminué localement suite à une diminution de l'aléa dans les zones fortement reboisées. Alors qu'à Valloire, le risque d'avalanche est stable en raison d'une faible exposition aux avalanches. Cela démontre clairement que même si les moteurs à grande échelle tel que le réchauffement climatique et les transitions socio-économiques sont explicites,

les dynamiques locales jouent un rôle crucial dans l'évolution du risque d'avalanche. Finalement, nous intégrons les changements du couvert forestier dans un cadre d'évaluation quantitative des risques reposant sur un modèle statistique-dynamique d'avalanche. Nous montrons sur une étude de cas typique, sur laquelle le reboisement a été intense au cours de la période 1825-2017, que les périodes de retour, les pressions d'impact et par conséquent les estimations des risques ont été considérablement modifiées. L'ensemble de ce travail illustre l'évolution spatio-temporelle du risque, de ses composants et de ses moteurs. Les travaux proposés sont d'un grand intérêt pour les acteurs qui recherchent à élaborer des stratégies efficaces de protection contre les risques tenant compte de la dynamique complexe des systèmes humains et naturels.

Mots clés: Avalanche de neige, dynamiques spatio-temporelles, évaluation qualitative du risque, forêt, évaluation quantitative du risque

Contents

Chapter 1

General Introduction

Contents

1.1 Context

Disasters like snow avalanches threaten mountain communities. The natural process is characterized by a rapid flow of snow moving down mountain slopes (Hopfinger, 1983; Schweizer et al., 2003). Snow avalanches can be naturally triggered by a combination of several factors such as weather conditions (temperature, snowfall, wind direction, etc.), slope, surface roughness (McClung and Schaerer, 2006; Bebi et al., 2009) and seismic activity (Podolskiy et al., 2010; Kargel et al., 2016). The sudden nature of the phenomena and the complexity of the interaction between the triggering factors endanger people (Techel et al., 2016)(i.e fatalities, injuries), block roads (Leone et al., 2014) and impact the environment all over mountain areas (Berlin et al., 2019; Höller, 2007; Rapin and Ancey, 2000).

Several destructive avalanches occurred over the past centuries. For instance the 1916 avalanche disaster in Italy during World War I (WWI) killed thousands of soldiers as well as civilians and caused severe disruption to the supply channels in the area (Brugnara et al., 2017). Similarly, the avalanches of 1951 in the Swiss, Italian and Austrian Alps (Estienne, 1951), and those of 1970 in the French Alps (Val-d'Isère) (Loup, 1971) resulted in casualties, injuries and building destruction (Ancey, 2009). The series of devastating avalanches continue well into the twenty first-century. As examples, we mention (*i*) the 2012 avalanche in the Mont-Blanc massif that killed 9 people (Estachy, 2014) and (*ii*) the 2017 Rigopiano avalanche (Italy) that killed 29 people and is considered the most fatal in Italy after the aforementionedc 1916 avalanche (Frigo et al., 2020) and the deadliest in Europe since Galtür in 1999 (Heumader, 2000). Beyond such naturally occurring events, avalanches can also be triggered by people traveling in snow cover terrain for recreation or other activities (Schweizer and Lütschg, 2001). These accidental avalanches are also a recurring cause for casualties in mountainous areas, but are not covered by this research.

These continuously occurring avalanche events, are met with increased efforts to manage and mitigate the rising risk through either passive (Sulzlée, 1950) (e.g. avalanche dams, snow sheds) or active (e.g. land use planning) mitigation measures (Schweizer, 2004). Despite the effectiveness of such methods, they are based mostly on purely hazard-oriented approaches that do not explicitly consider the elements at risk (buildings, people, roads, etc.). Therefore, more recently, risk based methods (e.g. Barbolini et al. (2004b); Favier et al. (2014b)) emerged in the snow avalanche field in an attempt to account for all the components defined by the risk concept.

The concept of risk in the natural hazard field identifies hazard and vulnerability as determinants of risk (UN/ISDR, 2004; Birkmann, 2013). Several other risk formulations emerged where most of the differences center around societal coping capacity and the definition of vulnerability (Villagrán De León, 2006). The first school of though considers the double structure of vulnerability where the external side involves exposure to risk (Chambers, 1989; Bohle, 2001). The second approach, widely adopted in the disaster risk community, views vulnerability as an independent factor from coping capacity and exposure (Bollin et al., 2003; Field et al., 2012). Alternatively, the global environmental change community and integrated approaches views vulnerability as the combination of exposure, susceptibility and coping capacity (Fuchs et al., 2011; Turner et al., 2003; Weis et al., 2016). Notwithstanding the formulation used, the majority considers risk as the combination of the likelihood of occurrence of a damageable event

(hazard), and the degree to which the exposed element can resist the impact of the hazard (vulnerability).

However, so far, the risk concept remains a static approach (Jónasson et al., 1999; Keylock et al., 1999) and fails at integrating the dynamic properties of its components (Fuchs et al., 2013). This is particularly problematic for mountain areas where risk is highly influenced by the dynamic nature of hazard, exposure and vulnerability, driven by shifts in the mountainous social and natural systems (Hock et al., 2020). Indeed, the spatio-temporal variability of weather and snow characteristics (Beniston et al., 2018) controlling the avalanche hazard (e.g. snowfall), coupled with changing socio-economic conditions and settlement patterns, induce shifts in risk to societies (Fuchs et al., 2013). Thus, the key challenge is putting forth effective and innovative risk management strategies to ensure the protection of people and their assets. To that end, addressing the spatio-temporal variability of risk, its components and their drivers in all their dimensions (social, economic, environmental, etc.) is essential for future sustainable risk management (Fuchs et al., 2013; Peduzzi, 2019).

This introductive chapter represent a comprehensive state of the art regarding snow avalanche risk assessment in a changing environment. First, the fundamentals of snow avalanches physical process are presented. Then, the avalanche risk assessment framework and the analysis of the different components (hazard, exposure, vulnerability) are explained. Thereafter, factors driving the spatio-temporal evolution of avalanche risk and its components are presented. Subsequently, methodologies integrating forest/avalanche interaction within hazard models are synthesized. The latter is a necessary step towards the quantification of the impact of land cover change, particularly reforestation on avalanche risk. Finally, grounded on the state of art, knowledge gaps are identified and objectives are defined and detailed.

1.2 Snow avalanches

Snow avalanches are gravity-driven flows characterized by an abrupt and rapid movement of large snow masses on a mountain slope (Hopfinger, 1983; Schweizer et al., 2003). The UNESCO (1981) (Table 1.1) morphological classification of snow avalanches is used internationally by the majority of scientists and practitioners in the field of avalanches. The latter categorize avalanches based on observable features in the three principal zones of an avalanche path (starting zone, transition and runout area) e.g. their release type (loose or slab snow avalanches), liquid water in snow (wet and dry snow avalanches) and form of the path (confined, unconfined) (see Table 1.1 for the different typologies of snow avalanches).

Table 1.1: International snow avalanche classification (Schweizer et al. (2015) based on UNESCO (1981)).

Zone	**Criterion**	**Characteristic and denomination**	
Origin	Manner of starting	From a point	From a line
		Loose snow avalanche	**Slab avalanche**
	Position of failure layer	Within the snowpack	On the ground
		Surface Layer avalanche	**Full depth avalanche**
	Liquid water in snow	Absent	Present
		Dry snow avalanche	**wet snow avalanche**
Transition	Form of path	Open slope	Gully or channel
		Unconfined avalanche	**Channeled avalanche**
	Form of movement	Snowdust cloud	Flowing along ground
		Powder snow avalanche	**Flowing snow avalanche**
Deposition	Surface roughness of deposit	Coarse	Fine
		Coarse deposit	**Fine deposit**
	Liquid water in deposit	Absent	Present
		dry deposit	**wet deposit**
	Contamination of deposit	No apparent contamination	Rock debris, soil, brances, trees
		clean deposit	**contaminated deposit**

A typical avalanche path consists of three zone: the starting zone, the track (transition area) and the runout area. Avalanche release occurs in the starting zone of the path. Then, the avalanche flows downstream along the transition area to finally reach the runout zone where it stops, and the snow is deposited.

The complex interaction between topography, snowpack and meteorological conditions define snow avalanche activity in a given site (Schweizer et al., 2003). The key terrain characteristics essential for avalanche formation are : (1) slope ($\geq$ 30 degrees), (2) cross slope curvature and (3) vegetation type, particularly forest cover/density. Given suitable topography for avalanche formation, failure occurs following one or a combination of the below-mentioned, most common, natural or artificial triggers:

1. Accumulation of new snow adds additional stress thus influencing slope failure and avalanche release (Föhn et al., 2002).
2. Wind-transported snow actively contributes to local snow loading. Snow deposited in irregular layers with different densities is more prone to avalanching (De Quervain, 1965;

Schweizer et al., 2003). Wind-deposited snow is influenced mostly by the topography and the location of the avalanche path.

3. Rainfall (Rain on snow events) affect the mechanical properties of the snow. The wetting and weakening of the snowpack release immediate and delayed snow avalanches (Conway and Raymond, 1993).
4. Temperature is also a decisive factor in snow avalanches release. A sudden increase in temperature develops instabilities due to (Schweizer et al., 2003) : (1) deformation of the surface layer of the slab, (2) alteration of the mechanical properties of the snow and (3) formation of a weak snow layer at the snow surface.
5. Snow stratigraphy, particularly the presence of a weak layer is a prerequisite but not sufficient for avalanche formation (Bader and Salm, 1990; Schweizer, 1999; Schweizer et al., 2015).
6. Explosive charges or gas mixtures are used in the starting zone to initiate the fracture of the slab and trigger the release of snow avalanches as a precautionary measures at ski slopes or above critical infrastructures (Gubler, 1977; Simioni et al., 2017).
7. Snow avalanches are also triggered by humans. The small weight of a skier can trigger a weak spot of the snowpack leading to its collapse (Schweizer and Lütschg, 2001; Gaume and Reuter, 2017).

Avalanche typology also varies depending on the processes leading to the release. In this case we can specifically distinguish dry and wet snow avalanches. For dry snow avalanches, stress increases mostly due to snow overloading (new snow, wind snow), leading to the failure of the weak layer followed by the collapse of the slab. They can also be triggered artificially (explosive, skier) and are responsible for most of avalanche fatalities (McClung and Schaerer, 2006). In comparison, wet snow avalanche release when the snowpack strength is weakened due to alteration of the mechanical properties of snow (temperature), water infiltration and overloading of partially wet snow (rainfall). Unlike dry avalanches, they typically cannot be triggered artificially, and primarily endanger communication lines and infrastructure (Schweizer et al., 2015).

Avalanche propagation begins shortly after snow is released. In the transition zone (the track area of the path), the avalanche first accelerates then it reaches a plateau, after which deceleration begins until the avalanche completely stops in the runout area (Schweizer et al., 2015). The depiction of avalanche speed, density, dimensions and impact pressures is a prerequisite for setting up efficient mitigation measures and requires modeling the avalanche flow either using statistical methods, numerical hydraulic models or combined statistical dynamical models (introduced in section 1.3.1).

1.3 Avalanche risk analysis

Long term risk mapping for land use planning is mostly based on purely hazard oriented approaches that ignore the elements at risk (buildings, people inside, etc.). In this context, high return periods are used as reference design events (e.g. 30, 100, 300 years return period event) to define three zones (Eckert et al., 2018): (i) the red zone (impact pressure $>$ 30 Kpa) i.e. zone

with highest risk where new constructions are forbidden, (*ii*) the blue zone where new buildings are permitted provided that specific construction methods and consideration are followed, and finally (*iii*) the white zone with no restrictions. However, hazard oriented approaches aren't a guarantee against excessive exposure/risk to snow avalanches (Favier et al., 2014b). Therefore, risk based mathematical methods (Keylock et al., 1999; Barbolini et al., 2004b; Fuchs and Bründl, 2005; Favier et al., 2014b) and cost benefit analysis (Bründl et al., 2006; Fuchs et al., 2007) emerged in the avalanche field in an attempt to include all the components defined by the risk concept (exposure, vulnerability, coping capacity, etc.). However, truly integrative quantitative avalanche risk assessment where vulnerability is assessed remains rare and only some research fits the criteria, e.g. Cappabianca et al. (2008) and Favier et al. (2014b).

1.3.1 Hazard analysis

In the field of natural hazards, risk is defined as the combination of a damageable event (hazard) and its consequences (expected damage) (Eckert et al., 2012). In the avalanche field, within the framework for probabilistic risk assessment, Eckert et al. (2012) assesses avalanche risk as follows:

$$r_z = \lambda \int p(y) V_z(y) dy, \tag{1.1}$$

where λ is the annual occurrence frequency of an avalanche. $p(y)$ is the joint probability distribution of all variables describing avalanche magnitude (runout, flow depth, etc.) and $V_z(y)$ is the vulnerability of the general type of element z to the hazard y.

Quantitative risk assessment methods combine a model describing avalanche hazard with consequence analysis for an element at risk (building, people, etc.). The avalanche hazard model $p(y)$ represent the variability of snow avalanche events for a specific site (Eckert et al., 2012). The model is assessed either by (*i*) purely statistical approaches (direct statistical inference, extreme value theory) (Lied and Bakkehøi, 1980; Keylock, 2005; Lavigne, 2013; Lavigne et al., 2015) that, despite their advantages (simplicity, reality-based), remain inefficient for hazard zoning since they don't produce velocity and impact pressure (Barbolini et al., 2000); (*ii*) deterministic propagation modeling (Naaim, 1998; Bartelt et al., 1999) describing singular events and highly criticized for their assumptions on the rheological behavior of snow (McClung and Schaerer, 2006), or (*iii*) a combined statistical-dynamical model (Eckert et al., 2010c; Fischer et al., 2020) analyzing the resulting joint distribution of the variables of interest (avalanche velocity, flow depth). Regardless of the method used, snow avalanche propagation remains a highly complex process that can only be approximated. The propagation is mostly characterized by the velocity, flow height, density of the flow, runout distance and impact pressures (in a risk context).

Assessment and calibration of the aforementioned parameters highly depends on data from documented avalanche events. In France, such records are provided by the Avalanche Permanent Survey (referred to as EPA: Enquête Permanante des Avalanches (Bourova et al., 2016)). The database is the most extensive in France, and among the most comprehensive worldwide. Approximately 3900 avalanche paths are documented in the French Alps and the Pyrenees, with quantitative and qualitative information describing avalanche characteristics e.g. deposit volume, release elevation, runout distance, type of avalanche, etc. (Bourova et al., 2016).

1.3.2 Consequence analysis: Exposure

In the last decade, the growing interest in exposure to natural hazards as an important driver of risk stems from its association to social and economic development. Exposure analysis refers to the identification of elements at risk located in the areas where a hazard occur (UN/ISDR, 2004; Field et al., 2012). In the snow avalanche field, the three elements mostly considered either in a purely hazard approach or within a quantitative risk framework are: (*i*) buildings (urban areas) (Keiler et al., 2006; Bertrand et al., 2010; Favier et al., 2014a; Soloviev et al., 2019), (*ii*) people (Jónasson et al., 1999; Barbolini et al., 2004a; Favier et al., 2014b), and (*iii*) roads/infrastructure (Margreth et al., 2003; Hendrikx et al., 2006; Hendrikx and Owens, 2008).

Long term changes in land cover/use, particularly urban areas and buildings exposed to natural hazards are assessed using an array of multi-temporal data e.g. historical maps, cadastral plans, zoning plans, building register (building type, number of storeys and utilization), aerial photos, satellite images, official land cover/land use maps, governmental data (building inventory, land registry), etc. Where digital information is not available, data are digitized from maps or mapped directly from the field (Van Westen, 2013). However, exposure data sets derived from various sources, at different spatial and temporal scales, are often not comparable (Paprotny et al., 2018). Thus, the use of multi-source data for land cover/ land use change detection, population variation, etc., became the center of interest of several research attempting at enhancing comparability between various data sources. This is particularly pertinent in light of the growing interest in the quantification of the long term evolution of exposed elements (buildings, people, etc.) to natural hazards (Jongman et al., 2012; Fuchs et al., 2015; Kummu et al., 2016).

Several algorithms have been developed to enhance comparability of land cover data generated from heterogeneous sources, and a brief overview is presented by Lu et al. (2004). However, most of them focused on enhancing comparability of land cover/land use maps resulting from remotely sensed data, assessed from different sensors e.g. (*i*) Post-classification method for Landsat-Multispectral Scanner, Thematic Mapper (Serra et al., 2003) and Sentinel (Idowu et al., 2020); (*ii*) Principal component analysis for Landsat images (Li and Yeh, 1998), and (*iii*) Spectral–temporal combined analysis applied on Thematic Mapper images (Bruzzone and Serpico, 1997). To our knowledge only few studies assess land cover change using historical maps and remotely sensed data, thus enlarging the temporal scale of the analysis (Verheyen et al., 1999; Cousins, 2001; Petit and Lambin, 2002; Statuto et al., 2017). Their aim is to successfully combine heterogeneous data for land cover change analysis using thematic and spatial equalization techniques (Petit and Lambin, 2001, 2002).

1.3.3 Consequence analysis: Vulnerability

Hazard and damage potential analysis i.e exposure analysis are an effective quantitative proxy for risk. However, vulnerability assessment remains an essential part of risk analysis for the successful elaboration of disaster reduction strategies (Fuchs et al., 2011, 2019). Vulnerability, as a concept and phenomenon, is the subject of on-going debate despite its widespread use in risk research. Several definitions have been proposed for vulnerability where most of them consider susceptibility to harm, the capacity to cope/adapt and exposure as essential components (Fekete

and Montz, 2018). An overview of definitions of vulnerability is beyond the scope of the thesis, and will not be presented. However we refer the readers to Cardona (2004); Adger (2006) and Villagrán De León (2006) for a compilation of definitions.

Integrative risk assessment requires a comprehensive vulnerability analysis that considers all its dimensions (human, physical, economic, environmental, etc.). However, the foci mostly remain on the physical and human dimensions. The physical dimension of vulnerability includes the sensitivity of the built environment (e.g. buildings and infrastructure) to hazard and their susceptibility to damage (Fuchs and Thaler, 2018). To assess failure probability of structures exposed to snow avalanches, vulnerability relations are derived either from field data linking avalanche loading to the observed building damage level (e.g. Keylock and Barbolini (2001); Cappabianca et al. (2008)) or via numerical simulations assessing the collapse/failure of structures subjected to snow avalanche loading (e.g. Bertrand et al. (2010); Favier et al. (2014a)). The latter have the advantage of being transferable between study areas and adaptable to different building types (Favier et al., 2014b). On the other hand, the human dimension represent the susceptibility and coping capacity of the society subjected to the natural hazard. Human fragility curves for snow avalanches mostly assess the probability of death or lethality rate linked to flow speed (Arnalds et al., 2004) or building degree damage (Barbolini et al., 2004b; Favier et al., 2014b).

The multi-dimensional nature of vulnerability is at the core of its volatility and sensitivity to the underlying socio-economic forces to which each dimension is subjected. To that end, a broader understanding of the concept of vulnerability and the drivers triggering spatio-temporal shifts in all its dimensions is needed to reduce damages caused by natural hazards.

1.4 Spatio-temporal drivers of avalanche risk changes

1.4.1 Climate change drives shifts in avalanche activity

Snow avalanche activity occurs either due to meteorological factors (snow loading, rain on snow events, wind drift, air temperature, etc.) or human interventions (skier, explosives, etc.). The spatio-temporal variability of the former, particularly weather and snow characteristics have been already documented in most European regions (Beniston et al., 2018). For example, in the French Alps (1958–2005), Durand et al. (2009a) highlight a marked snow depth decrease at low elevation versus less significant changes at high elevation. Also, in the Swiss-Austrian Alps (1961–2012), snow depth decreased in southern regions compared to no marked change in the northeast (Schöner et al., 2019). In the Austrian Alps, rate of decrease in the number of snow cover days depends on the studied elevation belt (1948-2009) (Marke et al., 2018). More recent studies concurs with the aforementioned results showing a decrease in the mean snow depth with different trends in the European Alps (1971-2019) (Matiu et al., 2020) and the Pyrenees (1958-2017) (López-Moreno et al., 2020) with marked differences among massifs, elevations and regions.

Considering the spatio-temporal variability of the aforementioned meteorological factors, inherited changes in avalanche activity and dynamics (flow regime) are also expected (Naaim et al., 2013; Steinkogler et al., 2014; Hock et al., 2020). Thus, assessing the evolution of avalanche hazard in a changing climate is crucial in order to determine shifts in future activity and the

associated risk. So far, a stagnation in avalanche occurrence numbers due to climate changes is observed in the European Alps (Laternser and Schneebeli, 2002; Eckert et al., 2010d). However, the stagnation results from the combination of a decrease at low elevations due to scarcer snow conditions (Eckert et al., 2013; Lavigne et al., 2015) and an increase at high elevations (Lavigne et al., 2015). This confirms the spatio-temporal variability of avalanche hazard driven by spatio-temporal snow and weather patterns (Laternser and Schneebeli, 2002; Durand et al., 2009a,b; Schöner et al., 2019) interacting with elevation gradients (Durand et al., 2009a,b). Modifications to the nature of avalanching has also occurred in the French Alps (1958-2010) (Naaim et al., 2016) and Swiss Alps (1952-2013) (Pielmeier et al., 2013), where the proportion of wet snow avalanches has substantially increased during the past decades. Such a modification of the nature of avalanches is particularly worth considering since, compared to dry snow avalanches, wet snow avalanches are denser with considerably higher impact pressures (Sovilla et al., 2010). These pressures can reach high levels that surpass those used for dimensioning avalanche protection structures (Ancey and Bain, 2015).

1.4.2 Exposure and vulnerability changes with socio-economic development

Land abandonment in European mountains began as early as the nineteenth century (Debussche et al., 1999; MacDonald et al., 2000; Taillefumier and Piégay, 2003; Lasanta et al., 2017) and continued into the twentieth century (Tasser et al., 2007; García-Ruiz and Lana-Renault, 2011; San Roman Sanz et al., 2013). Most farming communities depends on small extensive farming systems particularly vulnerable to marginalization (Baldock et al., 1996). In remote poorly accessible areas, farms lost their competitive capacity in the free market economy as a result of the technical and structural difficulties impeding the progress of agricultural practices (e.g. mechanization steep slopes) (MacDonald et al., 2000; Lasanta et al., 2017). Thus, the steepest, most marginal lands were abandoned and no longer cultivated (Sluiter and de Jong, 2007). In addition, waves of rural-urban migration (Allix, 1949; Bogdanov and Rangelova, 2012) and the shift of active population toward the tertiary sector lead to the discontinuation of agricultural practices (Strijker, 2005; Bernués et al., 2005; Lasanta et al., 2017) and contributed to abandonment. The latter heavily shaped the mountains we know today. The readers are referred to Lasanta et al. (2017) for an extensive detailed overview on the external and internal drivers of abandonment in Europe.

The twentieth century represents a critical period, during which mountain socio-economic systems transitioned from traditional agriculture toward service-based activities following a period of intense rural depopulation, marginalization and abandonment (MacDonald et al., 2000; Statuto et al., 2017). The transition toward service and leisure-oriented societies encouraged population and tourist influx. Consequently, demand for accommodation and infrastructure increased leading to peri-urbanization of European mountain areas e.g. the Alps (Bätzing et al., 1996; Perlik et al., 2001; Romano and Zullo, 2016) and the Pyrenees (Mottet et al., 2006; Lasanta Martínez et al., 2013).

However, not all mountainous areas are suitable for construction and expansion. Geographical constraints (steep slopes, narrow valleys) (Fuchs and Keiler, 2008) and the multiplicity of natural hazards in mountain environments reduces possible development sites. This, coupled with the increasing demand for touristic facilities raises the question of the safety of settle-

ments against natural hazards in general and snow avalanches in particular. Indeed, where suitable zones for expansion are scarce, settlements were centralized in confined areas, thus the peri-urban sprawl occured in the vicinity of avalanche paths (Keiler et al., 2005; Fuchs and Bründl, 2005). This led to more buildings being exposed to avalanche risk and reflect an increase in the potential overall loss. However, only few studies have focused on the temporal evolution of avalanche risk driven by shifts in exposure to snow avalanche, e.g. in Davos (Switzerland), Galtür (Austria) (Fuchs et al., 2005; Keiler et al., 2006) and the Sakhalin Island (Russia) (Podolskiy et al., 2014). While in Europe most studies suggest a decrease in avalanche risk to settlements due to risk reduction measures, Fuchs et al. (2004) states that avalanche risk to residential buildings increased for events with medium recurrence intervals.

1.4.3 Reforestation and avalanche activity

Since the mid-twentieth century, land cover change, particularly reforestation, has been linked to socio-economic changes especially depopulation and land abandonment in European mountains e.g. the European Alps (Gehrig-Fasel et al., 2007; Tasser et al., 2007; Rutherford et al., 2008; Bebi et al., 2017; Mainieri et al., 2020), the Pyrenees (García-Ruiz et al., 1996; Lasanta-Martínez et al., 2005), the Apennines (Bracchetti et al., 2012; Malavasi et al., 2018), the Cantabrian mountains (García-Llamas et al., 2018; Bergua et al., 2019). In turn, colonization of abandoned pastures can impact avalanche activity (García-Llamas et al., 2018; Giacona et al., 2018) especially since forests are known for their avalanche protection services (Brang et al., 2001, 2006).

The primary role of protective forests is preventing initiation of snow avalanches (Salm, 1978; De Quervain, 1978; Viglietti et al., 2010). This is possible due to : (*i*) snowfall interception by trees inhibiting stratification of the snowpack below the forest canopy and the consequent release of snow avalanches (Schneebeli and Bebi, 2004) , (*ii*) reduced wind speed in forests preventing the formation of large wind-slabs (Schneebeli and Bebi, 2004), (*iii*) moderate temperature fluctuation of snowpack surface beneath the canopy thus preventing surface hoar (Lutz and Birkeland, 2011) (i.e. surface frost, major cause of avalanche formation) and avalanche release (Schneebeli and Bebi, 2004) and (*iv*) direct snowpack support by the tree stems (Schneebeli and Bebi, 2004). Forests capacity to inhibit avalanche formation depends on its structural characteristics (crown cover, size of forest gaps, etc.) and path topography (slope) (Bebi et al., 2009). For additional details on forest structural characteristics refer to the review article of Bebi et al. (2009).

Mountain forests have also the capacity to decelerate and reduce the runout distance of flowing avalanches (Malanson and Butler, 1992; Anderson and McClung, 2012). However, the protective potential is directly linked to forest structural parameters, e.g. stem density for small-medium avalanches (i.e., $< 10{,}000$ m^3) (Teich et al., 2012a, 2014), topography and the distance traveled before penetrating into forests for large avalanches (i.e., $> 10{,}000$ m^3) initiating above the timberline (McClung, 2003; Anderson and McClung, 2012; Takeuchi et al., 2011; Teich et al., 2012a). According to Bartelt and Stöckli (2001), forests lose their protective capacity once they are destroyed by large avalanches initiating above the timberline. Conversely, tree fracturing doesn't consume enough energy to cause significant deceleration (De Quervain, 1965; Bartelt and Stöckli, 2001). However, Takeuchi et al. (2011, 2018) showed that an avalanche destroying

the forest during its descent can still be decelerated. Thus, the controversy is not yet settled and requires more in depth research and studies.

In light of the above, temporal changes in forests (structure, extent) can indeed impact snow avalanches activity. For example, García-Hernández et al. (2017) highlighted a decrease in snow avalanche damage in the Asturian massif (Spain) linked to reforestation. Similarly, Mainieri et al. (2020) showed a decrease in avalanche hazard in the Queyras massif (France). Additional studies analyzing the spatio-temporal evolution of the forest cover and its impact on avalanche activity are needed for more robust understanding of the dynamics of avalanche/forest interactions.

However, the protection capacity of mountain forests, especially its influence on avalanche runout, is rarely considered in risk studies. This process requires in-depth knowledge and understanding of forest/ avalanche stopping mechanisms and is mostly included in dynamic avalanche modeling. Grêt-Regamey and Straub (2006), performed avalanche risk calculations considering the presence of the protective forest. Teich and Bebi (2009) also considered the impact of various forest structure and its presence on risk. They found that collective risk depends on forest structure and decreases by half in the presence of protection forests (compared to unforested areas). To our knowledge in the avalanche field other than the above-mentioned, no studies assessed the impact of forests and/or its temporal evolution within a quantitative risk analysis framework. Thus, so far, the generated risk estimates remain static and independent of the protective potential offered by forests (conditional on its structure and characteristics). Therefore, studies assessing the effect of forest on avalanche risk, within a quantitative risk framework, are essential for the advancement of avalanche management, particularly ecosystem-based solutions for disaster risk reduction (Eco-DRR). In this context, protection forests (Eco-DRR example in mountains) present a holistic cost-efficent approach with the potential to simultaneously reduce natural hazard risks and to provide ecosystem services (e.g. wood production) (Moos et al., 2018).

1.5 Modeling avalanches in forested terrain

1.5.1 The friction approach

Earliest efforts to model forest-avalanche interaction considered a local friction increase in forested terrain (Buser and Frutiger, 1980; Schaerer and McClung, 2006; Takeuchi et al., 2011, 2018). The increase is supposedly caused by a combination of different processes (breaking, overturning, entrainment, etc.) (Bartelt and Stöckli, 2001). This method is nowadays known as the friction approach. In this context, most physical avalanche models employ a Voellmy-fluid law (flow rheology theory). The Voellmy friction law (Voellmy, 1955) considers the total resisting friction (basal resistance) F as a combination of the dry Coulomb (static) friction and a velocity-dependent turbulent friction (Equation 4.3). The dry–Coulomb friction parameter μ is thought to summarize snow properties, whereas the velocity-dependent friction parameter ξ represent the geometry and roughness of the avalanche path (Salm et al., 1990; Ancey et al., 2003).

$$F = \mu g cos\phi + \frac{g}{\xi h} v^2. \tag{1.2}$$

To model avalanche runout shortening in forested paths using the friction approach, the turbulent friction parameter ξ is decreased and set to 400 ms^{-2}, while μ is slightly increased by $\Delta\mu$ ranging between 0.02 and 0.05 (e.g. Gruber and Bartelt (2007); Christen et al. (2010)). The major focus on ξ to characterize forest-avalanche interaction (Salm et al., 1990; Gubler and Rychetnik, 1991; Bartelt and Stöckli, 2001) potentially stems from the belief that the parameter represent the roughness of the path and that processes like overturning, breaking, etc. mostly act on the velocity-dependent friction (Bartelt and Stöckli, 2001). However, this interpretation of the Voellmy friction parameters is controversial since it is based on expert considerations rather than on measurements (Eckert et al., 2010c). In fact, studies like Heredia et al. (2020) and Barbolini et al. (2000) explain that snow avalanche models are highly sensitive to variation of the static friction parameter μ that in turn substantially controls the runout distance of an avalanche.

Over the years, the friction approach has been the center of criticism. Although it has been tested for large scale fast moving avalanches (Bartelt and Stöckli, 2001), some authors suggest that it is not valid for small avalanches (Teich et al., 2014) since snow detrainment is not well represented in the Voellmy friction (Maggioni et al., 2012).

1.5.2 The detrainment approach

Recently, the detrainment approach was proposed by Feistl et al. (2014) to model the breaking effect of forest against small and medium avalanches. In this case, the trees act as a rigid obstacle behind which wedge-like snow depositions are formed. Thus, the approach assumes that the mass deposited behind the trees is deduced from the flow leading to reduction in momentum of the avalanche flow and runout shortening (Teich et al., 2012a, 2014; Feistl et al., 2014). To this end, in addition to the Voellmy friction parameters μ and ξ, a new detrainment coefficient K is introduced to quantify mass extraction from the flow (Teich et al., 2014). K depends on forest parameters (forest type, crown coverage, etc.) and the property of flowing snow (Teich et al., 2014; Feistl et al., 2014) and is formulated by Feistl et al. (2014) as follows :

$$\rho \frac{\delta h_d}{\delta t} = \frac{K}{\|\mathbf{V}\|'} \tag{1.3}$$

Where ρ is the avalanche flow density and h_d is the mean deposition height. This approach is however only valid for small and medium avalanches, under the condition that no tree breakage occur (Feistl et al., 2014).

1.6 Research gaps, objectives and thesis content

1.6.1 Research gaps

The state of the art summarized above highlights several gaps that need to be addressed by avalanche risk assessment. Risk studies in the avalanche field are often based on a static approach that neglects long term evolution of the risk. Yet, it is clear that avalanche risk is subject to the temporal variability of its components (vulnerability, hazard and exposure) driven by shifts in the social (e.g. population dynamics, economy, etc.) and natural systems (e.g. reforestation, climate change, etc.) and all the mechanisms underlying their interaction and dynamics (Field et al., 2012; Birkmann, 2013). Consequently, in their *High Mountains Areas* chapter in the *Special Report on the Ocean and Cryosphere in a Changing Climate* (SROCC), the Intergovernmental Panel on Climate Change (IPCC) convey the need for integrative risk assessment techniques mobilizing interdisciplinary knowledge and expertise of various biophysical and social disciplines (Hock et al., 2020). The latter is in line with the recommendations of several worldwide organizations e.g. the the World Meteorological Organization (WMO) and the United Nations office for Disaster Risk Reduction (UNDRR), notably the *Sendai framework for disaster risk reduction* (Pearson and Pelling, 2015). However, until now, the need for such dynamic integrative risk methodologies remains unfulfilled, which prevents the understanding of past risk trajectories and impedes efforts to elaborate effective adaptation strategies in a context of increasing future risks related to combined socio-economic and environmental transitions.

Additionally, although Alpine and European Mountains underwent relatively the same trends (e.g. land abandonment, depopulation, tourism, etc.), socio-economic, environmental and climatic local peculiarities can lead to spatio-temporal disparities in avalanche risk trajectories. To our knowledge, differences in avalanche risk trajectories linked to such local variations have not yet been considered in the avalanche risk community. Such studies potentially allow a deeper understanding of the processes governing the evolution of hazard, vulnerability and ultimately avalanche risk. The latter can help adapt management strategies to the real local needs/constraints, potentially very different from one area to another.

Finally, forests are known for their protective capacity against natural hazards, notably snow avalanches. Yet, to our knowledge quantitative risk assessment rarely considers forests and its temporal variability as a preventive measure against snow avalanches. Dynamic risk estimates that take into account temporal environmental changes (e.g. forest and its structure) and different building technologies could allow optimization of risk protection under budget constraints.

1.6.2 Thesis objectives

Considering the aforementioned gaps, the aims and objectives of this thesis are the following: (1) developing an integrative approach combining knowledge from natural and social sciences to assess long term changes in avalanche risk and all its dimensions (hazard, vulnerability, exposure), driven by socio-economic, land cover and climatic changes (Figure 4.1); (2) Investigate local socio-economic, land cover and climatic peculiarities that lead to spatial and temporal disparities in risk trajectories (Figure 4.1) and (3) Generate risk estimates that take into account temporal evolution of the forest cover in avalanche paths (Figure 4.2).

Herein, the focus is on the high mountains of the French Alps (more specifically on three typical high valleys, namely the municipality of Valloire, the Guil valley and the upper Maurienne valley) for the 1860-2017 period. The climate conditions of the French Alps, combined with high altitude and steep slopes highly promote avalanche initiation. In addition, the area witnessed important socio-economic and environmental changes over the years. All this, combined with the data availability (avalanche records, historical maps, climate and socio-economic data) makes it an ideal territory to fulfill the objectives of this PhD.

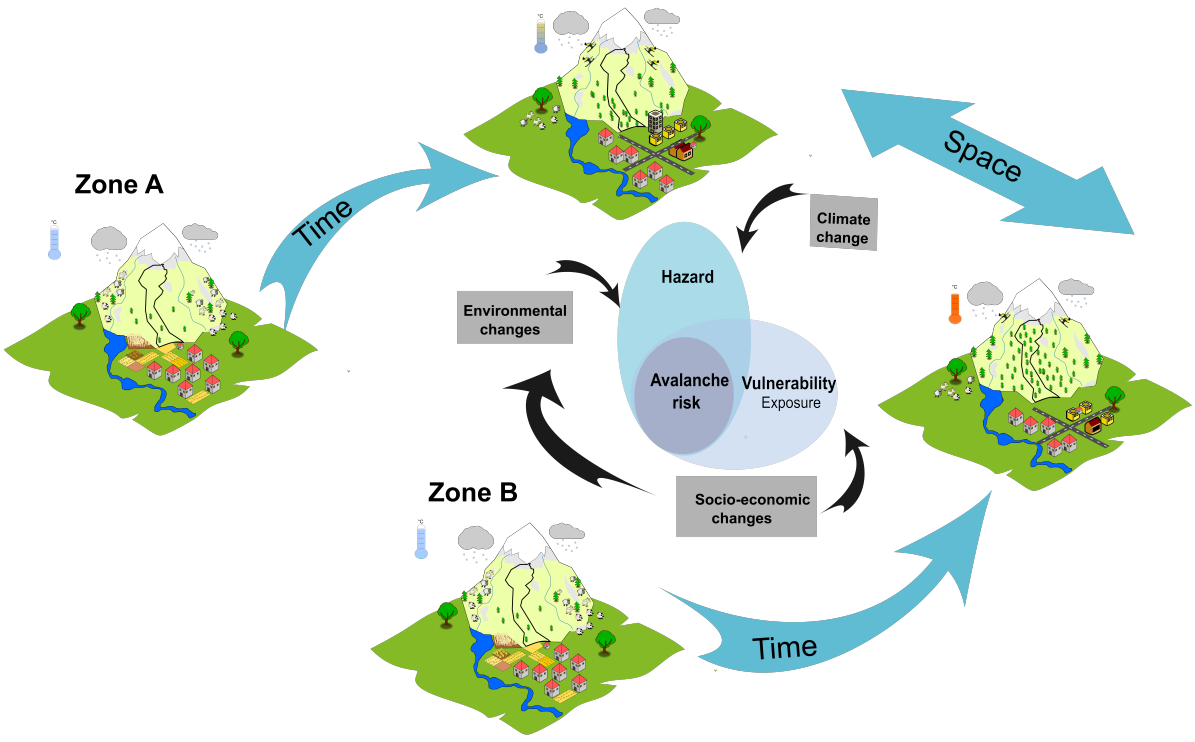

Figure 1.1: The proposed holistic dynamic risk analysis framework: Spatio-temporal evolution of the socioeconomic, land cover and climatic processes leading to changes in hazard, vulnerability, exposure and ultimately risk. The figure represents two almost identical systems (Zone A and Zone B) subjected to different socio-economic, land cover and climatic changes. This leads to spatial and temporal disparities in avalanche risk trajectories

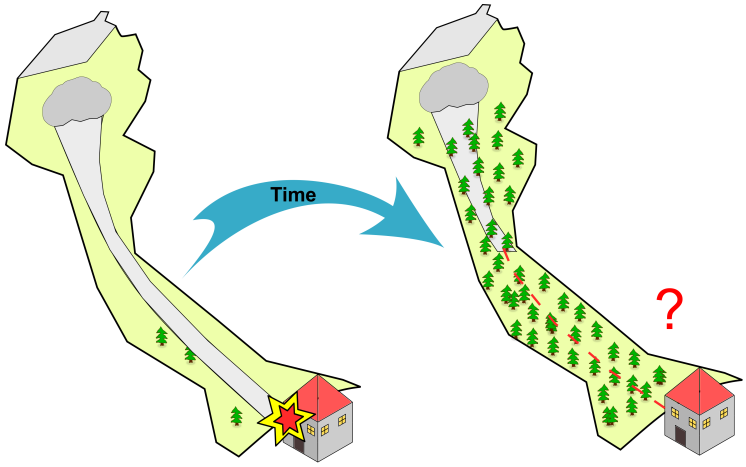

Figure 1.2: Considering the temporal changes in forests to quantitatively assess avalanche risk to reinforced concrete buildings located in the avalanche path.

Each fulfilled objective is intended to be a self-contained published journal article. The development of the integrative avalanche risk methodology taking into account socio-economic and environmental changes is presented in **Chapter 2**. The corresponding article has been published in *Global Environmental Change*. In **Chapter 3**, the approach presented in **Chapter 2** is extended to include the impact of climate on avalanche risk. Then, within this chapter, the local spatio-temporal disparities of risk linked to local socio-economic, land cover and climatic variations, are addressed. The article is currently in revision in *Regional Environmental Change*. Finally, **Chapter 4** develops the final objective that considers the generation of integrative dynamic risk estimates. In this chapter we zoom into the avalanche path level to quantitatively assess the evolution of avalanche risk to reinforced concrete buildings located in the avalanche paths. Here, the integrative methodology only considers land cover changes, notably forest changes as a driver of risk. This chapter is a draft article and will be submitted later.

1.6.3 Overview of the thesis

In **chapter 2**, we develop the first integrative avalanche risk methodology assessing the long term evolution of avalanche risk in all its dimensions, driven by socio-economic and environmental changes. Our methodology combines land cover change detection using advanced image processing techniques, geohistorical investigations and qualitative modeling of risk changes in order to infer the evolution of avalanche risk and its drivers in the upper Maurienne (French Alps) from 1860 to 2017. Herein, we consider that risk is the combination of hazard and vulnerability. The latter not only depends on exposure (a driver of vulnerability), but it is also reinforced by human actions, such as urban development, that can alter the location of elements at risk and its resulting vulnerability. Prior to avalanche risk analysis, the simultaneous evolution of the socio-economic and environmental system is assessed by cross analyzing various data sources (pastoral inquiries, population data, etc.). For land cover change analysis, a series of historical maps and aerial photos were spatially and thematically homogenized to enhance their inter-comparability using the methodology proposed by Petit and Lambin (2002). Then, a

bias correction was used to create one complete series of comparable landscape matrices. Land cover analysis was conducted on the scale of the entire upper Maurienne and in the vicinity of avalanche paths, thus allowing inference of the evolution of avalanche risk to settlements. Ultimately, the qualitative model highlighting the impact of long-term socio-economic and environmental changes on avalanche risk to settlement was elaborated. The results show that avalanche risk in the study area increased locally, due to an increase in the vulnerability of exposed settlements. Our approach, transferable to other natural hazards, notably in wider mountain environments, is a contribution to the elaboration of effective adaptation strategies in a context of increasing risks related to combined climate change and socio-economic transitions.

The holistic risk methodology for qualitative avalanche risk assesment applied for the upper Maurienne valley in **chapter 2**, has been extended in **chapter 3** to consider climate as an additional driver of risk. In this chapter, we address the need for studies assessing the spatial variability of risk driven by local disparities. The extended methodology is thus applied to three upper basins of the French Alps - The upper Maurienne valley, the Guil valley and the municipality of Valloire - to track local spatio-temporal variation of the socio-economic, land cover and climatic drivers of avalanche risk and its components (hazard, vulnerability, exposure). The analysis, conducted from 1860 to 2017, focuses on avalanche-prone terrain defined as the maximal extension of avalanches potentially occurring on all paths of the French avalanche cadaster. We show that from 1860 to 2017, avalanche risk in the upper Maurienne increased, whereas it might have locally decreased in the Guil valley. As for Valloire, risk remains stationary. This study demonstrates the crucial role of local dynamics in avalanche risk evolution.

In **chapter 4**, we address the need for quantitative studies integrating the impact of environmental changes on the evolution of avalanche risk. We thus consider the impact of a changing forest fraction in the avalanche path on risk estimates within a quantitative risk assessment framework. In this chapter, risk is considered as the combination of the likelihood of occurrence of a damageable event (hazard), and degree to which the exposed element can resist the impact of the hazard (vulnerability). For hazard analysis, the Bayesian statistical-dynamical model of Eckert et al. (2010c) is expanded to account for potentially multiple release areas and is calibrated using local data for the *Ravin de Côte Belle* avalanche path in Abriès (Queyras massif, French Alps). Then, the local distribution of avalanche hazard is evaluated according to observed changes in the forest fraction i.e. the aerial percentage of the terrain covered by forests within the extension of the avalanche path. Results of the hazard models are then coupled with Favier et al. (2014a) fragility curves to assess changes of individual risk to a building located in the avalanche path. The fragility curves are associated to different failure limit states for various construction technologies depending on their boundary conditions. In this chapter we show that the probability of exceedance of runout distances, the impact pressure at the building abscissa and ultimately avalanche risk decreases with increasing forest fraction. The study emphasizes the importance of the protective role of the forest and the impact of a changing forest cover on risk estimates. It also highlights the potential of elaborating successful risk reduction strategies that combines nature based solution and construction technology to reduce risk to acceptable levels, all while respecting budget constraints.

Last, in **chapter 5**, we recapitulate the main results and conclusions of the thesis, then we propose possible perspectives for future developments.

Chapter 2

One and a half centuries of avalanche risk to settlements in the upper Maurienne valley inferred from land cover and socio-environmental changes.

This chapter present the article "One and a half centuries of avalanche risk to settlements in the upper Maurienne valley inferred from land cover and socio-environmental changes." published in *Global Environmental Change*, 65:102–149, 2020.doi: 10.1016/j.gloenvcha.2020.102149.
The following authors contributed to the work: Florie Giacona, Anne-Marie Granet-Abisset, Samuel Morin, and Nicolas Eckert.

Abstract: Changes in mountain landscape can affect avalanche activity, causing changes in risk, potentially enhanced by a transition of the socio-environmental system and its underlying dynamics. Thus, integrative approaches combining biophysical and social sciences are required to assess changes in risk in all its dimensions. This study proposes a holistic methodology combining land cover change detection using advanced image processing techniques, geohistorical investigations and qualitative modelling of risk changes in order to infer the evolution of avalanche risk and its drivers in the upper Maurienne (French Alps) from 1860 to 2017. Results show that a continuous increase of forested areas associated with the retraction of agro-pastoral zones followed a period of land abandonment and depopulation. However, reforestation within avalanche paths remains largely incomplete and mostly absent in the majority of release areas, making a decrease in avalanche occurrence and propagation unlikely. This, combined with marked urban sprawl partially concentrated in avalanche prone areas, locally increased the exposure of residential settlements to avalanches. Hence, even if new defense structures have been set up, our analysis indicates that avalanche risk in the upper Maurienne increased through the study period. Even if local specificity related to physical dissimilarities and/or distinguished socio-economic trends always exist, our results may be valid for many high alpine valleys. Our approach is also transferable to other natural hazards, notably in wider mountain environments, as a contribution to the elaboration of effective adaptation strategies in a context of increasing risks related to combined climate change and socio-economic transitions.

Keywords: Avalanche risk, exposure, diachronic analysis, land cover changes, geohistory.

Contents

2.1 Introduction

Snow avalanches are prevalent in mountain areas. The natural process is characterized by a rapid snow flow (Hopfinger, 1983; Schweizer et al., 2003). Snow avalanches are naturally triggered by a combination of factors such as weather conditions (temperature, snowfall, wind direction, etc.), slope, surface roughness (McClung and Schaerer, 2006; Bebi et al., 2009) and seismic activity (Podolskiy et al., 2010; Kargel et al., 2016). The sudden nature of the phenomenon and the complexity of the interaction between the triggering factors endanger people, buildings and infrastructures, causing damages and fatalities all over Alpine environments (e.g.Berlin et al. (2019); Höller (2007); Rapin and Ancey (2000)). Worldwide rise of losses due to natural disasters e.g. floods, snow avalanches etc., and, more widely, the need to take socio-economic considerations into account in mitigation approaches pushed forward the emergence of the concept of risk in the natural hazard field (Keiler et al., 2006; Bründl et al., 2009, 2015) as a tool for risk zoning in land use planning (Eckert et al., 2012, 2018) and as a facilitator for decision making including optimal design of defense structures (Bohnenblust and Troxler, 1987; Eckert et al., 2009; Favier et al., 2016).

The general concept of risk in the natural hazard field identifies hazard and vulnerability as determinants of risk (UN/ISDR, 2004). The most palpable differences in risk formulations center on the definition of vulnerability (Villagrán De León, 2006). The earliest social science definitions consider that vulnerability comprises an *internal* and *external* side, where the latter involves exposure to risk (Chambers, 1989; Watts and Bohle, 1993). Other approaches consider exposure as an important, independent factor of risk (Field et al., 2012). Natural sciences emphasize the importance of susceptibility assessment as a requirement for the set up of technical mitigation structures (Fuchs et al., 2011). Lastly, integrated approaches present vulnerability as a function of exposure, susceptibility and coping capacity (Fuchs et al., 2011; Turner et al., 2003; Weis et al., 2016). In this context, vulnerability not only depends on exposure (among other things), but it is also reinforced by human actions, such as urban development, that can alter the location of elements at risk and its resulting vulnerability.

So far, the concept of risk often does not integrate the dynamic properties of its components and the approach remains static (Fuchs et al., 2013). However, in a changing climate, the intensity and frequency of natural hazard change (Klein et al., 2014). This, coupled with changing socio-economic conditions and settlement patterns, induce shifts in risk to societies. Therefore, addressing the spatio-temporal variability of risk drivers is essential for future sustainable risk management (Fuchs et al., 2013; Peduzzi, 2019). Accordingly, avalanche risk is subject to spatio-temporal variability driven by shifts in the social and natural systems and the mechanisms underlying their interaction and dynamics (Field et al., 2012; Birkmann, 2013). Consequently, integrative approaches to risk based on knowledge transfer between social and natural sciences are now recognised as essential for addressing the complexity of risk, its drivers and inherent spatio-temporal variability (Hock et al., 2020).

The twentieth century represents a critical period, during which mountain socio-economic systems transitioned from traditional agriculture toward service-based activities following a period of rural exodus, marginalization and abandonment (MacDonald et al., 2000; Statuto et al., 2017). Accordingly, land abandonment induced the vegetation succession process from shrubs to forests (Mather et al., 1999; Bebi et al., 2009). In parallel, the transition toward

service and leisure-oriented societies, especially outdoor activities (e.g. ski tourism, trekking etc.), encouraged population and tourist influx (Barbier, 1989). This amplified the demand for accommodation and infrastructure, mostly concentrated around tourist centers and key transportation routes (Barker, 1982). Where suitable zones for expansion are scarce, settlements were centralized in confined areas (Fuchs and Keiler, 2008). Therefore, peri-urban sprawl occurred in the vicinity of active avalanche paths, causing an increase in the damage potential resulting from snow avalanches in settlements (Keiler et al., 2005; Fuchs and Keiler, 2008). Only few studies have focused on the temporal evolution of avalanche risk driven by shifts in exposure to snow avalanche, e.g. in Davos (Switzerland), Galtür (Austria) (Fuchs et al., 2005; Keiler et al., 2005; Fuchs and Keiler, 2008) and the Sakhalin Island (Russia) (Podolskiy et al., 2014). Although, in Europe, results suggest a decrease in avalanche risk to settlements due to risk reduction measures, Fuchs et al. (2004) states that avalanche risk to residential buildings increased following an increase in exposure to avalanches.

Assessing the evolution of avalanche hazard in a changing climate is crucial in order to determine shifts in future activity and the associated risk. Changes in avalanche activity and dynamics are governed by changes in snowfall, snow cover amount, properties and duration (Naaim et al., 2013; Steinkogler et al., 2014). Spatio-temporal variability of the weather and snow characteristics (e.g. snow depth) is already documented in most European regions (Beniston et al., 2018). For example, in the French Alps (1958-2005), Durand et al. (2009a) highlight marked snow depth decrease at low elevation versus less significant changes at high elevation. Also, in the Swiss-Austrian Alps (1961-2012), snow depth decreased in southern regions versus no marked change in the northeast (Schöner et al., 2019). Consequently, spatio-temporal disparities in avalanche activity are also expected. However, weather conditions and snow characteristics are not the only space-time varying factors affecting avalanche hazard. Land cover changes, mostly driven by socio-economic changes, have an impact on snow avalanches (Giacona et al., 2018; Hock et al., 2020). Indeed, vegetation cover, particularly forests, may play a crucial role in decreasing snow avalanche hazard (Salm, 1978; Viglietti et al., 2010; Teich et al., 2012b) and related damages (García-Hernández et al., 2017), notably by decelerating the flow (Malanson and Butler, 1992; Anderson and McClung, 2012; Takeuchi et al., 2018).

To our knowledge, research has not yet addressed the growing need for approaches assessing simultaneous socio-environmental changes and their influence on the long term evolution of avalanche hazard, vulnerability and risk. On this basis, in this study we present an integrative procedure to analyze the evolution of avalanche risk to settlements in one prototypical avalanche prone area of the French Alps, the upper Maurienne valley (Figure 2.1). Information collected from a wide corpus of supports, including historical sources, is combined with an integrative methodology associating land cover change detection using advanced image processing techniques, geohistorical investigations, and qualitative modelling of risk changes. This optimizes documentation and analysis of changes in the socio-environmental system driving the evolution of avalanche risk in all its components. We consider that avalanche risk hinges on the interaction between avalanche hazard and vulnerability of the elements at risk (Figure 2.2), where exposure is considered one of the drivers of vulnerability whereas sensitivity and adaption capacity are not considered. The objectives of our study are: i) to analyze the co-evolution of the socio-economic and environmental system in the upper Maurienne valley from 1860 to 2017 using a diachronic analysis of historical maps and aerial photographs. ii) Zoom into the

extent of avalanche paths to examine the temporal variability of exposed settlements to snow avalanches; iii) Assess how changes in vegetation cover could have influenced the variation of hazard over time, iv) and finally, infer on the evolution of avalanche risk to settlements in the study area since 1860.

2.2 Materials and Methods

2.2.1 Study area

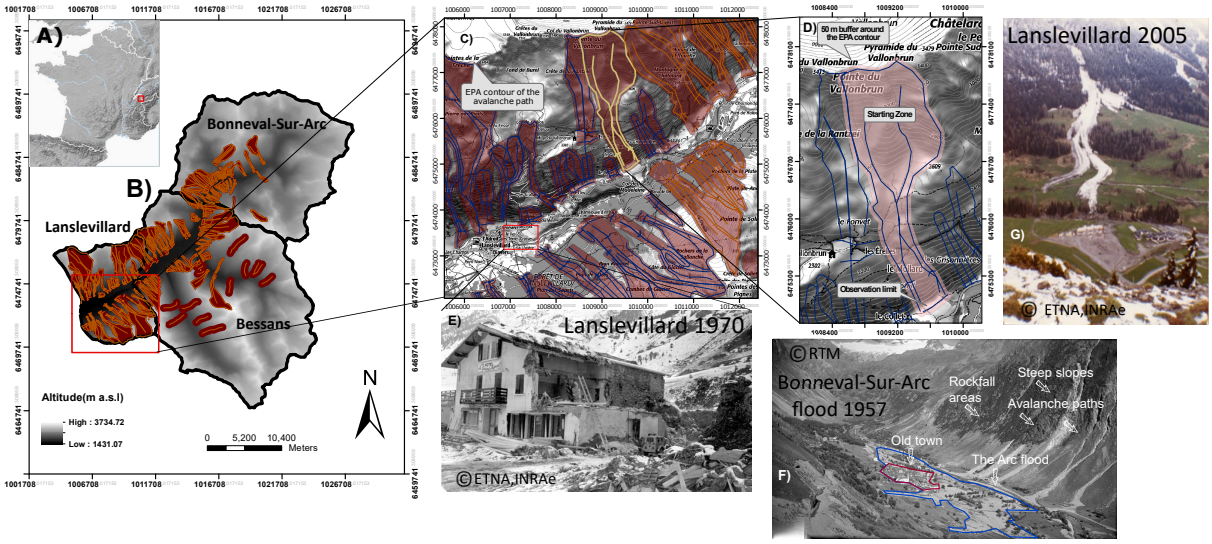

Figure 2.1: (A,B) Location of the study area, (C,D) Avalanche Permenant Survey (EPA) avalanche path contour and 50 m buffer around it, (E) Destroyed hotel in Lanslevillard due to the tragic 1970 avalanche (F) A view of Bonneval-Sur-Arc following the 1957 flood of the Arc river. The old city is visible in the narrow valley. It is surrounded by avalanche paths and rockfall areas located on steep slopes larger than 30 °. (G) Avalanche in 2005 in Lanslevillard.

The three municipalities under study are located in the highest part of the Maurienne valley commonly referred to as the upper Maurienne (Savoy region, Northern French Alps). Bessans, Lanslevillard and Bonneval-Sur-Arc are positioned along the French-Italian borders, between 1500 and 3700 m a.s.l (Table 3.1, Figure 2.1B). The climate of the upper Maurienne is cold with relatively low mean annual precipitation (884±167mm, according to the closest station located in Bessans at 1715 m. asl) in comparison with the rest of the French Alps. Snowfall is abundant with an average of 170 days of snow between November and the end of April (Bessans meteorogical station).

These climate conditions combined with high altitude and steep slopes, highly promote avalanche initiation. Indeed, in the Avalanche Permanent Survey (referred to as EPA: Enquête Permanante des Avalanches (Bourova et al., 2016)), 129 avalanche paths are registered in the study area (59 in Bessans, 33 in Lanslevillard and 37 in Bonneval-Sur-Arc). In addition, more than 3000 avalanche events have been documented since 1900 (Table 3.1), which makes the Haute

Maurienne a valuable territory for avalanche studies (Ancey et al., 2004; Eckert et al., 2008b; Favier et al., 2014b). The avalanche permanent survey (EPA) is the only regular and up to date avalanche monitoring system in France. Avalanche events are recorded on approximately 3900 avalanche paths in the French Alps and the Pyrenees, with quantitative and qualitative information describing avalanche characteristics e.g. deposit volume, release elevation, runout distance, type of avalanche, etc. (Bourova et al., 2016).

However, in the upper Maurienne, snow avalanches are not the sole natural hazard. Flooding, rockfalls and landslides contribute, in addition to topography, to the complexity of the area (e.g. Figure 2.1F shows the multiplicity of natural hazards in Bonneval-Sur-Arc). Apart from climate and topography, the socio-economic development of the study area makes it an interesting case study. Over the last two centuries, the area went through a depopulation and agricultural decline period (Folliasson, 1916; Onde, 1942; Jail, 1977), followed by a flourishing of the tourism sector that transformed its landscape (Rambaud and Vincienne, 1964; Jail, 1973, 1977). However, the increasing demand for touristic facilities, coupled with the scarcity of suitable areas for development raises the question of the safety of settlements against natural hazards in general and snow avalanches in particular.

Table 2.1: Characteristics of the study area

	Whole study area	Lanslevillard	Bessans	Bonneval-sur-arc
Area(km^2)	311	45	154	112
Max. elevation (m)	3735	3572	3735	3633
Min. elevation (m)	1431	1431	1655	1758
Mean elevation (m)	2630	2393	2641	2704
Number of avalanche paths in the EPA record	129	33	59	37
% Area covered by avalanche paths from the EPA	24%	53%	23%	12%
Mean elevation of EPA paths	2215	2171	2270	2205
Number of avalanche events since 1900 in the EPA record	3275	599	1358	1318

2.2.2 Overall methodology to infer the co-evolution of the socio-economic system and avalanche risk

A holistic interdisciplinary approach based on the cross analysis of different data sources is proposed to asses the evolution of avalanche risk in the upper Maurienne (Figure 2.2). Prior to avalanche risk analysis, the co-evolution of the socio-economic and environmental system is assessed by cross analysing various data sources. Population counts for each of the studied municipalities (Lanslevillard, Bessans, Bonneval-Sur-Arc) were obtained from 1861 to 2015. For the first century of the study (1861-1967), data were collected from the School of Advanced Studies in the Social Sciences (EHESS, *http://cassini.ehess.fr*) with 5 to 20 years interval. From 1968 to 2015, data were collected from the National Institute of Statistics and Economic Studies (INSEE), per decade (on average, 1968-2006) and every two years for 2006-2015. Livestock inventories (1862-2013, every 20 years on average), the number of shepherds of the entire Maurienne valley (1860-1968) and the number of cultivated areas (1862-2010, every 20 years on average) were obtained from published data (Rambaud and Vincienne, 1964; Jail, 1969, 1977), the agricultural census published by the Ministry of Food and Agriculture (recensement agri-

cole), and the pastoral inquiries ("enquête pastorale", *http://enquete-pastorale.irstea.fr*). Land cover data from 1860 until 2017 were produced using the methodology explained in section 2.2.3.1.

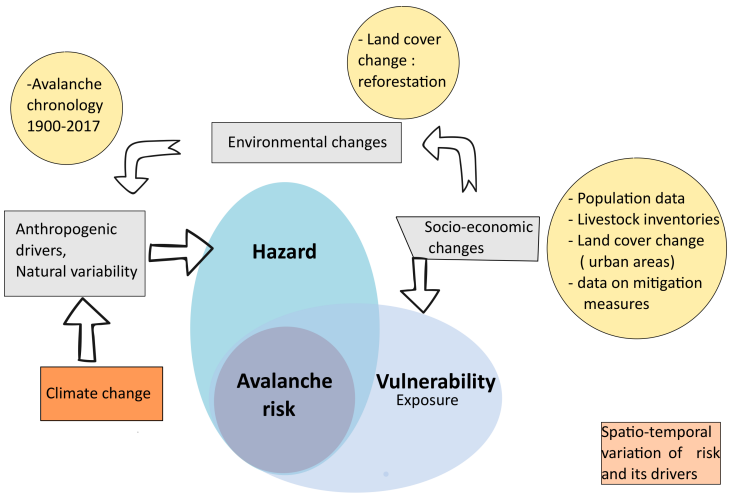

Figure 2.2: Co-evolution between changes in socioeconomic and environmental processes and avalanche risk as function of changes in hazard and vulnerability. Yellow circles indicate data sources used for the study.

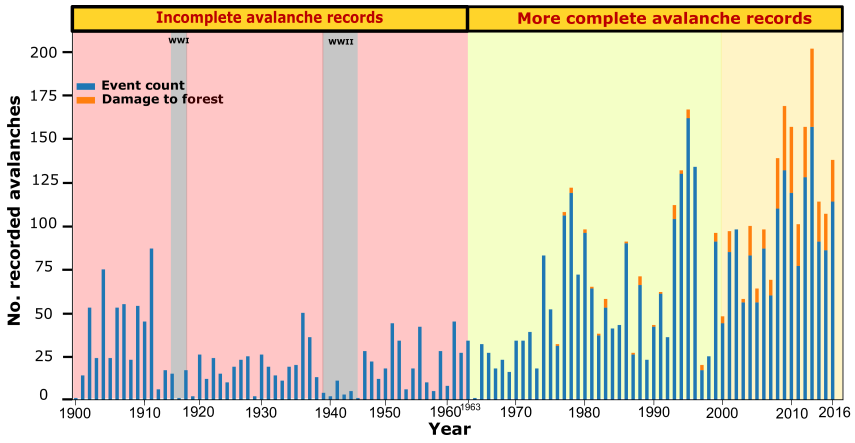

Figure 2.3: Chronology of avalanches reported in the upper Maurienne from 1900 to 2017 within the EPA database. Avalanches that caused forest stand disturbances are also represented. Collected data are more reliable and comprehensive following a series of reforms since 1963. Prior to that date, mainly damaging and/or large avalanches were recorded.

The chronology of recorded avalanche events (EPA database) (Figure 2.3), the local avalanche cadaster (referred to as CLPA: Carte de Localisation des Phénomènes d'Avalanche, (Bonnefoy et al., 2010)) and information on protection structures were used to further identify areas at risk

and infer the evolution of avalanche risk. The CLPA is the French Avalanche map. It records the widest limits of all known avalanches that occurred in the French Alps and Pyrenees (Bonnefoy et al., 2010). Avalanche limits are assessed with a combination of photo-interpretation and eyewitness testimonies (Bonnefoy et al., 2010). Eventually, a qualitative model highlighting changes in land cover and avalanche risk to settlements in the upper Maurienne was elaborated following the geohistorical methodology proposed by Giacona et al. (2019).

2.2.3 Land cover change analysis

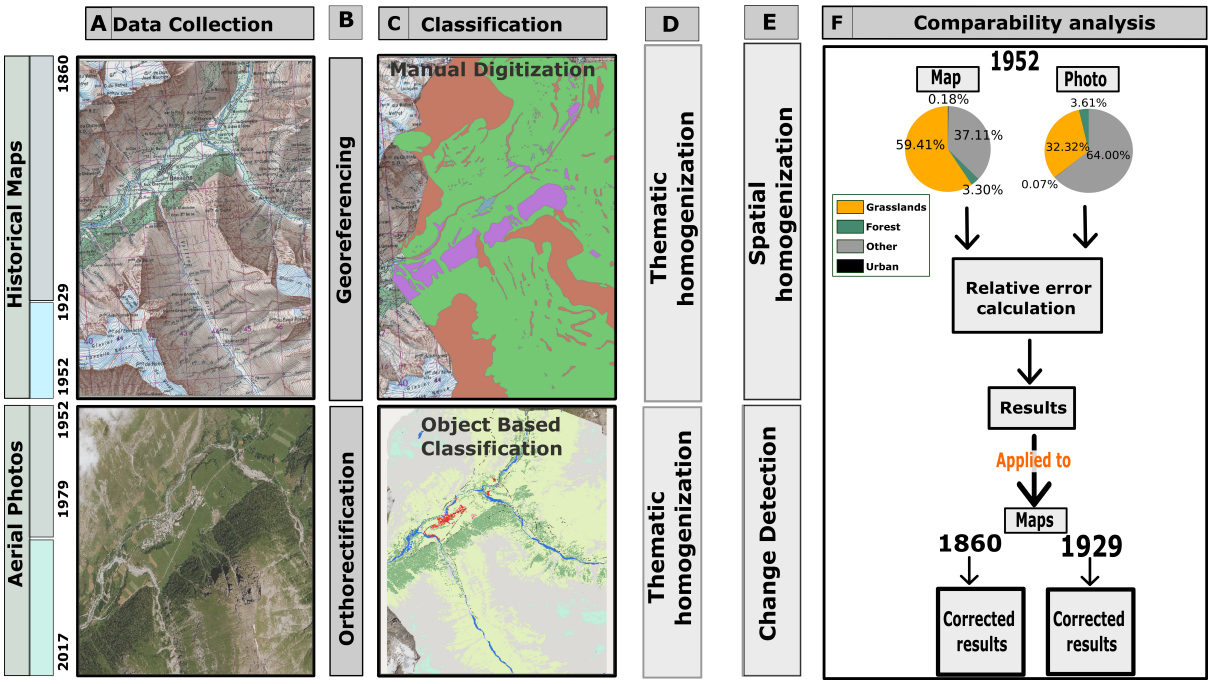

Figure 2.4: Methodology for land cover change analysis: (A,B) collection and preprocessing of historical maps (georeferencing) and aerial photographs (orthorectification) (C) land cover classification and (D,E,F) Change detection and comparability analysis. In (F), the pie charts represent the percent area composition of the whole upper Maurienne for the 1952 historical map (MAP) and aerial photo (Photo).

2.2.3.1 Historical maps: Manual digitization for land cover analysis

Historical maps were provided by the French National Geographic Institut (IGN). The maps used are the *Etat-Major* map of 1860 and the 1952 map scanned and georeferenced by IGN. Alternatively, the 1929 maps also acquired from IGN needed to be georeferenced prior to proceeding to the digitization phase. Additional information on the collected maps and their characteristics can be found in Appendix A, Table 2.3.
All historical maps were manually digitized (Figure 2.4C). Eight land cover classes were delimited, when possible, following the old maps digitization manual proposed by Favre et al. (2013):

forest, grasslands, agricultural lands, urban areas, glaciers, water bodies, main roads, rocks and sands.

2.2.3.2 Aerial photos for land cover interpretation

Aerial photographs are a valuable, spatially complete and temporally continuous tool to analyze historical changes in land cover (Morgan et al., 2010). Therefore, three additional aerial photo collections for 1952, 1979 and 2017 were collected to provide land cover evolution from mid twentieth century until today. All the dates for the analysis are chosen based on availability and as key dates relative to agricultural decline, depopulation and world wars.

Pre-processing: Pre-processed aerial photos for 2017 and 1952 were obtained from IGN. The 2017 image is a true-color aerial photo while the 1952 is in black and white. For 1979, color infra-red photos were gathered in their raw form (https://remonterletemps.ign.fr). Prior to the photographic interpretation, raw aerial photographs needs to be ortho-rectified and preprocessed (Figure 2.4B) to compensate the errors due to distortions and displacements (Morgan et al., 2010; Linder, 2016). In order to successfully perform an orthorectification, several additional information needs to be known. The most essential ones are the type of camera used and its characteristics such as the interior, exterior orientation and the focal length. The majority of the required information is provided in the camera calibration reports acquired from the IGN. In addition to the calibration reports, the IGN's 1 meter resolution digital evelation model (DEM) was used as the vertical reference during the ortho-rectification process. The software used to complete this task is ERDAS LPS® (Leica Photogrammetry Suite) (Intergraph, 2015). Additional information concerning the aerial photos are found in Appendix A, Table 2.3.

Object Based Classification: Over the past years, basic pixel based classification methods were superseded by object based image analysis (OBIA) (Ma et al., 2017; Blaschke, 2001). The concept of OBIA depends upon widely used feature extraction and segmentation techniques (Blaschke, 2010) crucial for good classification results (Baatz, 2000).
The chosen technique for land cover analysis is Multiresolution segmentation (MS) offered within eCognition software that specializes in object oriented image analysis. MS is a bottom-up region based algorithm that merges two image objects based on the combination of spectral information, shape properties and a user defined scale parameter (Baatz, 2000; Darwish et al., 2003).
Accordingly, the 1979 and 2017 aerial photos were classified into seven classes : urban, forest, grasslands, rocks, snow, water bodies and roads. Alternatively, the black and white 1952 image was digitized by hand. The land covers recognised are : grasslands, urban, forest and other.

2.2.3.3 Data comparability and change detection analysis

The result of all the steps described before is two series of land cover maps. The first one is produced from the digitization of historical maps and the second series is generated from the analysis of aerial photographies.

As previously mentioned in other studies, leveling thematic and spatial details prior to combining and comparing heterogeneous data is necessary to reduce errors on change-detection caused by map inconsistencies (Petit and Lambin, 2001, 2002; Falcucci et al., 2007; Pelorosso et al., 2009). For this purpose, the technique proposed by Petit and Lambin (2001) for integration by pairs of successive maps was used to conduct the change detection analysis.
First a thematic generalization (Figure 2.4D) is applied to the 5 land cover maps. Original land cover categories were merged into four classes: urban, forest, grasslands and other. Since the difference in the aerial photographs resolution is relatively minor, the change detection analysis is directly analyzed from the thematically homogenized maps. However, for the historical maps, a spatial homogenization is required before proceeding to the change detection phase (Petit and Lambin, 2001).
To spatially homogenize the layers digitized from the historical maps, the map with the coarser resolution of each successive pair is selected as the target map while the other map is transformed from vector form to a 1 meter resolution raster. Thereafter, it is spatially aggregated from 2 up to 20 meter using the majority rule for the aggregation procedure. This step is essential in order to compensate for scale dependency problems of landscape patterns (Turner et al., 1989; Wu, 2004; Falcucci et al., 2007).
Next, landscape metrics were computed in order to detect the resolution that present the highest landscape similarity between the target and the generalized data. Five landscape metrics (the landscape shape index, Shannon's diversity index, the mean patch fractal dimension, the total core area index and the Total edge contrast index) are sufficient to explain more than 80% of the variability in the landscape pattern (Riitters et al., 1995; Petit and Lambin, 2001, 2002). These metrics were calculated using Fragstats4.2. The normalized euclidean distance was then computed and the resolution with the smallest distance between the metrics was selected as the optimal resolution.
Performing a historical reconstruction of land cover change is a challenging task since it often involves comparing maps derived from different sources. For some applications, the data integration method provided consistent results when maps of different sources were used (Petit and Lambin, 2002). However, in our case, the analysis failed to detect the proper transition of the urban areas between 1929 (historical map) and 1952 (aerial photos). Change detection showed a decrease in the urban area, that is inconsistent with the real urban evolution in the zone. Thus having 1952 as a pivot year common to both the maps and aerial photos series ensures the continuity of change analysis results and translates the dynamics of land cover evolution from 1860 until 2017. However, this does not ensure the proper comparison between the landscape composition matrices derived from the historical maps and aerial photographs. Hence, the 1952 pivot year can be used to quantify the bias resulting from the maps and, once assessed, to have a complete homogenized series of comparable landscape matrices.
To calculate the bias (Figure 2.4F), let 1952 be the pivot year, common to both aerial photographs and historical maps. First let S_k be the surface area corresponding to land cover type k.

$$S_k = P_k \times S_0, \tag{2.1}$$

where S_0 is the total surface of the study area and P_k is the fraction of land cover type k. Knowing that $\sum P_k = 1$ and $\sum S_k = S_0$ we can calculate the relative error ε_k per land cover class using the 1952 aerial photography as reference as follows:

$$\varepsilon_k = \frac{S_0 P_{km} - S_0 P_{kp}}{S_0 P_{kp}} = \frac{P_{km} - P_{kp}}{P_{kp}}, \tag{2.2}$$

leading

$$P_{kp} = \frac{P_{km}}{\varepsilon_k + 1}, \tag{2.3}$$

where P_{km} is the fraction of k resulting from the 1952 historical map and P_{kp} is the fraction of k recorded from the analysis of the 1952 aerial photos.
Since all the land cover data, generated from historical maps, were already homogenized to a comparable resolution following the methodology suggested by Petit and Lambin (2001), we can assume that the relative error derived for the pivot year applies to the previous years. Thus we can create virtual matrices that represent the landscape composition as if it was analyzed from aerial photographies.
Let S_{kp}' be the virtual area corresponding to land cover type k knowing that only the area digitized from the map is available :

$$S_{kp}' = \frac{P_{km}}{\varepsilon_k + 1} \times S_0. \tag{2.4}$$

Thus, P_{kp}', that represents the potential fraction of land cover k as if it was generated from an aerial photos, is :

$$P_{kp}' = \frac{S_{kp}'}{\sum S_{kp}'} = \frac{S_0 \frac{P_{km}}{\varepsilon_k + 1}}{\sum S_0 \frac{P_{km}}{\varepsilon_k + 1}} = \frac{\frac{P_{km}}{\varepsilon_k + 1}}{\sum \frac{P_{km}}{\varepsilon_k + 1}}. \tag{2.5}$$

2.2.3.4 Land cover change analysis in avalanche paths

To asses land cover change in avalanche prone areas, a 50 m buffer was created around the contour of the 129 avalanche paths from the EPA database within the study area. Then, change detection analysis was applied within this newly created buffer following the methodology explained above. Mean evolutions within avalanche-prone terrain were then computed for further analysis.

2.3 Results

2.3.1 Evolution of land cover, population and livestock in the upper Maurienne

By applying the methodology suggested above, we were able to trace the co-evolution of land cover, population and livestock in the upper Maurienne valley as function of five sub-periods: 1860-1929, 1929-1952, 1952-1979 and 1979-2017. Overall, land cover trends shows that the study area is mostly covered by grasslands zones that fluctuate with time. On the other hand, forested areas show an increasing trend in terms of percentage total area. They hit the 5%

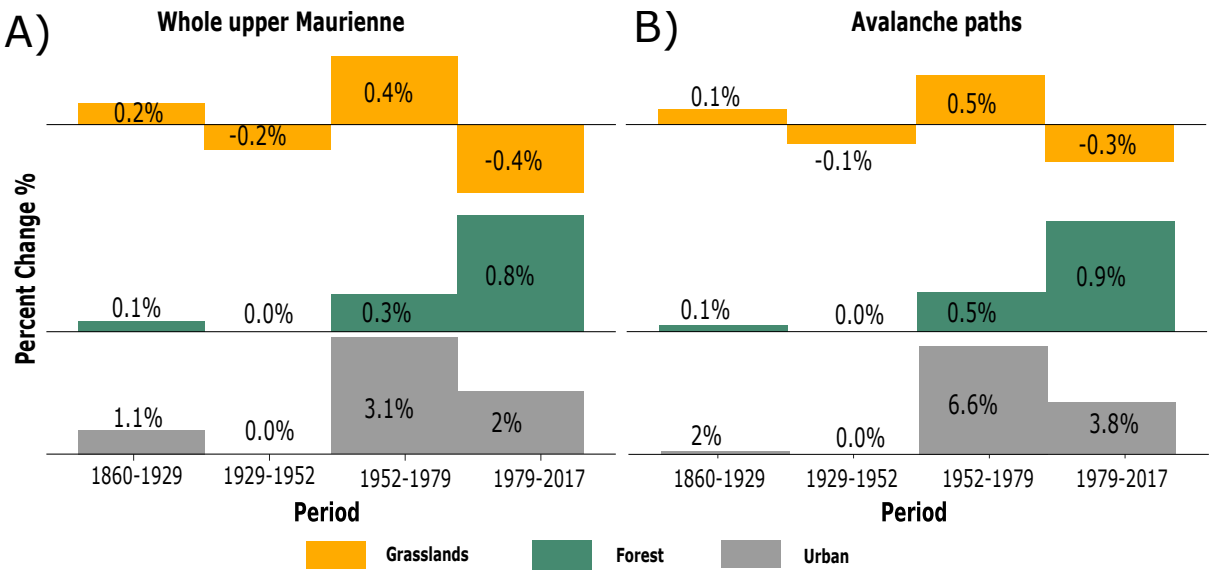

Figure 2.5: (A) Yearly land cover changes in the whole upper Maurienne (values rounded to the nearest tenth) (B) Yearly land cover changes within the extension of all avalanche paths from the EPA record (values rounded to the nearest tenth).

coverage mark in 2017 after being stuck in the 3% zone for more than a century. Urban areas remain the least dominant landcover, never surpassing 0.25% of the area, but with a significant increasing trend over the study period (Figure 2.6).

Between 1860 and 1929, grasslands area increased by 14% (0.2%/year) whereas forests were very slowly stabilizing and expanding (0.1%/year) (Figure 2.6, Figure 2.5A). Cross analysis of the population and agro-pastoral data shows that, from 1861 until 1926, while population declined by 35%, 33% and 38% in Lanslevillard, Bonneval-Sur-Arc and Bessans, respectively, the number of breeders (1860-1914), cattle and sheep (1861-1923) also declined by 38%, 43% and 84%, respectively (Figure 2.10). In addition, around 70 to 80% of cultured areas vanished between 1862 and 1930 (Figure 2.10). In addition, during this period, the urban area increased by 56% (1.1%/year) (Figure 2.6, Figure 2.5A).

For the second period (1929-1952), analysis shows a 5% decline in the grassland areas (Figure 2.5A). The decline coincides with an intensification of the depopulation (additional 30% loss by 1954) and a further decline of the number of breeders (50% decline since 1914) and cattle (additional 9 % loss since 1929) (Figure 2.10). A stagnation in the establishment of the forests and development of urban areas is also observed (Figure 2.6, Figure 2.5A).

In the second half of the twentieth century, the rate at which the population was declining slowed down, especially in Lanslevillard and Bonneval-Sur-arc (Figure 2.10). Between 1952 and 1979, grasslands increased by 11.2% (Figure 2.6, Figure 2.5A). Forest growth rate also increased (0.3% yearly increase) and urbanization surged (87% increase 1952-1979) (Figure 2.5A). The maximum yearly urban growth of 3.5% was recorded during this period (Figure 2.5).

After the increase in 1952-1979, grasslands decreased by 15.6% between 1979 and 2017 (Figure 2.5). The major decline in pastoral areas was accompanied by a fast reforestation

process (31% increase from 1979 to 2017) (Figure 2.5). Shortly after 1979, depopulation halted. The population in the entire area increased by almost 50% (1975-2017) (Figure 2.10) which coincides with an expansion of the urban areas (78%) (Figure 2.6, Figure 2.5A).

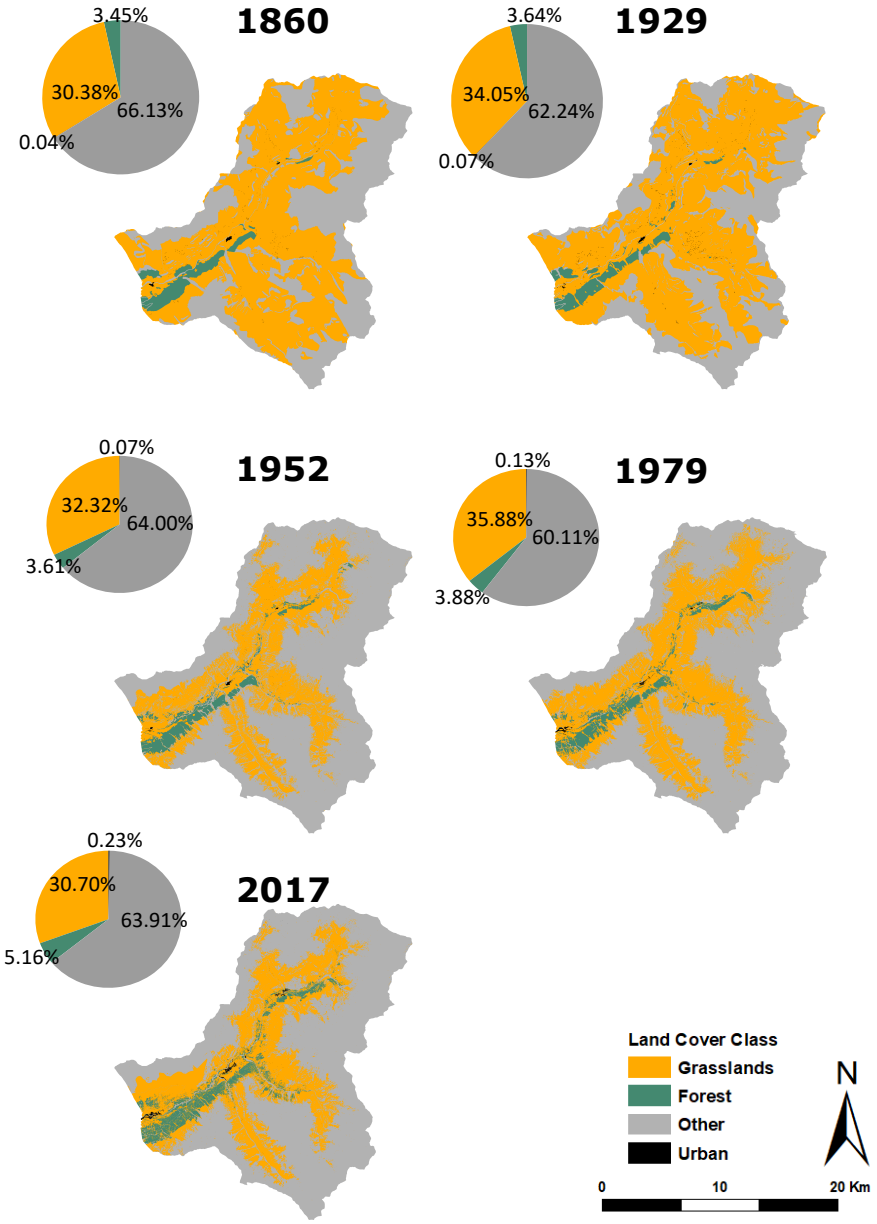

Figure 2.6: Diachronic land cover analysis of the upper Maurienne between 1860 and 2017. Pie charts represent the percent area composition of the whole upper Maurienne for each land cover map.

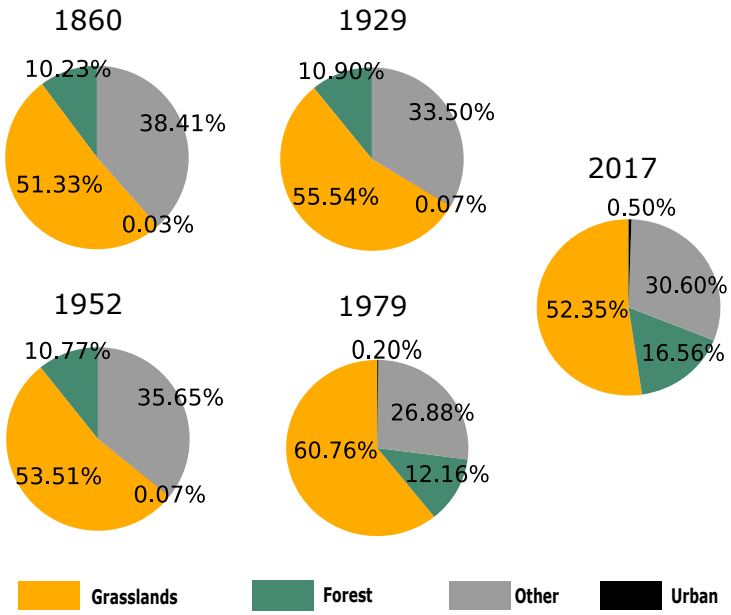

Figure 2.7: Percent area composition within the extension of avalanche paths from the EPA record in the Upper Maurienne from 1860 until 2017.

2.3.2 Evolution of land cover in avalanche paths

2.3.2.1 Evolution of settlements exposed to avalanches

In 2017, urbanization covered on average 0.5% of the areas (Figure 2.7). Between 1952 and 1979, urban areas increased by 6.6% per year in the vicinity of avalanche paths in the upper Maurienne (Figure 2.5B), and by 3.8% per year from 1979 to 2017. This phenomena is particularly observed in Lanslevillard and Bonneval-Sur-Arc.

Figure 2.8, shows the evolution of the urban area within the extent of the deadliest avalanche that ever hit Lanslevillard. In February 1970, the Northern Alps were hit by a heavy snowfall wave during which it continuously snowed for ten to twenty days (Jail, 1970). Heavy snowfall, combined with abnormally low temperatures and a considerable accumulation of snow staged the perfect situation for disastrous avalanches formation. On February 24, 1970, an avalanche deviated from its usual path (*La Combe de Pisselerand* EPA 5 track into *couloir du Pichet*) to hit the newly constructed urban area of Lanslevillard. That day, eight people died, ten were injured and five buildings were destroyed (Jail, 1970; Ancey, 2009). The majority of buildings affected in 1970 did not exist in 1952 (Figure 2.8). So, already, the urban transition during this period increased the exposure of the newly constructed urban area that was left unprotected despite that a similar avalanche took the same exceptional path a century ago (Jail, 1970). Therefore, in 1972, four snow deflection structures were installed to protect the affected area (Figure 2.8). Two structures were positioned at 2430 and 2410 m a.s.l. at the *Plan de la Cha* (PPR, 2004). Their main role was to restrict the deviation of avalanches initiating in *La Combe de Pisselerand* to avoid a repeat of this exceptional avalanche.
Fifty years later, the urban area within the avalanche extent continues to grow and reaches a maximum in 2017 (Figure 2.8). Nowadays, EPA sites 5 and 205 where the avalanche occurred

are labeled as highly sensitive inhabited zones. The fact that the 1970 avalanche was never seen again doesn't reduce the vulnerability of the expanded urban area. In fact, the same area is also affected by the *Rocher Roux* avalanche that initiates below 2300 a.s.l. on the same *Pichet* track (EPA 3) (PPR, 2004). Contrary to the *Pisselerand* one, this avalanche is very frequent and occured 15 times between 1902 and 1966. However, until today, the two other deviation structures located upstream of the village grant a good level of protection against it.

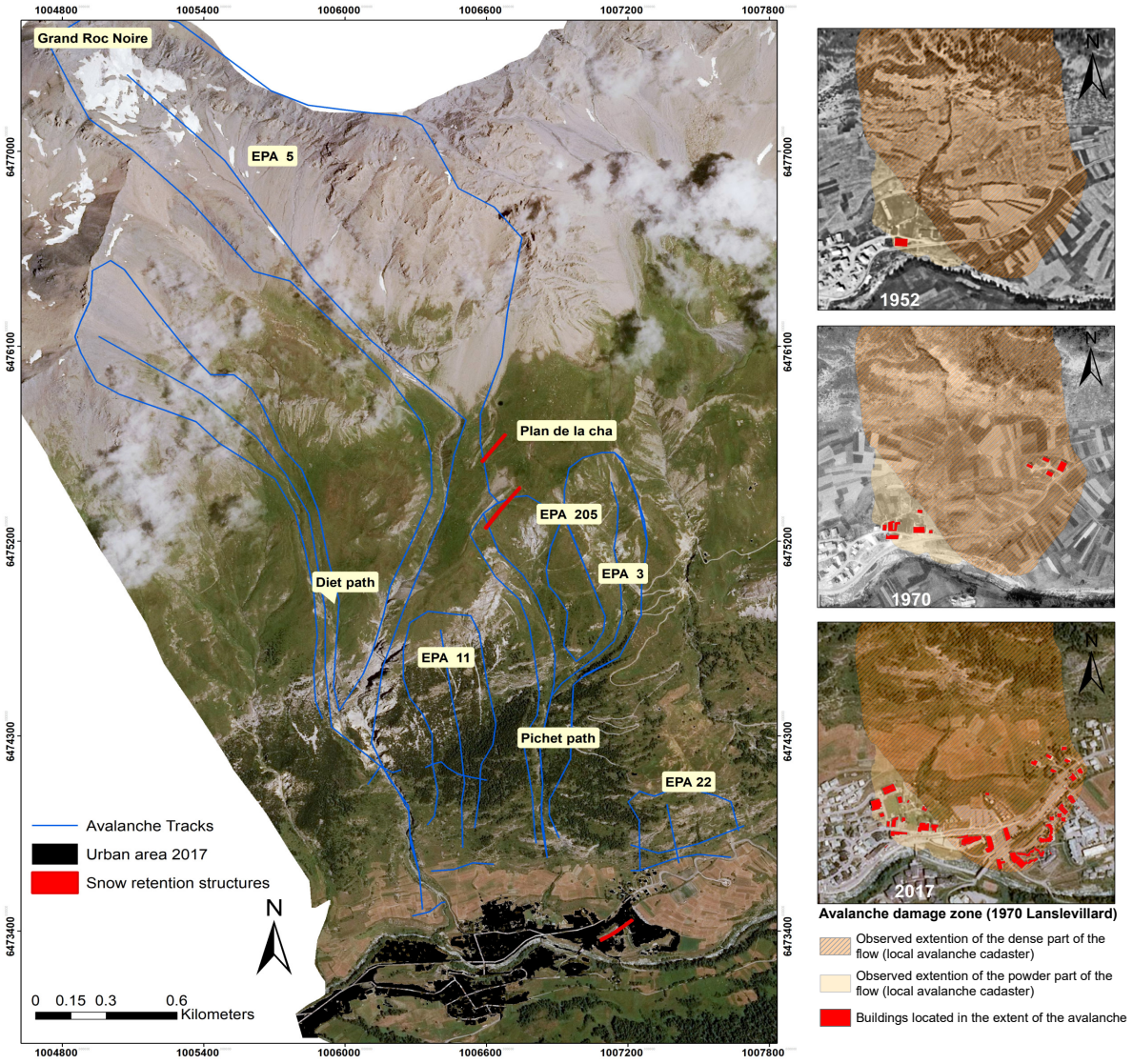

Figure 2.8: Left: location of snow deflection structures within the paths concerned by the major avalanche of 1970 in Lanslevillard. Right: extent of the 1970 avalanche in Lanslevillard and evolution of the urban area at risk (red) from 1952 to 2017.

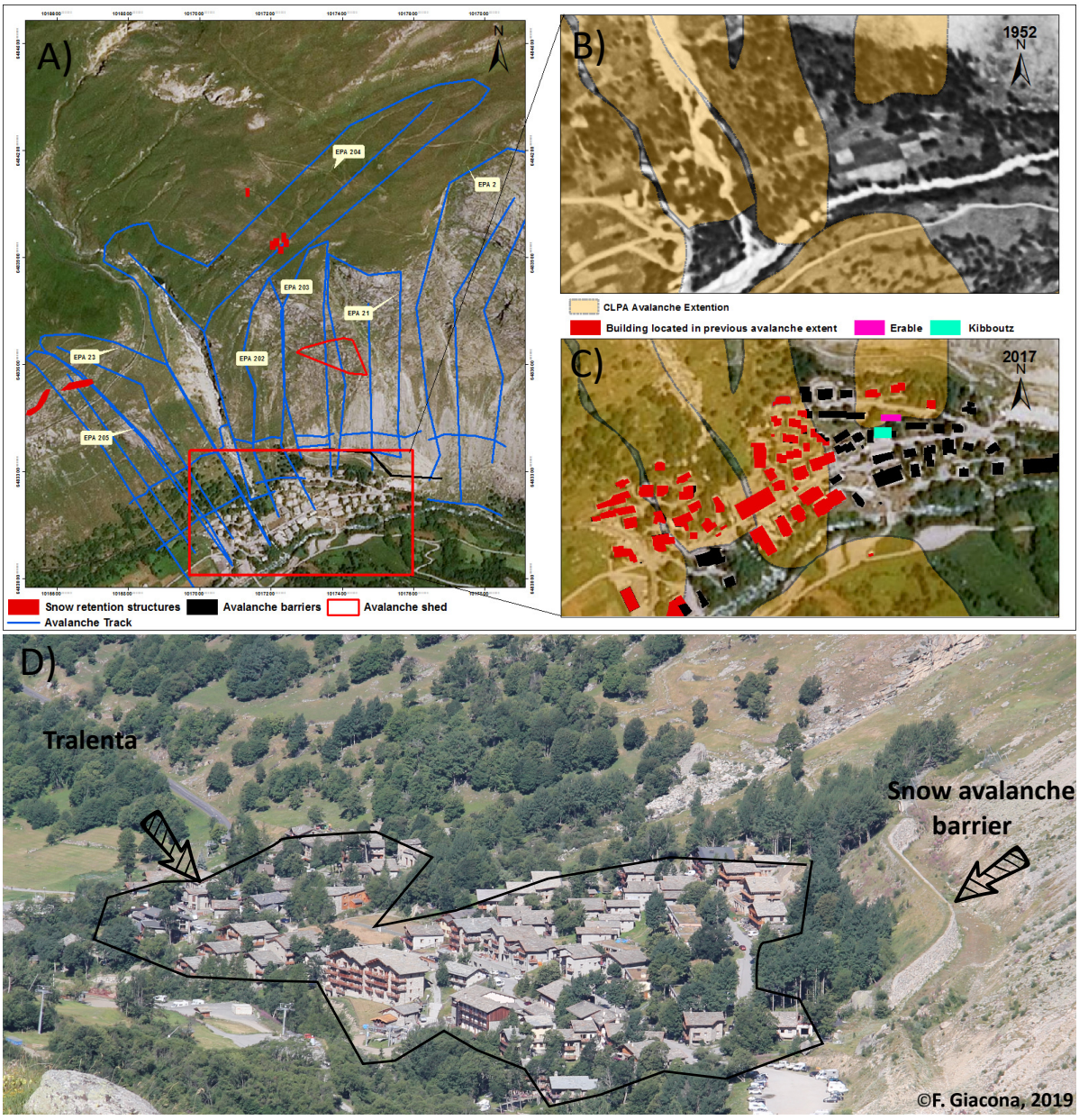

Figure 2.9: The Tralenta district in Bonneval-Sur-Arc: (A) aerial photography of Tralenta surrounded by avalanche paths and their numbers according to the EPA database, (B) the situation of the urban area in 1952, (C) the complete development of Tralenta in 2017 and (D) a picture of the study area taken in 2019 showing the protective barricade.

Another example is Bonneval-Sur-Arc. The village is located in the narrow upper part of the valley. Therefore, an urban expansion was a must to accommodate the increasing touristic demand. The Tralenta district, east of the old city, is the last inhabited place (farthest) in the upper Maurienne. The development of the Tralenta in late 1960's (Megerle, 2018), coincides with the opening of the ski resort and flourishing of tourism in the area. The newly constructed

accommodations were mostly owned by locals and offered exclusively to tourists (Megerle, 2018). The Tralenta is directly affected by *Tralenta, Merlon, Gabions* and *Clappier Faudon* pathways that were respectively subjected to a 14.33%, 2.54%, 8.5% and 0.75% increase of their urban area between 1952 and 2017 (Table 2.2). Today, the urban areas below the aforementioned avalanche paths in the Tralenta district are classified as highly sensitive inhabited zones, namely zone where avalanche risk to settlements is high.
According to a witness, prior to the establishment of Tralenta, an avalanche usually passed at the location of *Kibboutz* and *Erable* chalets (CLPA no.31694) (Figure 2.9). However, in general, no deadly avalanche have ever occurred in these paths. However, the lack of victims or severe damage does not necessarily alleviate the vulnerability of the exposed urban area. In fact, with the construction of the Tralenta, the local vulnerability largely increased and, as a result, protective barricades against avalanches were built in the *Merlon* Zone (Figure 2.9) in 1972 (PPR, 2011). After that, the urban envelope continued to expand until late 1980's. To alleviate the increasing vulnerability and to insure additional protection of the heavily populated area, the barricade built in 1972 was shifted upward in 2011 (PPR, 2011).

Table 2.2: List of most affected paths by the urban expansion in Bonneval-Sur-Arc (1952-2017).

District	Path Name	EPA Path Number	CLPA[1] Number	% change in urban area[2]	Avalanche Events[3]
Tralenta	*Clappier Faudon*	21	7	+0.8%	9
	Gabions	23	11	+8.5%	7
	Tralenta	202	9	+14.3%	None
	Merlon	203	8	+2.5%	None
	La Lenta	204	10	+2.8%	None
	L'Oratoire	205	12	+4.7%	None
Old City	*Druges*	25	14	+2%	9

[1] *Carte de Localisation des Phénoménes d'Avalanche (avalanche cadaster).*
[2] *Change as a percentage of area within the extension of each path.*
[3] *Recorded between 1952 and 2017 in the EPA.*

2.3.2.2 Evolution of forest cover within avalanche paths

Figure 2.5B and Figure 2.7 show continuous forest increase in avalanche paths over the study period, from 10.2% in 1860 to 16.6% in 2017. Before 1952, reforestation rates were slow (<0.1% /year) (Figure 2.5B). However, after 1952, reforestation rates sped up (0.5%/year) and by 1979 the forest area in avalanche paths increased by 14%. Thereafter, the forest continued to expand at a more rapid pace (0.93%/year) and by 2017 it increased by an additional 36% (Figure 2.5B).

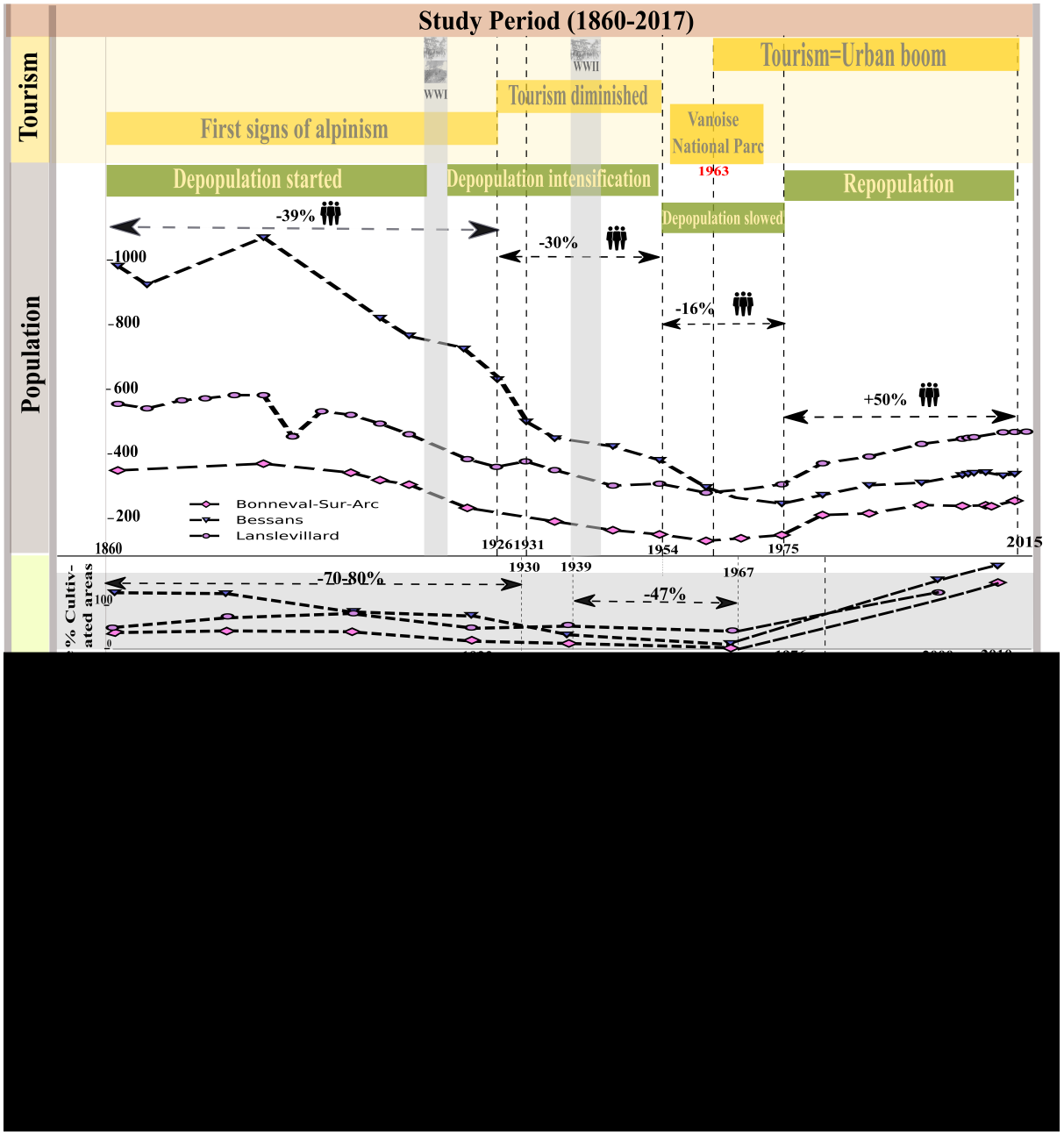

Figure 2.10: Diachronic evolution of the socio-environmental context in the upper Maurienne from 1860 until 2017. Qualitative data highlighting the evolution of tourism are deduced from Jail (1977) and discussed, when needed, in the discussion.

2.4 Discussion

2.4.1 Diachronic analysis of land cover

Two series of historical maps and aerial photos were used to asses the evolution of land cover in the upper Maurienne valley. As for other of such studies, our analysis is subject to a range of uncertainties. Most common uncertainties associated with land cover analysis stems from the classification and change detection phase. Thus, to reduce the errors associated with both, we adopted the methodology suggested by Petit and Lambin (2001) that facilitate change detection analysis through the homogenization of spatial and thematic information across data sources. The methodology was applied to layers digitized from historical maps. Three types of errors are recognized when performing thematic and spatial equalization.

First, aggregation errors caused by the aggregation from small to a broader level. Aggregation errors are also associated with the change from vector coverage to raster coverage. We checked that these errors were negligible and less than 1% for all land cover types in all the years (Appendix B, table 2.4).

The second type of errors is related to the thematic aggregation of the different maps. In this study, the thematic aggregation errors were not included in the analysis since, before the classification phase, the different land cover were identified and grouped into similar categories.

No explicit measure of the error associated with the classification is performed due to the absence of ground truth data. However, by reducing the number of classes to the four most relevant land-cover types, it was possible to cut down the potential occurrence of misclassification errors.

The comparison of the land cover composition between the 1952 map and aerial photos shows several discrepancies especially in the grasslands, other and urban class that were over-represented in the historical maps (appendix C, Figure 2.12). The higher representation of grasslands in the map is related directly to the under representation of rocks. Small patches of rocks dispersed among the grasslands in higher altitude were most probably only represented as grasslands on the maps. This discrepancy propagates also to older maps. As for the urban areas, the difference is mostly due to cartographic generalization techniques (mostly scale variation). Finally, it is important to note that maps represent a simplification of a much complex reality. Thus, a large part of the uncertainty stems from the different sematic models used to create the map and its intended use.

Comparability between landscape matrices generated from aerial photography and historical maps remained an issue. Thus, for the pivot year (1952), the relative error was calculated (Appendix C: table 2.5) and applied to correct the maps and,thus, create new matrices that potentially represent the state of land cover as if they were analyzed from aerial photos. This innovative method helps create one complete series of comparable landscape matrices. However, overall, the procedure did not modify the trajectory of the evolution. A comparison between the rate of changes analyzed before the correction (appendix C: Figure 2.13) and after (Figure 2.5) shows the coherence of the results.

Finally, the 50 m buffer zone around avalanche paths is also a source of spatial error. The 50 m extension beyond the current limits of avalanche paths in local avalanche cadaster and chronicles was made as a pragmatic compromise between: i) including all potential avalanche prone terrain (current extensions are regularly exceeded), and ii) not exaggerating the number

of exposed elements.

2.4.2 Evolution of the socio-environmental context in the upper Maurienne

We assessed the co-evolution of the socio-economic and environmental system in the upper Maurienne valley as function of five sub-periods: 1860-1929, 1929-1952, 1952-1979 and 1979-2017. These changes could be successfully linked with the evolution of population and social practices.

2.4.2.1 1860-1929: Start of the depopulation phase

Mountains have long been considered as migration territories (Fontaine, 2005). The decrease in population, number of breeders, livestock and cultivated areas, between 1860 and 1929, clearly implies the start of the depopulation and land abandonment phase (Onde, 1942; Rambaud and Vincienne, 1964; Jail, 1969, 1977). Although depopulation and abandonment are the main reason that explains the decreasing population trend (Jail, 1977), the First World War (1914-1918) and its subsequent impact on the society also inderectly contributed to the population loss. Indeed, according to Gex (1922) the deaths during the First World War in our study areas accounted for 5% of the population in 1911 (1566 in Bessans, Lanslevillard and Bonneval-Sur-Arc). Still, since no sharp population decline is observed during the war period (1914-1918) (Figure 2.10), it is very likely that the subsequent impacts of war, e.g. decrease in birth rates linked to postponed marriages, displaced and fragmented families, also contributed, in addition to the abandonment, to depopulation. This has been confirmed for different departments in France e.g. Savoy department (France) (Gex, 1922) and Hérault department (France) (Raynal, 1946).

This period also marks the start of the transition from deforestation to reforestation in the entire Maurienne valley (Battipaglia et al., 2014) and in France in general (Mather et al., 1999; Kauppi et al., 2006). The reforestation observed between 1860 and 1929 is attributed to the combination of factors that helped reduce pressures and restore forests e.g. depopulation (Mather et al., 1999), forest policies (Brugnot, 2002) and agricultural intensification (Mather and Needle, 1998). Indeed, as areas in high altitudes were abandoned (Mather et al., 1999), forest encroachment in the study area occurred mostly between 1800 and 2350 m.asl (Appendix E, Figure 2.17). The intensification of grazing on sowed grasslands at lower elevations (Mather and Needle, 1998) explains the increase in grasslands observed between 1860 and 1929.

During this period, except agro-pastoralism, all three villages had little to no activity (Jail, 1977). So they all slowly turned towards tourism as a second source of income. The first signs of touristic activity appeared at the end of the nineteenth century with alpinism in Bessans and Bonneval-Sur-Arc Jail (1969, 1977). The different touristic activities during this period led to the construction of several hostels to accommodate the tourists (Jail, 1973), that might have modestly contributed to the urban expansion during this period.

2.4.2.2 1929-1952: Population and agricultural decline

Overall, the 1929-1952 period marks a stagnation in the development of the area due to the combined effect of abandonment, depopulation and wars.

The combined decline in grasslands, livestock and breeders is potentially a delayed consequence of the agricultural abandonment that began during the previous period. However, this should have encouraged a faster reforestation between 1929 and 1952. Hence, the observed delay in forest regeneration is potentially associated with a rise in transient livestock reported by Jail (1969) between 1928 and 1964.

During the Second World War tourism completely stopped in some areas, such as Bessans, contributing to population decline in the area (Jail, 1977). Likely, the effect of the war on the overall development of the area is somewhat reflected in the stagnation of urban development, especially since Bessans and Lanslevillard were completely destroyed during the Second World War (Millere, 1997). This caused a housing crisis (Millere, 1997) due to the combined effect of building destruction and the economic recession that occured in the interwar period (Loiseau et al., 2005).

2.4.2.3 1952-1979: Major urbanization of the valley

Between 1952 and 1979, grasslands increased. One possible explanation is the shift toward more profitable activities such as the creation of high value cheese label (Chauchard et al., 2010). This, in addition to the implementation, in 1962, of the European Common Agricultural Policy (CAP), encouraged intensive cattle farming and pastoral activities. The aim of this new policy was to encourage agricultural productivity via modernization of farms to achieve food self-sufficiency in Europe, and France in particular (Ackrill, 2000).

Another important finding was the peak in urbanization. This is likely to be related to tourism. Indeed, during this period, the tourism sector started to redevelop (Jail, 1973). The presence of the Vanoise national park in 1963 played a role in boosting summer tourism, and heavily contributed to a much needed economical boost in the area (Mauz, 2007). The impact of tourism can be seen in the increase in the number of available beds for tourists from 250 (before the second war, (Pairaudeau, 1983)) to 2890 in 1978 (Marnezy, 1979). In addition, complete districts were exclusively built and reserved for tourism. For example, the Tralenta area developed in the 1960's, and exclusively reserved for touristic and secondary accommodations (Megerle, 2018). In 1978, the district alone held 27% (786 beds) of the available beds in the upper Maurienne (Pairaudeau, 1983).

2.4.2.4 1979-2017: Major reforestation and urbanization driven by a surge in tourism

The small push in grasslands during the previous period (1952-1979) lasted until the European dairy crisis in 1983 (Chauchard et al., 2010). Thereafter, the pastoral lands returned rapidly to their previously declining trends. As a result, forest encroachment sped up.

The combined impact of repopulation and tourism contributed to the increase in urban areas between 1979 and 2017. This is reflected in the rise of primary residences (1975-2016) (INSEE, 2016), secondary residence (Megerle, 2018) and the number of beds available for tourists (30% increase, 1978-2017) (INSEE, 2017). Similarly, Roca (2013) highlight a tripling of mountain vacation properties in France between 1968 and 2008.

2.4.3 Evolution of avalanche hazard

Land cover changes in avalanche paths are a direct result of socio-economic changes that occurred in the study area between 1860 and 2017. These changes can impact avalanche activity (García-Hernández et al., 2017; Giacona et al., 2018), especially forests which are valued for their avalanche protection services (García-Hernández et al., 2017). Their primary role is to stabilize the snow in release areas, thus preventing initiation of snow avalanches (Salm, 1978). However, in the upper Maurienne, only 2 out of 129 avalanche paths (1 in Bessans and the other in Lanslevillard) are forested up to their release area. Therefore, the forest, despite the major reforestation that occurred, is not able to provide protection by preventing snow avalanche release. However, this trend is not specific to our study area since the majority of the release areas in alpine environments are located above the treeline (Giacona et al., 2018).
Mountain forests have also the capacity to decelerate flowing avalanches (Malanson and Butler, 1992; Anderson and McClung, 2012). However, identifying if the reforestation process in the upper Maurienne plays a role in slowing down avalanches without explicit modeling of the physical processes is challenging (Zgheib et al., 2019). According to Bartelt and Stöckli (2001), forests loose their protective capacity once they are destroyed by large avalanches initiating above the timberline. Since 1976, 380 events that damaged the forest are recorded in the study area (Figure 2.3). In line with the ideas of Bartelt and Stöckli (2001), it can be concluded that reforestation in the upper Maurienne have no power against large flowing avalanches. However, we acknowledge that there are considerable discussions among researchers with respect to the capacity of forests to decelerate avalanches : while scientists generally believe that destroyed forest can't decelerate large avalanches, others showed that this may be possible in some circumstances (Takeuchi et al., 2018).

A direct analysis of the evolution of avalanche occurrence numbers using historical data of recorded avalanches (Figure 2.3) introduces bias related to sources and does not reflect the natural evolution of avalanche activity (Giacona et al., 2017). As a result, the increasing trend observed in the upper Maurienne from 1900 to 2017 (Figure 2.3) mostly reflects that the record is much more comprehensive over the recent decades. Therefore, in order to objectively show the evolution of avalanche hazard in the upper Maurienne, we mostly refer to studies made on the French Alps where, using advanced statistical methods, researchers were able to depict evolution trends in avalanche occurrence. Indeed, in addition to land cover, changes in avalanche activity are also governed by modification in snow and weather variables (Naaim et al., 2013). While snow cover at low elevations has generally declined, at high elevations changes are either insignificant or unknown (Hock et al., 2020). In addition, Eckert et al. (2010d) showed that, overall, climate change had little impact on avalanche occurrence numbers in the Northern French Alps from 1948 to 2005, in good agreement with other studies by Laternser and Schneebeli (2002) and Schneebeli et al. (1997) in Switzerland. Eventually, Lavigne et al. (2015) showed that the overall stagnation in the French Alps results from combined decrease in avalanche occurrence numbers at low elevations due to scarcer snow conditions versus potential increase of avalanche occurrence numbers at high elevations areas such as upper Maurienne. In summary, the impact of climate change on avalanches in high mountains, like the upper Maurienne, is most likely a change in the magnitude and nature of events (Eckert et al., 2010a, 2013; Corona et al., 2013; Pielmeier et al., 2013; Naaim et al., 2016; Hock et al., 2020). This,

combined with the lack of protection provided by the reforestation against avalanche initiation and propagation, in the upper Maurienne, suggest that avalanche hazard in the study area was and still is very high with no clear decreasing trend.

2.4.4 Evolution of avalanche risk in the upper Maurienne

The temporal evolution of avalanche risk depends on the change of hazard and vulnerability in which we include exposure. These changes are driven by shifts in the socio-economic and natural systems of the upper Maurienne valley since 1860. As avalanche activity in the upper Maurienne was arguably more or less steady for the entire period, the evolution of avalanche risk primarily depends on changes in the vulnerability of the elements at risk (Figure 2.11). Since 1952, the number of buildings exposed to snow avalanches has been increasing due to the development of tourism e.g. Tralenta district in Bonneval-Sur-Arc (section 2.3.2.1,2.4.2.3). With the growing number of tourists, tourism-related businesses bloomed, increasing the attractiveness of the area and leading to its consequent re-population (Figure 2.10). This result ties well with previous studies wherein increase of exposure of buildings to avalanches was observed in the European Alps (Fuchs et al., 2005; Keiler et al., 2006; Fuchs and Keiler, 2008). Similarly, Hock et al. (2020) assess with high confidence that over the recent decades people and infrastructures, in high mountains, became more exposed to cryospheric hazards such as snow avalanches.

Changes in vulnerability can also occur due to the presence of technical risk reduction measures (Fuchs et al., 2017). The aforementioned results (section 2.3.2.1) shows that in Lanslevillard and Bonneval-Sur-Arc barricades and deflection structures were indeed built in 1972 to protect the urban area. However, mitigation structures cannot decrease exposure to the point where risk is non-existent. This is important to acknowledge because if mitigation methods were infallible, extreme winters such as 1998/1999 wouldn't have been so fatal for the European Alps (Gruber and Margreth, 2001; Rousselot et al., 2010). As examples, we mention i) the Taconnaz avalanche in 1999 (Chamonix) that broke through all the barriers installed and destroyed a part of the forest and few houses located below (Rapin and Ancey, 2000); ii) the Montroc avalanche (1999, Chamonix) that left comparable damages to the horrific winter of 1970 in Val-D'isère (Rapin and Ancey, 2000) and Lanslevillard; iii) the 1999 Evolène avalanche in Switzerland (Wilhelm et al., 2000). Hence, despite the presence of technical risk reduction structures in our study area, their effectiveness cannot be entirely guaranteed on the long term. For this reason, the presence of technical mitigation measures is not considered in zoning plans in France. Indeed, DGPR (2015) in general prohibits the construction in highly hazardous areas even if protection structures are installed. Only if several criteria are met, such as the lack of available space for development outside of risk areas, construction is permitted (DGPR, 2015). This seems to be the case of Bonneval-Sur-Arc where, due to the low availability of suitable land for development, areas like Tralenta have developed even if they are surrounded by avalanche paths.

Therefore, avalanche risk in the upper Maurienne arguably increased between 1860 and 2017, mostly due to a concentration of settlements in the vicinity of avalanche paths. Thus, more people are exposed, making them more vulnerable to snow avalanches. One might argue that being exposed does not imply vulnerability to natural hazards (Field et al., 2012). However, as Birkmann (2006) explains, although vulnerability controls the degree of loss of a given element,

exposure controls the number of elements that can potentially be affected, so that focusing on exposure may be sufficient to catch the first-order trend in risk evolution which is highlighted in our qualiltative diachronic model (Figure 2.11). Also, one may argue that our interpretation of risk evolution is valid only if avalanche activity in the study area was constant. Under this assumption, risk changes depend on the evolution of vulnerability including the change in exposure driven by socio-economic and environmental factors. We gave arguments to justify why a more or less steady avalanche hazard may be realistic for our case-study. However, further work could clearly refine our results. These would imply fully quantitative risk assessment, including quantitative probabilistic-numerical avalanche modelling (Eckert et al., 2010c), analysis of the vulnerability in all its dimensions (physical, social, economic, etc.) and dynamic evolutions induced by changes in environmental and socio-economic drivers (Farvacque et al., 2019). This would allow designing successful disaster risk reduction strategies (Fuchs et al., 2019).

Eventually, in the context of our currently changing climate, future projections predict an increase in wet snow avalanche activity (Castebrunet et al., 2014; Hock et al., 2020). This, coupled with an expected increase in exposure and the possibility that current risk reduction approaches become increasingly ineffective (mitigation structures, warning systems, etc.) to climate change (Hock et al., 2020), imply further potential increase in avalanche risk in high mountains of the world. Thus, expansion of our work to future conditions would be beneficial, as a contribution to the elaboration of effective adaptation strategies.

2.4.5 Wider relevance of the results obtained

Even if we have never attempted to extrapolate our data outside the study area, we are convinced that similar results could have been obtained for many high alpine valleys. The upper Maurienne has indeed been chosen as an archetypal case-study, so that overall trends in socio-environmental conditions and avalanche risk are arguably more or less similar. Notably, socio-economic and environmental patterns associated with land abandonment and depopulation are common to the majority of Alps, e.g. in Italy (Velli et al., 2018), Switzerland (Gellrich et al., 2007) and other European mountains e.g. Pyrenees (Mottet et al., 2006), Cantabrian mountains (Spain) (García-Llamas et al., 2018). Also, climate warming affects the whole mountain environment in a similar drastic way.

However, patterns of change may vary locally depending on socio-economic and/or environmental peculiarities. Exposure of local communities to avalanche risk may vary regionally (Hock et al., 2020), and depend on the historical development of the settlements under study (Fuchs et al., 2004). For example, exposure highly depends on the combination of the size of tourism industry, infrastructure development and availability of suitable areas for expansion. In turn, development is regulated by urban planning strategies and laws that also vary from one place to another. Also, factors affecting snow avalanche occurrence such as altitude, slope, climate, the location and number of avalanche paths etc., vary locally. As an illustration of this spatial variability, in our study area, most of the reforestation took place in Lanselvillard due to more favorable condition (altitude, climate) and the existence of a larger forest cover in 1860 facilitating forest recovery. Similarly, urban expansion was the largest in Lanslevillard due to the closeness to the largest ski resort in Val Cenis. However, it is in Bonneval-Sur-Arc that the highest number of buildings exposed to avalanches exist mostly due to the lack of

space for development and the large number of active avalanche paths (Refer to Appendix D for an overview of land cover change in each of three municipalities: Bessans, Lanslevillard and Bonneval-Sur-Arc). All in all, even if the case study choice and our extensive methodology should be seen as guarantees of the robustness of the conclusions reached, the work should be reproduced in other contexts to generalise our results and, hence, refine our understanding of the profound ongoing changes affecting mountain socio-environmental systems.

2.5 Conclusion

By combining a large corpus of sources including historical maps, aerial photographs, population and livestock inventories with advanced processing techniques, we assessed the co-evolution of land cover and the socio-economic system in the upper Maurienne from 1860 to 2017. First, different land cover classes were identified and digitized. Then, the land cover maps stemming from the historical map series were spatially and thematically homogenized to enhance their inter-comparability. Finally, a bias correction was used to create one complete series of comparable landscape matrices using 1952 as the common correction year. Using the same approach, the evolution of land cover in avalanche paths was also assessed, allowing inference of the evolution of avalanche risk to settlements. Ultimately, a qualitative model highlighting changes in land cover and avalanche risk to settlements in the upper Maurienne was elaborated.

The 1860-1929 period marks the start of the rural depopulation that intensified between 1929 and 1952. As a result, agricultural lands were slowly abandoned and pastoral activities reduced. The impact of abandonment is mostly visible in the 1929-1952 period, with the decrease in grasslands and in the number of cattle and sheep in the area. After 1952, winter and summer tourism grew and new touristic accommodations were established in the upper valley to host the incoming visitors. Most of the newly constructed areas were built in the vicinity of avalanche paths, increasing their exposure and consequent vulnerability to snow avalanches. Reforestation was also a result of agricultural abandonment. It began in 1860 and sped up mid twentieth century. However, reforestation of avalanche paths remains incomplete with still almost no forests in avalanche release zones. This, coupled with the complexity of forest-avalanche interactions, indicate that a drastic hazard reduction compensating vulnerability increase is unlikely. Hence, despite the technical protection measures installed by the local authorities in the 1970's, avalanche risk in the study area increased locally, due to an increase in the vulnerability of exposed settlements.

In the future, scientists predict an increase in risks due to natural hazards in high mountain areas. As illustrated with our work, spatio-temporal evolution of risk depends not only on changes in hazard, and may even be mostly driven by the evolution of vulnerability in all its dimensions. Thus, integrative assessment techniques that mobilizes the knowledge and expertise of various biophysical and social disciplines are mandatory to elaborate efficient mitigation strategies. To this aim, our approach could be transferred with benefit to other areas and natural hazards.

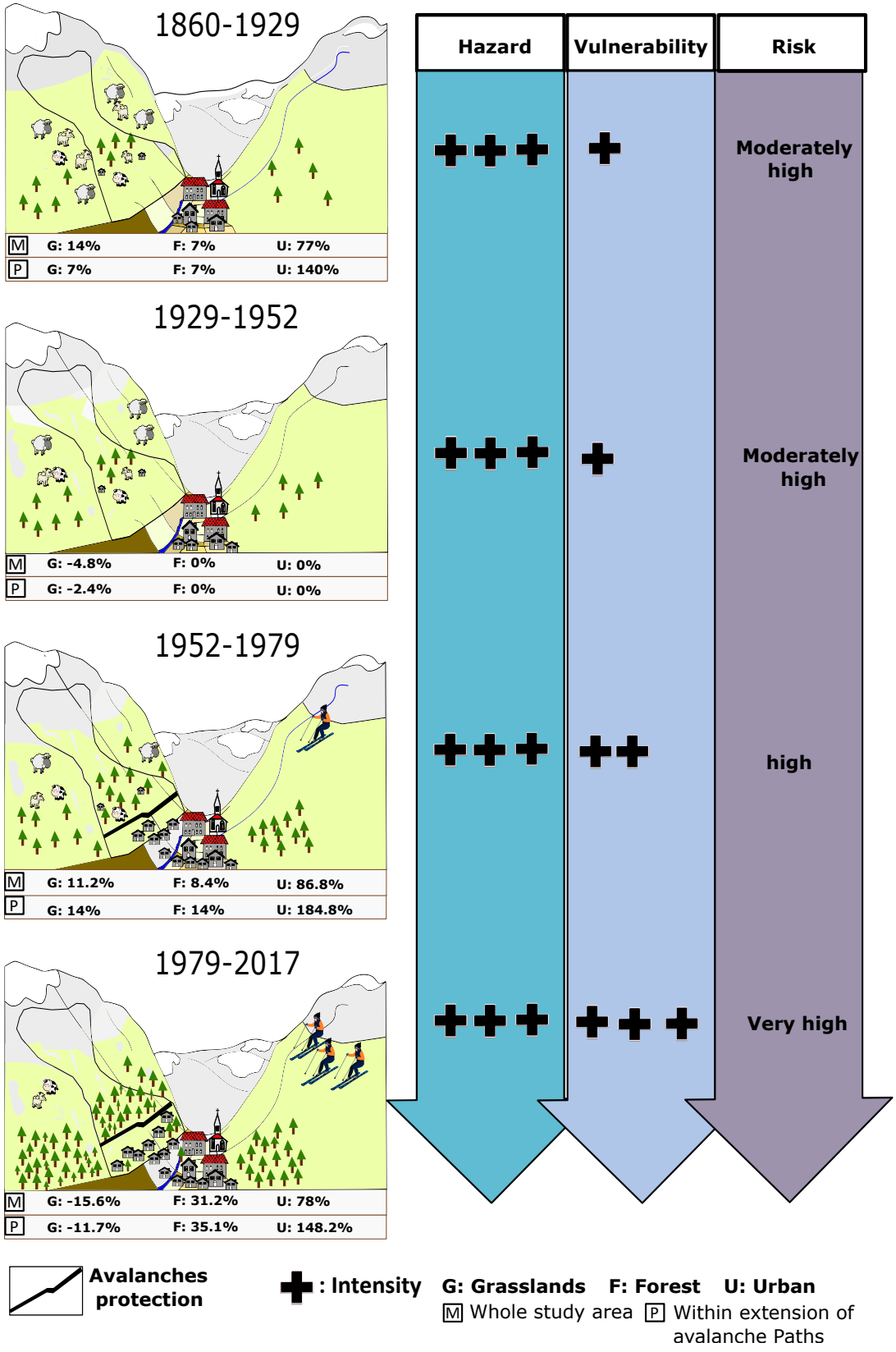

Figure 2.11: Co-evolution of land cover, avalanche risk and its components from 1860 to 2017 in the upper Maurienne valley. For each of the four sub-periods, this qualitative model sums-up changes in land-cover and in the different components of avalanche risk to settlements.

2.6 Appendix

2.6.1 Appendix A: Characteristics of the collected data

Table 2.3: Characteristics of the maps and aerial photographs used to document the evolution of land cover in the study area.

	Year	Name	Scale/resolution	Source
Historical maps	1860	Etat Major	1/40000	IGN
	1927	Lanslebourg	1/50000	IGN,EPA
	1929	Tignes	1/50000	IGN,EPA
	1952	Lanslebourg	1/50000	IGN
	1952(partially updated)	Tignes	1/50000	IGN
Aerial photos	1952	-	0.5m	IGN
	1979	-	1.5m	IGN
	2017	-	1.5m	IGN

2.6.2 Appendix B:Errors associated with change detection

Table 2.4: Spacial aggregation errors associated with the transformation from vector to raster formats.

Land cover class	1860	1929	1952 (map)
Grasslands	0.00%	0.00%	0.00%
Forest	0.00%	-0.01%	0.00%
Urban	-0.02%	0.05%	-0.92%
Other	0.00%	0.00%	0.00%
Average	-0.01%	0.01%	-0.23%

2.6.3 Appendix C: Data comparability analysis

Table 2.5: Relative error per land cover class ε_k in absolute value calculated using the 1952 aerial photography as reference for the entire study area and within the extension of EPA avalanche paths.

	Forest	Grasslands	Urban	Other
Relative error (entire area)	-0.08	0.83	1.78	-0.42
Relative error (within EPA avalanche path)	-0.07	0.33	3.00	-0.48

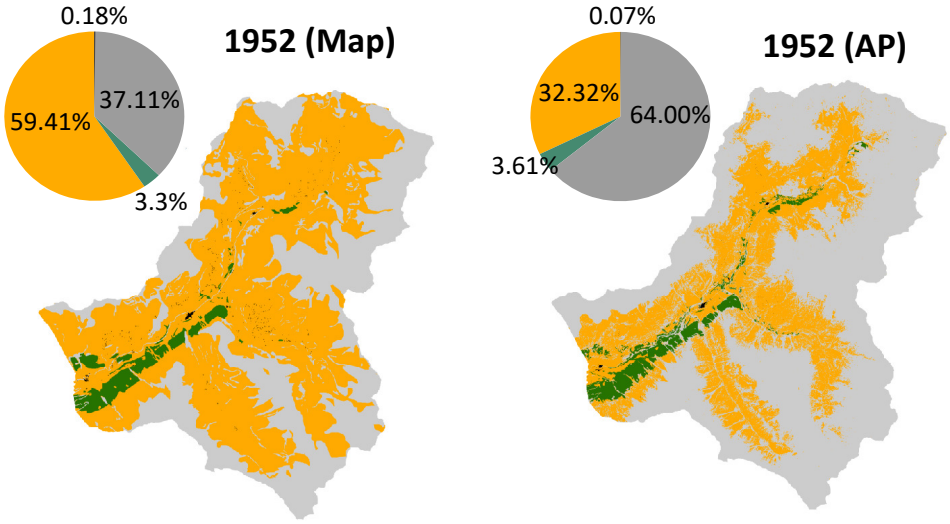

Figure 2.12: 1952 Land cover digitized from the historical map (MAP) and analyzed from aerial photography (AP).

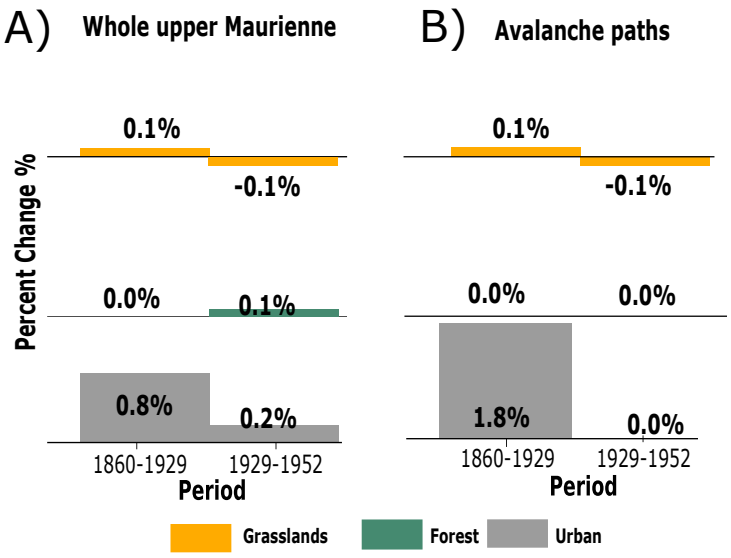

Figure 2.13: Yearly land cover changes for the first two periods obtained by direct comparison of the homogenized maps prior to correction: A) for the entire study area B) within the extension of EPA avalanche paths.

2.6.4 Appendix D: Highlights of land cover evolution for the three municipalities of the upper Maurienne

First we notice a continuous increase in forested areas for the three municipalities and within the extension of their avalanche paths, but with some local disparities. Overall, forest is most abundant in Lanslevillard followed by Bessans and Bonneval-Sur-Arc. The lower elevation of Lanslevillard creates a more favorable situation for reforestation in general. This, coupled

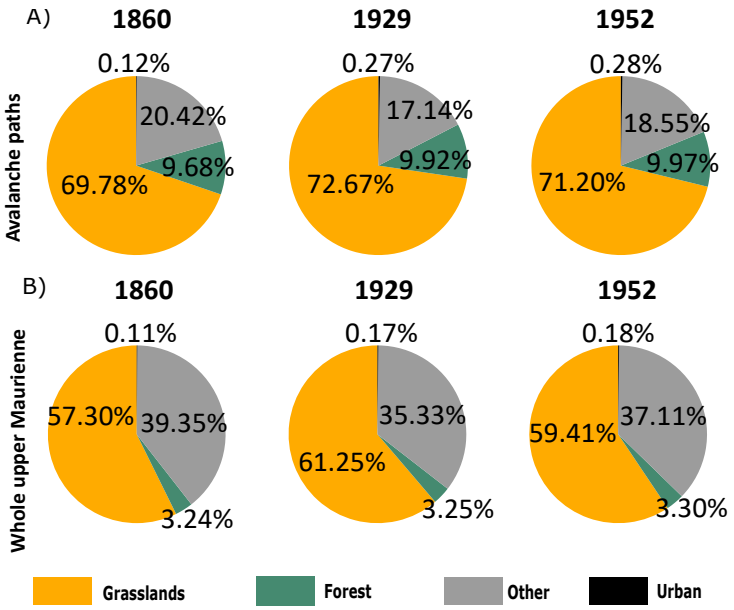

Figure 2.14: Land cover composition results obtained from the digitization of historical maps and prior to correction: A) within the extension of EPA avalanche paths, B) for the entire study area.

with the fact that initially (in 1860) Lansevillard was covered by more forests than the other municipalities, explains why Lanslevillard has the highest percentage of forests in 2017 (Figure 2.15,2.16).
Similarly, Lanslevillard is the municipality with the highest percentage of settlements (Figure 2.15). However, according the extension of avalanche paths, settlements in Bonneval-Sur-Arc are more exposed to snow avalanche (Figure 2.16). Bonneval-Sur-Arc is located in the narrowest part of the Maurienne valley. The Low availability of suitable areas for development combined with the high touristic demand for accommodations explains this large number of settlements in the vicinity of avalanche paths. The significant increase over the last part of the study period corresponds to the Tralenta area.
The evolution of grasslands is less homogeneous. We notice at first that after 1952 grasslands show a decreasing trend in the three municipalities (Figure 2.15). The pattern is more complex when we try to compare 1860 with 1952 especially in Lanslevillard. Pie charts show an increase from 26.43% to 41.10% in Lanslevillard from 1860 and 1952 (Figure 2.15,B). This increase is most probably an error inherited from the adjustment methodology used. Clearly, the creation of a comparable matrix was impossible for Lanslevillard. The same problem is found also when concentarting on the areas within the extension of avalanche paths (Figure 2.16,B). In these, we notice an increase in grasslands after 1952. It is possible that some bare lands (classified as rocks) were colonized by grass species in 2017 thus explaining the slight increase in grasslands.
Overall, what we can conclude is:

1. Forest fraction increased in the three municipalities, mostly as a result of the retraction of pastoral activities highlighted by the decrease in cattle, sheep and spearheads (Fig-

ure 2.10).

2. Urban settlements expanded, sometimes close to avalanche prone areas. This is mostly associated with the lack of suitable areas available to build and the increasing touristic pressure .

3. Most of the exposed buildings are located in the Tralenta area in Bonneval-Sur-Arc.

4. The majority of the forest is located in Lanslevillard and Bessans.

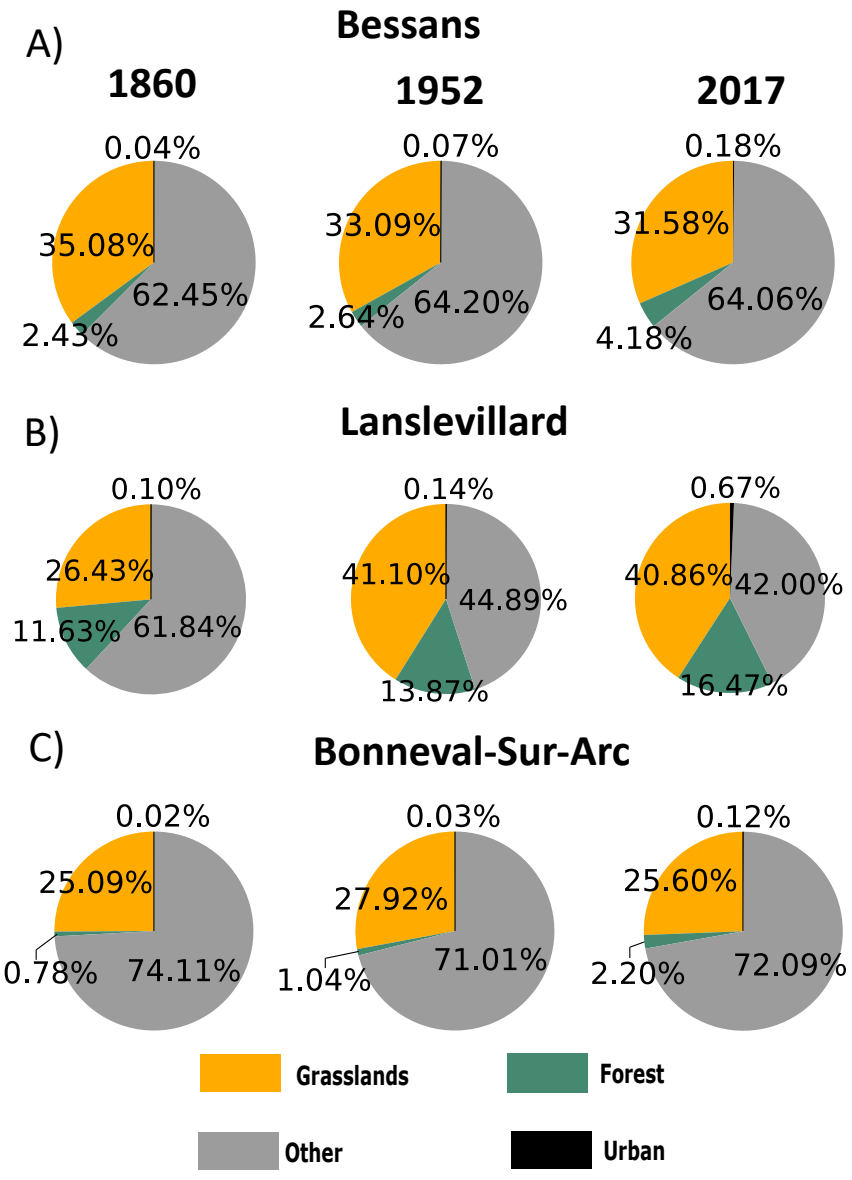

Figure 2.15: Land cover composition from 1860 to 2017 for A) Bessans B) Lanslevillard C) Bonneval-Sur-Arc.

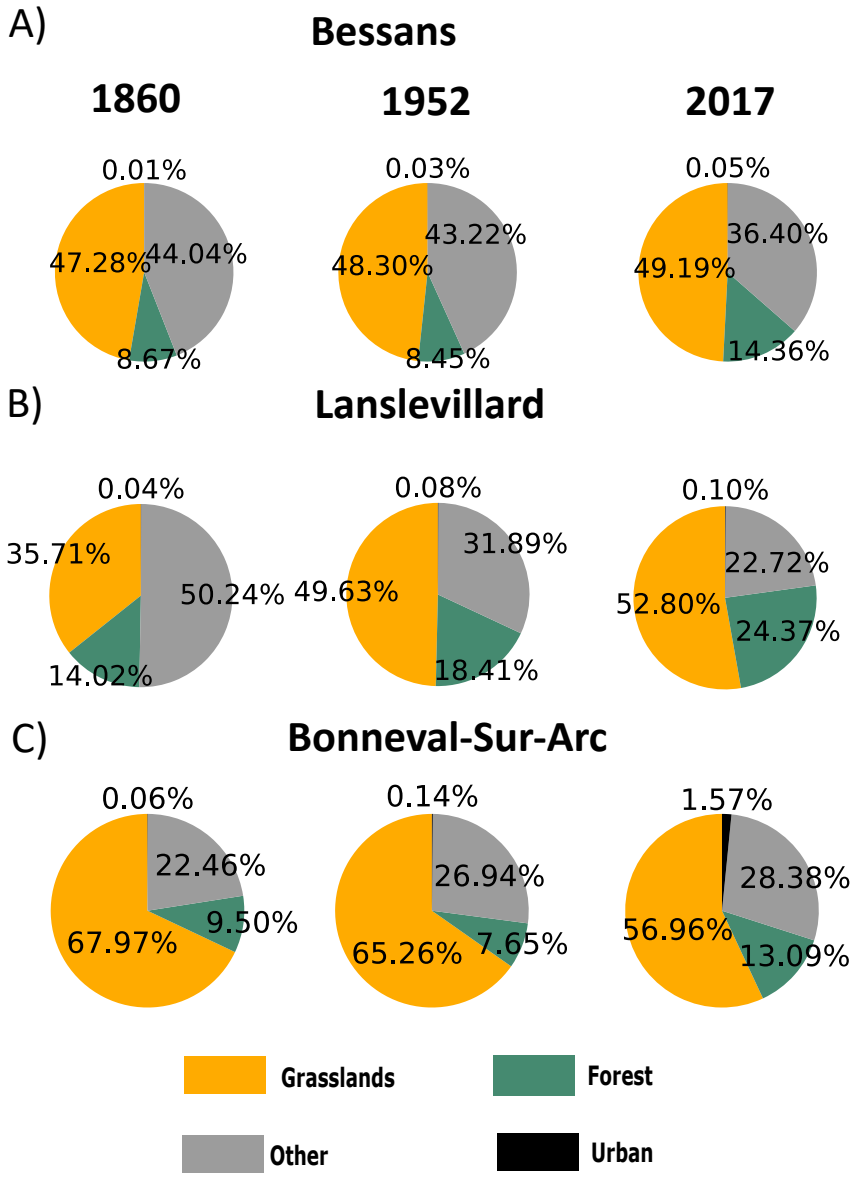

Figure 2.16: Land cover composition within the extension of EPA avalanche paths from 1860 to 2017 for A) Bessans B) Lanslevillard C) Bonneval-Sur-Arc.

2.6.5 Appendix E:Attitudinal distribution of forest pixels in 1860 and 1929.

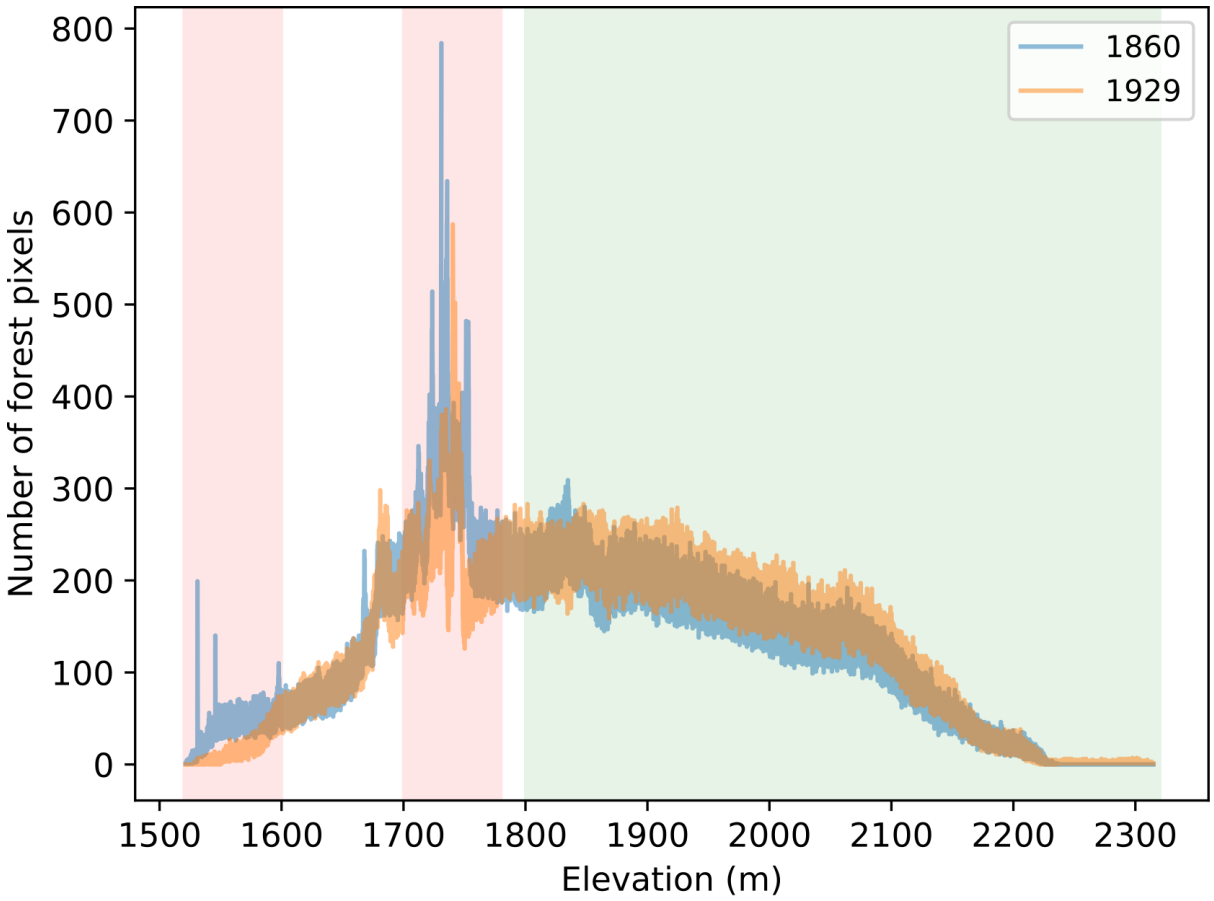

Figure 2.17: Attitudinal distribution of the forest pixels in 1860 and 1929. The zones highlighted in 'red' represent attitudinal zones where forest cover decreased from 1860 to 1929. Zones in 'green': altitude where forest cover increased (1860-1929).

Chapter 3

Spatio-temporal variability of avalanche risk inferred from land cover, climate and socio-environmental changes in three upper valleys of the French Alps

---

This chapter present the article "Spatio-temporal variability of avalanche risk inferred from land cover, climate and socio-environmental changes in three upper valleys of the French Alps" currently in revision in *Regional Environmental Change*.The following authors contributed to the work: Florie Giacona, Anne-Marie Granet-Abisset, Samuel Morin, Aurore Lavigne and Nicolas Eckert.

Abstract: Avalanche risk changes through time due to climate, landscape and social transformations. These drivers exhibit space-time variations as function of local peculiarities that may alter local avalanche risk trajectories. Here we use an integrative methodology to track the co-evolution of the socio-economic, land cover and climatic drivers of avalanche risk and its components in three upper basins of the French Alps: The Upper Maurienne valley, the Guil valley and the municipality of Valloire. The analysis, conducted from 1860 to 2017, focuses on avalanche-prone terrain defined as the maximal extension of avalanches potentially occurring on all paths of the French avalanche cadaster. Avalanche occurrence numbers have likely increased over the last decades, more strongly at higher elevation. By contrast, a quasi-complete afforestation of avalanche prone areas took place in the Guil valley, whereas, in the Upper Maurienne and Valloire, afforestation remains incomplete. This suggests a significant increase of protection from avalanches for people downslope due to the presence of forests in the Guil valley only. In parallel, recent expansion of urban areas in avalanche-prone terrain is prominent in the Upper Maurienne, and more modest and controlled in the Guil valley and in Valloire. Hence, overall, avalanche risk for buildings and their inhabitants may have slightly decreased over the study period in the Guil valley, remained rather stationary in Valloire and has arguably rather strongly increased in the Upper Maurienne. This demonstrates the crucial role of local dynamics in avalanche risk evolution. Our results help understanding the complex patterns resulting in mountain risks changing faster than ever and very differently from one location to another, which may, in turn, contribute to the development of improved disaster risk reduction strategies.

Keywords: Snow avalanches, spatio-temporal variability, diachronic analysis, qualitative Risk Modeling.

Contents

3.1 Introduction

The general concept of risk in the field of natural hazards acknowledges hazard, vulnerability and exposure as founding pillars (UN/ISDR, 2004). Through the years, different risk formulations branched out. While some chose to consider exposure to hazard as an independent determinant of risk (Field et al., 2012), others adhered to the original formulation and assessed vulnerability as a function of exposure (Turner et al., 2003; Weis et al., 2016). Despite these differences, all proposals recognize the spatio-temporal dynamics of risk. The latter is driven by changes in social and natural systems and the mechanisms underlying their interactions and dynamics (Field et al., 2012; Birkmann, 2013). Consequently, integrative methodologies to risk that breach barriers, and reinforce and facilitate knowledge transfer between social and natural sciences are essential to address the complexity of risk (Hock et al., 2020).

Snow avalanches are prevalent in mountain areas. The natural process is characterized by a rapid snow flow (Hopfinger, 1983; Schweizer et al., 2003). Snow avalanches can be naturally triggered by a combination of several factors such as weather conditions (temperature, snowfall, wind direction, etc.), slope, surface roughness (McClung and Schaerer, 2006; Bebi et al., 2009) and seismic activity (Podolskiy et al., 2010; Kargel et al., 2016). The sudden nature of the phenomenon and the complexity of the interaction between the triggering factors endanger people (i.e fatalities, injuries), block roads (Leone et al., 2014) and impact the environment all over mountain areas (e.g.Berlin et al. (2019); Höller (2007); Rapin and Ancey (2000)). Consequently, risk assessment integrating hazard, vulnerability and exposure emerged (Keylock et al., 1999; Keiler et al., 2006) as a tool for zoning in land use planning (Eckert et al., 2012, 2018) and as a facilitator for decision making including optimal design of defense structures (Bohnenblust and Troxler, 1987; Eckert et al., 2009; Favier et al., 2016).

Landscape alterations, especially reforestation, have been previously linked to agricultural abandonment (Barker, 1982; Gellrich et al., 2007; García-Llamas et al., 2018). In turn, land cover modification, particularly reforestation, is thought to impact avalanche activity (Bebi et al., 2009). Mid-20th century, the gradual shift from traditional farming towards service-based economies encouraged rural depopulation and amplified abandonment behaviors that started mid-19th century, notably in the European Alps (MacDonald et al., 2000; Statuto et al., 2017). Slowly, forests recolonized abandoned lands (Mather et al., 1999; Bebi et al., 2009). They played a crucial role in decreasing snow avalanche hazard (Salm, 1978; Viglietti et al., 2010; Teich et al., 2012b) and related damages by decelerating the flow (Malanson and Butler, 1992; Anderson and McClung, 2012; Takeuchi et al., 2018) and inhibiting avalanche initiation. For instance, García-Hernández et al. (2017) demonstrated causality between reforestation following land abandonment and decreased snow avalanche damage in the Asturian massif, Spain. Similarly, Mainieri et al. (2020) showed that progressive colonization of avalanche paths reduced snow avalanche initiation in some areas of the French Alps.

Human influence also extends to the climate system (IPCC, 2014). The consequent modification of snow cover characteristics and weather variables impacts avalanche magnitude and frequency (Castebrunet et al., 2012; Eckert et al., 2010c, 2013; Castebrunet et al., 2014; Stoffel and Corona, 2018; Naaim et al., 2013; Steinkogler et al., 2014) and increases the proportion of wet snow avalanches (Pielmeier et al., 2013; Naaim et al., 2016). In details, studies suggest that no major shift in avalanche occurrence numbers due to climate change has occurred so far in the

European Alps (Laternser and Schneebeli, 2002; Eckert et al., 2010d). However, Lavigne et al. (2015) explains that this apparent stagnation results from combined decrease at low elevations due to scarcer snow conditions versus increase at high elevations. This confirms the spatio-temporal variability of avalanche hazard driven by spatio-temporal snow and weather patterns (Laternser and Schneebeli, 2002; Durand et al., 2009a,b; Schöner et al., 2019) interacting with elevation gradients (Durand et al., 2009a,b).

In addition to hazard, exposure to snow avalanches is also subject to spatio-temporal variations. Only few studies focused on the spatio-temporal evolution of avalanche risk driven by exposure to snow avalanches e.g. in Davos (Switzerland), (Fuchs et al., 2005; Fuchs and Keiler, 2008). They mostly suggest an increase in the number of exposed elements, and a decrease in risk due to the presence of avalanche protection measures with the exception of Fuchs et al. (2004) who demonstrated an increase in avalanche risk in Galtür (Austria), particularly in residential buildings.

All in all, by contrast to the need of integrated studies addressing the different components of avalanche risk changes altogether, research has to date not considered how the simultaneous evolution of socio-economic factors, the environmental system and climate drive avalanche hazard, vulnerability and ultimately avalanche risk on a long time frame. Zgheib et al. (2020) proposed a comprehensive methodology that combines land cover change detection using advanced image processing techniques, geohistorical investigations and qualitative modeling of risk changes to asses the spatio-temporal evolution of avalanche risk and its socio-economic and environmental drivers. Here, we assess the evolution of the socio-economic and environmental system and introduce the analysis of climate as an additional driver of avalanche hazard to compare the spatio-temporal evolution of avalanche risk in three upper valleys of the French Alps : the Upper Maurienne, the Guil valley and Valloire (Figure 3.1). The ultimate objective of our study is to document the spatio-temporal variability of avalanche risk and relate it to local variations in hazard, vulnerability and their socio-economic, environmental and climatic drivers.

In details, our study : i) analyzes the co-evolution of the socio-economic and environmental system in the Upper Maurienne valley, Valloire and Guil valley from 1860 to 2017 using a diachronic analysis of historical maps and aerial photographs; ii) asses the spatio-temporel co-evolution of climate variables and avalanche hazard; iii) assess how changes in vegetation cover could have influenced the variation of hazard over space and time; iv) examine the spatio-temporal variability of exposed settlements to snow avalanches; v) and finally, infer and explain the spatio-temporal evolution of avalanche risk to settlements in the study areas since 1860.

3.2 Material and Methods

3.2.1 Study areas

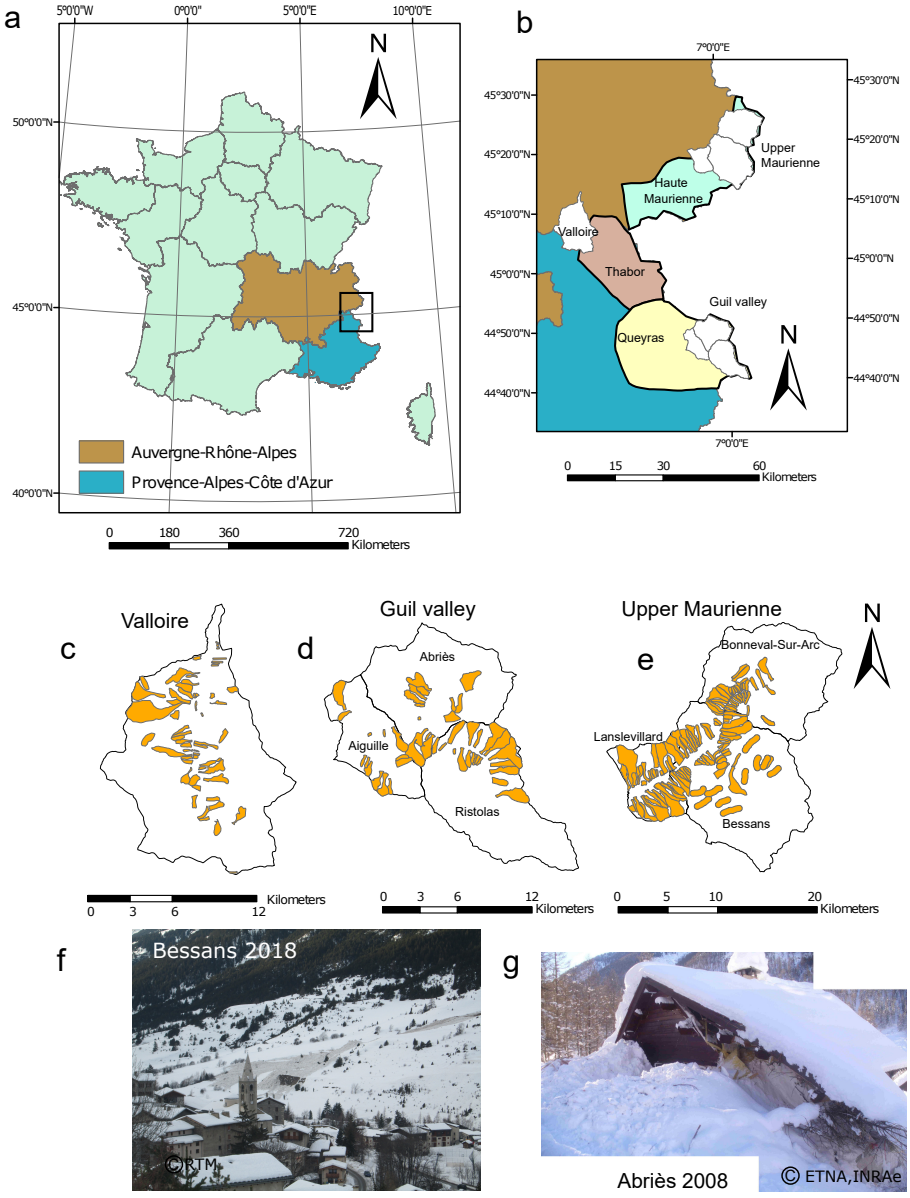

Figure 3.1: a,b) Location of the study areas within the French Alps, Extention of avalanche paths from the EPA record in c) Valloire, d) Guil valley, e) Upper Maurienne, f) Avalanche in Bessans (Upper Maurienne) in December 2018 and g) House destroyed by an avalanche in Abriès (Guil valley) in 2008.

To analyse the spatio-temporal evolution of avalanche risk within the French Alps, we focus on three archetypal upper valleys: three municipalities of the Guil valley, three municipalities

of the Upper Maurienne valley and the municipality of Valloire. The three municipalities of the Guil valley are part of the Queyras massif located in the Southern French Alps, Provence-Alpes-Côtes d'Azur region (Figure 3.1 a, b, d). Abriès, Ristolas and Aiguilles are positioned between 1400 and 3300 m a.s.l (Table 3.1) and adjacent to the Italian border. Northwest of the Guil valley is Valloire, a municipality of the middle mountains of the Maurienne valley in Auvergne-Rhône-Alpes region (Figure 3.1 b, c). It spans an altitudinal range between 685 and 3500 a.s.l (Table 3.1). Finally, the three municipalities of the Upper Maurienne valley, Lanslevillard, Bessans and Bonneval-Sur-Arc are part of the highest mountains of the Maurienne valley in the Auvergne-Rhône-Alpes region, Northern French Alps (Figure 3.1 a, b, e). They are positioned along the French-Italian borders between 1500 and 3700 a.s.l (Table 3.1). In the Upper Maurienne, avalanche paths are located at higher mean elevation (2700 m a.s.l.) and include steeper slopes (31.8°) compared to Valloire (2100 m a.s.l. and 30.7°, respectively) and the Guil valley (2100 m a.s.l.and 30.6°, respectively) (Table 3.1). Due to the previously mentioned topographic characteristics and favorable climate (See Section 3.2.3), the three study areas witness significant avalanche activity (Table 3.1).

Table 3.1: Topography, avalanche activity and temperature in the three study areas : the Upper Maurienne, the Guil valley and Valloire. Mean avalanche release elevation is assessed in each study area from the corresponding EPA record. SAFRAN temperature data corresponds to the mean of the Nov-March reanalysis over the 1958-2019 period.

	Upper Maurienne	Guil valley	Valloire
Area (km^2)	309	202	138
Max. elevation (m)	3735	3300	3500
Min. elevation (m)	1431	1400	685
Mean elevation (m)	2630	2258	2245
Number of avalanche paths in the EPA record	129	45	57
% Area covered by avalanche paths from the EPA	24% (74 km^2)	16% (32 km^2)	13% (18 km^2)
Mean elevation of EPA paths (m)	2215	2160	1930
Mean slope of EPA paths (°)	31.8	30.6	30.7
Number of avalanche events since 1900 in the EPA record	3275	600	1600
Mean avalanche release elevation (m)	2500	2280	2010
SAFRAN average winter temperature at mean elevation of EPA paths (°C)	-6.21	-2.90	-3.22

3.2.2 Avalanche data

The Avalanche Permanent Survey (referred to as EPA: Enquête Permanante des Avalanches (Bourova et al., 2016)) is the most extensive avalanche survey in France, and among the most comprehensive worldwide. Avalanche series for our study areas date back to c. 1900, with several thousands of avalanche events recorded in total in each of our three study areas. A direct analysis of the evolution of avalanche activity using EPA chronologies introduces strong bias related to sources (Giacona et al., 2017) due to discrepancies in data collection protocols and criteria. Therefore, to investigate the evolution of avalanche hazard, we refer to the study of Lavigne et al. (2015) instead of to the raw data. The authors used advanced statistical methods to depict spatio-temporal avalanche evolution trends from 1946 to 2009 at the level of each municipality of the French Alps. Parameters of the statistical model are enhanced

and validated by adding expert contribution to the modelling. Also, this approach considers missing data within the series using statistical Bayesian techniques. This leads model-based homogenized series reflecting the evolution of natural avalanche activity as much as possible, but where a bias due to lower avalanche records as one goes further back in the past still exists.

3.2.3 Snow and climate data

We used daily reconstruction of weather and snow conditions (Vernay et al., 2019) reanalysed by the SAFRAN (Durand et al., 1999)-Crocus (Brun et al., 1989) model chain. The reanalysis was conducted at the massif scale. For our study, data were collected for the Upper Maurienne Massif, Queyras massif (Guil valley) and the Thabor massif (Valloire) from 1958 to 2019 at the elevation correspoding to the mean elevation of avalanche paths (Table 3.1). We selected for our analysis : i) SAFRAN mean winter temperature (°C) (Figure 3.2a); ii) SAFRAN winter cumulated snowfall (kg m^{-2}) (Figure 3.2b) and iii) Crocus mean winter snow depth (m) (Figure 3.2c). Here, by winter, we consider the months from November to March. Overall, all three areas are characterized by a cold climate. In winter, temperature in though lower at the mean elevation of avalanche paths in the Upper Maurienne compared to the Guil valley and Valloire (Table 3.1), which is primarily due to the significant difference in elevation between avalanche prone areas.

3.2.4 Socio-economic data

For the three study areas, population data (1860-2016) were obtained from the National Institute of Statistics and Economic Studies (INSEE) and the School of Advanced Studies in the Social Sciences (EHESS,http://cassini.ehess.fr). Livestock inventories were obtained from published data (Drogue, 1950; Rambaud and Vincienne, 1964; Jail, 1969; Digard, 1974; Jail, 1977; Perret et al., 1992; Vincent, 2007), the agricultural census published by the Ministry of Food and Agriculture ('recensement agricole'), and the pastoral inquiries ('enquête pastorale', http://enquete-pastorale.irstea.fr). All these data were crossed and compared with land cover data to infer the evolution of the socio-economic and environmental system.

3.2.5 Land cover change analysis

We used the methodology of Zgheib et al. (2020) to assess land cover changes and optimize intercomparison between historical maps and aerial photographs. To assess land cover change in avalanche hazard areas, a 50 m buffer was created around each of the reconstructed EPA avalanche paths. Long-range evolution of land cover was assessed from a series of maps and aerial photographs. Historical maps were provided by the French National Geographic Institut (IGN). The maps used are the *Etat-Major* maps of 1855-1860 and the maps of 1952-1958. Pre-processed aerial photos for 2017 and 1952 were obtained from IGN. The 2017 image is a true-color aerial photos while the 1948-1952 photos are in black and white. Additional information on the collected maps and aerial photos for each zone can be found in Table 3.2 (Appendix A). For each study area, two series of maps were created. The first set is the result of manual digitization of historical maps. The second set of land cover maps is the result of segmentation and interpretation of the aerial photographs using a combination of spectral information, shape

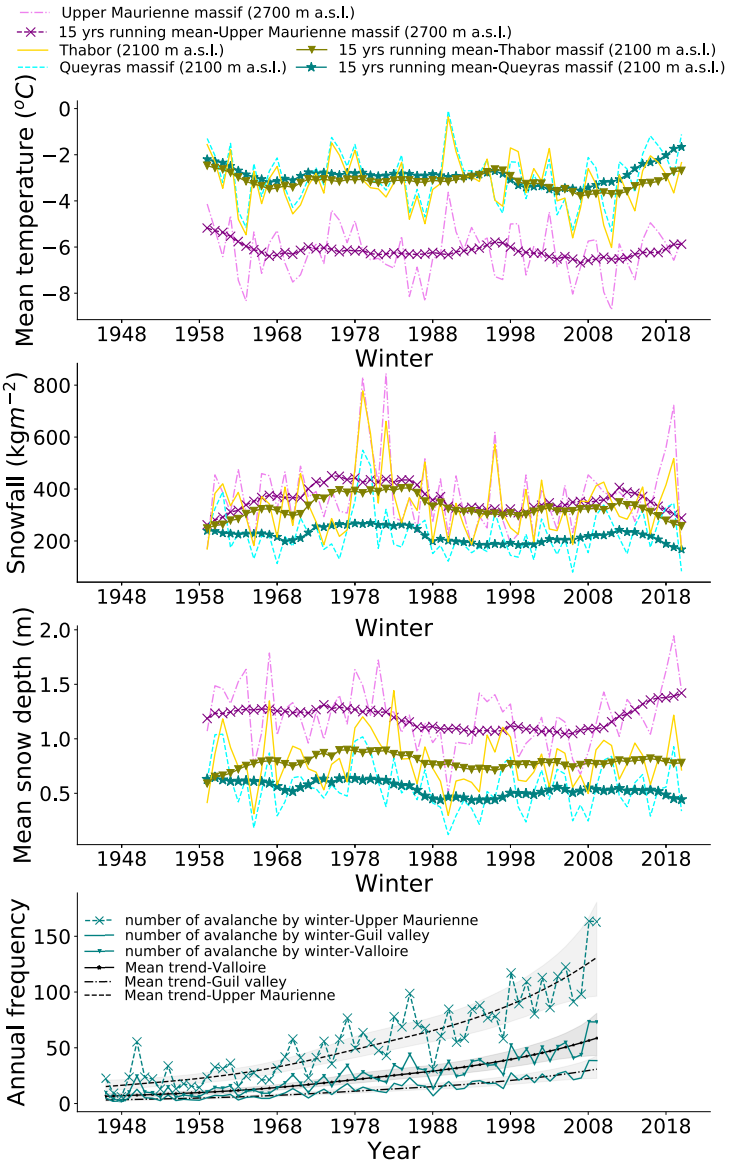

Figure 3.2: (a) SAFRAN mean winter (Nov-March) temperature. (b) SAFRAN winter cumulated snowfall (c) Crocus mean winter snow depth. (d) Mean avalanche number per winter and path from Lavigne et al. (2015). ▪ 95% credible interval of the trend. In a-c, climate and snow conditions are those provided by the massif scale reanalysis at the mean elevation of avalanche paths analysed from the EPA record : the Haute Maurienne massif at 2700 m a.s.l. for the Upper Maurienne study area, the Queyras massif at 2100 m a.s.l. for the Guil valley and the Thabor massif at 2100 m a.s.l. for Valloire.

properties and a user defined scale parameter. The primary land cover classes recognized are grasslands, urban, forest and other.

Once land cover maps are created, the next step is homogenization and comparability analysis. Spatial homogenization of the maps digitized from the historical maps was performed

using the methodology suggested by Petit and Lambin (2001). The main idea is to create a set of comparable maps, to reduce errors on change detection rising from thematic and spatial discrepancies (Petit and Lambin, 2001, 2002). Finally, to ensure the proper comparison between the landscape composition matrices derived from the historical maps and aerial photography the pivot year (common year between the two sets of maps in this case it is the 1950's) was used to i) quantify the bias resulting from the maps and, once assessed, ii) to have a complete homogenized series of comparable landscape matrices (Appendix B).

3.3 Results and discussion

3.3.1 Spatio-temporal variability of avalanche hazard

3.3.1.1 Impact of climate conditions on the spatio-temporal evolution of avalanche hazard

We inferred the co-evolution of climate variables and avalanche hazard using SAFRAN-Crocus reconstructed daily meteorological and snow conditions (Durand et al., 2009a,b) and the Lavigne et al. (2015) avalanche occurrence evolution trends. The latter shows an increasing number of avalanches between 1946 and 2009 in the three study areas (Figure 3.2d). The quality of the data underlying the approach still impacts the results (Lavigne et al., 2015), so that these trends need to be interpreted with caution. Notably, the increase may be overestimated with regards to reality. However, it is not just an artefact of the data as it relates to i) climate fluctuations at decennial time scale (e.g. low temperatures in the mid-80's, Figure 3.2a) and ii) a systematic increase with warming of extreme precipitation in a context where winter temperatures are still cold enough for these to fall in the form of snow (López-Moreno et al., 2011; Beniston et al., 2018; O'Gorman, 2014; Ballesteros-Cánovas et al., 2018). In line with this interpretation, a recent study by Faranda (2019) shows an increase in winter atmospheric circulation above the Mediterranean (1979-2018). In turn, such flows can evolve into easterly returns (Eckert et al., 2010b), which are responsible of heavy snowfall in the eastern part of the French Alps where our three study areas are located and where, as a consequence, avalanche activity is arguably increasing.

Despite their limitations, Lavigne et al. (2015) results show that mean avalanche activity and increasing rates are clearly different among the study areas. The higher mean activity in the Upper Maurienne can be explained by the position of avalanche paths at higher mean elevations (Table 3.1) leading to higher inter-annual variability of snow depth (Figure 3.2c) and snowfall amounts (Figure 3.2b) and to lower inter-annual mean temperatures (Figure 3.2a) compared with the two other areas. By contrast, the lower mean snowfall and higher mean temperature in the Guil valley explains the much lower avalanche activity. In addition to elevation differences, the more sheltered location of the Guil valley far from the atmospheric westerly flows that determine the climate in the French Alps (Durand et al., 2009b) also plays a role. Eventually, the difference in forest cover may also contribute since studies have shown that temperate forests have a moderate warming effect in winter (Li et al., 2015). This may partially explain why temperature/snowfall in the Guil valley (more heavily forested) are higher/lower than in Valloire at the same 2100 m.asl elevation. Anyhow, these differences in topography, location

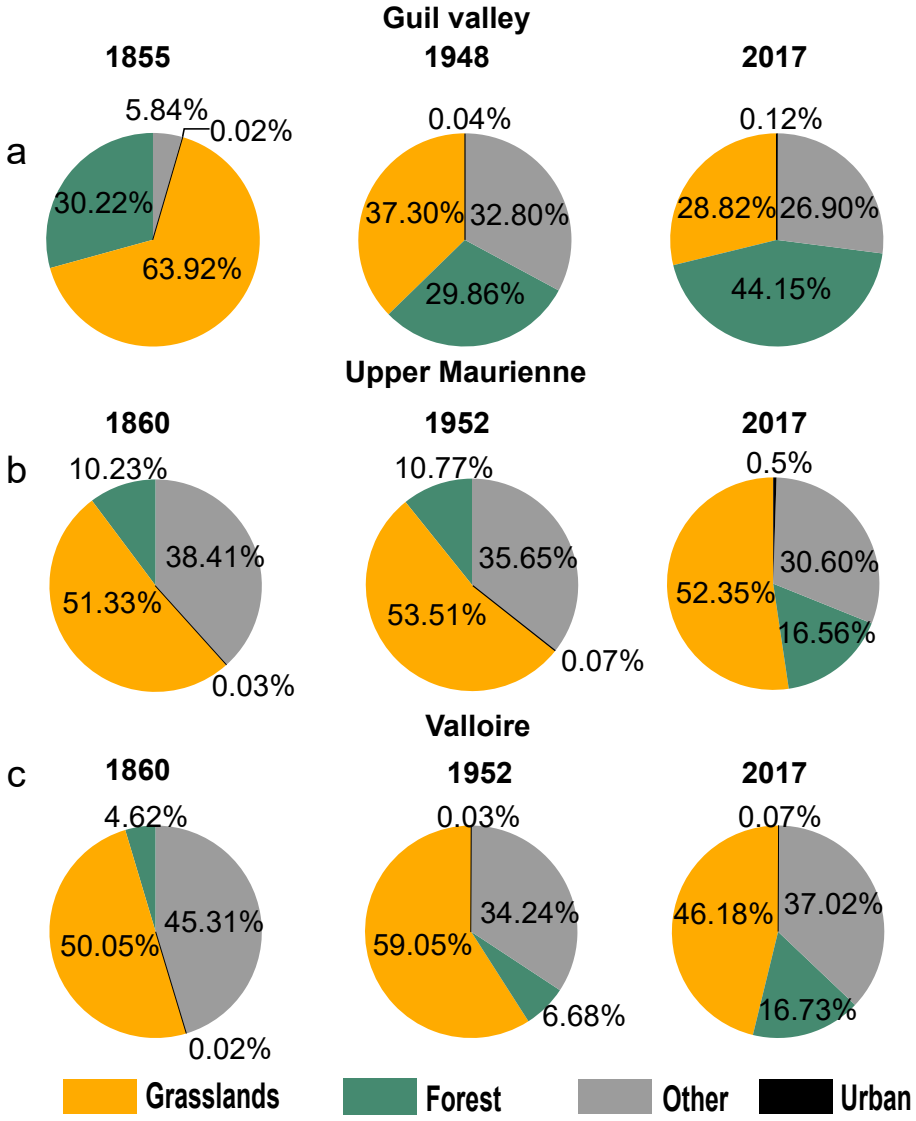

Figure 3.3: Diachronic land cover analysis within the extension of avalanche paths from the EPA record in : a) the Guil valley between 1855 and 2017 b) the Upper Maurienne between 1860 and 2017 and c) Valloire between 1860 and 2017. Pie charts represent the percent area composition for the selected zones.

and potentially forest cover also explain the strong differences in increasing rates in our three study areas: in Upper Maurienne, where winter temperatures are colder, the systematic increase in extreme precipitation arguably drives a much stronger increase in avalanche activity than in the two other study areas where the increase in winter precipitation is somewhat compensated by warmer temperatures above the 0°C freezing level.

3.3.1.2 Impact of reforestation on the spatio-temporal evolution of avalanche hazard

Land cover change analysis shows continuous reforestation of avalanche prone terrain in the three study areas (Fig. 3.3). In the Guil valley, the percentage of forest increased from 30% in 1855 to 44.15% in 2017 (Fig. 3.3a). In the Upper Maurienne and Valloire, forests percentages increased by 6% and 10% (measured as a percentage of area within the extension of avalanche paths) respectively between 1860 and 2017 (Fig. 3.3b,c). Cross analysis of population and pastoral data (Fig. 3.5) shows a decrease in population and cattle in all three study areas prior to 1950. This implies a heavy depopulation and abandonment phase (Rambaud and Vincienne, 1964; Jail, 1977; Granet-Abisset, 1991) that began during the early nineteenth century (Mather et al., 1999). The development of the forest policy in 1860 also played an important role in forest management (Brugnot, 2002).

Similarly, the shift towards intensive agro-pastoral practices, encouraged abandonment of high slopes towards intensive grazing on lower gentler slopes (Mather and Needle, 1998). This led to forest encroachment on higher altitude in the three study areas. Indeed, results highlight a slight increase in the mean forest elevation (Fig. 3.4c). In the Upper Maurienne, the mean forest elevation increased from 1890 m a.s.l. in 1860 to 1920 m a.s.l. in 2017 (Fig. 3.4c). Likewise, in the Guil valley, the mean forest elevation increased from 2030 m.asl in 1860 to 2050 m a.s.l. in 2017 (Fig. 3.4c). In Valloire the mean forest elevation increased from 1675 m a.s.l. in 1860 to 1687 m a.s.l. in 2017 (Fig. 3.4c). Cross-analysis of the aforementioned results with stocking rates (Fig. 3.5) shows an overall decrease in sheep grazing mostly at high elevations and on steep slopes since 1860 (Fig. 3.5), thus validating the impact of abandonment, depopulation and grazing intensification on attitudinal distribution of forest parcels. However, forest encroachment in the Guil valley, Valloire and the Upper Maurienne remains greater at lower elevations and less intense at progressively higher elevations (Fig. 3.4c). This is potentially due to less favorable soil and climate conditions in comparison with lower elevations (Körner, 2007).

Hence, despite all three areas have undergone agricultural abandonment and depopulation, spatial variability of forest evolution trends is clear. We believe that differences in reforestation trends between the three areas is governed by the complex interaction between topographic factors and socio-economic changes. Considering similar land cover and depopulation pattern, a possible explanation for the larger evolution of forest parcels in the Guil valley is the presence of large parcels in 1860. Indeed, studies in the central Pyrenees (Spain) (Gartzia et al., 2014) and in the Apennines (Italy) (Malandra et al., 2019) showed that recolonization and the in-filling of forest gaps and open areas is most prominent near pre-existing forests due to the influence of seed proximity on forest regeneration. Nevertheless, active reforestation work in the Guil valley cannot be excluded, especially since 28% of the reforestation of the Haute Alpes department (includes Queyras massif) between 1800 and 1973 is a result of active afforestation efforts (Bourcet, 1984).

We then examined the link between the evolution of the socio-economic and environmental systems since 1860 and the spatio-temporal evolution of snow avalanche activity. In general, the Guil valley is the most forested zone since 1855, with 20% of its paths being completely reforested in 2017 (Fig. 3.4a). In addition, the mean avalanche release elevation (2282 m a.s.l,Table 3.1)

is slightly above the mean forest elevation (2000 m a.s.l., Fig. 3.4c). Interestingly, the Guil valley also has the slowest increase rate in snow avalanche numbers since 1946 (Fig. 3.2d). This emphasizes the role of forests in preventing avalanche initiation by stabilizing the snow cover in release areas (Salm, 1978; Teich et al., 2012a). Indeed, a recent small-scale study conducted by Mainieri et al. (2020) in the Queyras, confirms a decrease in snow avalanche activity associated with the progressive afforestation of avalanche release areas. Alternatively, in the Upper Maurienne, from 1860 to 2017, only 3% of the paths were covered by more than 75% of forests whereas the majority remained under 25% (Fig. 3.4a). Similarly, in Valloire, prior to 2017, no avalanche path was covered by more than 75% of forests (Fig. 3.4a). In fact, in 1860, the forest fraction in the majority of the forested paths was less than 25%. In 2017, only 4% of the path were almost completely reforested whereas the majority stayed below 25% (Fig. 3.4a). All of this indicates that no further complete or quasi-complete (re)-forestation occurred in the Upper Maurienne and Valloire. As a consequence, reforestation had arguably little impact on avalanche hazard in these areas since the majority of release areas are far above the forested part of the path (if any). This is a common issue in Alpine environments where the majority of avalanche release areas are located above the treeline (Giacona et al., 2018).

In addition to reducing avalanche release susceptibility, forests can also decelerate flowing avalanches (Malanson and Butler, 1992; Anderson and McClung, 2012) but this is unlikely in the Upper Maurienne and Valloire, since, during the entire study period, the forest fraction in the majority of avalanche paths stayed below 25%. Alternatively, avalanche deceleration in the Guil valley is a possibility with 50% of the paths forested by more than their half (Fig. 3.4a). Without explicit modeling of avalanche dynamics, avalanche deceleration and, hence, reduction of damage potential is hard to fully quantify, especially since there is no consensus in the snow avalanche literature regarding the protection capacity of forests against large, fully developed, avalanche flows (Bartelt and Stöckli, 2001; Takeuchi et al., 2018).

All in all, our results show a quasi-complete afforestation of avalanche prone terrain in the Guil valley, which suggests a significant increase of protection from avalanches for people downslope that more than compensates the arguably weak increase of avalanche occurrence numbers in this area. By contrast, in the Upper Maurienne and Valloire, afforestation remains incomplete. Likely, in Valloire, avalanche hazard has to the minimum remained stationary for people downslope with an increasing trend in avalanche occurrence numbers stronger than in the Guil valley but partially compensated by an increase of the forest protective effect. Eventually, in Upper Maurienne, afforestation was clearly not sufficient to compensate the strong increase in avalanche occurrence numbers, so that avalanche hazard downslope has likely notably increased (Figure 3.6).

3.3.2 Spatio-temporal evolution of exposure to snow avalanches

We studied spatio-temporal changes in the exposure of buildings to avalanche hazard from 1860 to 2017 and their relation to the socio-economic context. Overall, the urban area in avalanche paths roughly doubled in all three study areas between 1860 and 1950 (Fig. 3.3). Interestingly, the majority of the expansion in the 1950s occurred below 1600 m a.s.l. in the Guil valley, whereas, at the same time, in Valloire, settlements located above 2100 m a.s.l. disappeared and the density of those above 1800 m a.s.l. decreased (Fig. 3.4d). Similar changes

occurred in the Upper Maurienne, where the density of settlements above 2000 m a.s.l. decreased (Fig. 3.4d). These trends are most likely linked to agricultural abandonment, depopulation and agricultural intensification. As stated in Section 3.3.1.2, agro-pastoral practices at high altitudes were abandoned and replaced by intensive activity at gentler, more accessible slopes. Hence, densification of settlements at lower elevation and the diminishment of the use of higher altitude buildings between 1860 and 1950 explains the decrease in mean urban elevation. From Fig. 3.3, it can be seen that by far the most prominent expansion of urban areas in avalanche paths occurred between 1952 and 2017 in the Upper Maurienne (from 0.07% in 1952 to 0.5% in 2017) followed by Guil valley (from 0.04% in 1948 to 0.12% in 2017) and Valloire (from 0.03% in 1952 to 0.07% in 2017). The rise in settlements may be explained by repopulation and the development of tourism. Indeed, during this period, the economic attractiveness of touristic sector appealed to several investors, who financed the construction of large building complex, hotels and infrastructures intended for tourists in the Upper Maurienne (Megerle, 2018), the Guil valley (Barbier, 1989) and Valloire (Arcuset, 2009). The impact of the repopulation is reflected in the increase of primary residences after 1968 (INSEE, 2016), as a result of the attractiveness and availability of employment in the tertiary sector (CCE, 1975).

In more details, despite their geographical proximity and overall similar evolution trends, exposure of settlement to snow avalanches present further disparities between our three study linked to socio-economic and geographical differences. In the Upper Maurienne, the narrow valley and the high number of avalanche paths (Table 3.1) reduces the availability of suitable zones for development. Therefore, as the demand for accommodation increased, expansion occurred in avalanche prone terrain, thus increasing exposure of settlements to snow avalanches. This is consistent with previous studies published in high mountains in general (Hock et al., 2020) and the European Alps in particular (Fuchs et al., 2005; Keiler et al., 2006; Fuchs and Keiler, 2008). By contrast, in the Guil valley, the evolution of settlements in avalanche prone terrain (Fig. 3.3, Fig. 3.4a) and within the entire Guil valley (Fig. 3.5), is more limited. This is potentially a result of a later kickoff of winter tourism (in 1930) (CCE, 1975; Vandenhove, 1984) combined with a series of winter without snow (e.g. winter 1963-64 and 1988-90 (Barbier, 1989; Gauchon, 2009)) that hindered winter tourism. Finally, in Valloire, exposure to snow avalanches is quasi-constant (Fig. 3.3). This finding was unexpected, since tourism developed fast after the creation of Valloire station in 1934 (Prieur, 1989), and the number of buildings increased approximately as much as in the Upper Maurienne between 1968 and 2016 (Fig. 3.5). It can be explained by a more open landscape with larger flat areas in Valloire w.r.t. the Maurienne valley. This, coupled with a lower number of avalanche paths (Table 3.1) permitted the development of the Valloire settlements primarily outside from avalanche prone terrain.

3.3.3 Spatio-temporal variability of avalanche risk

Eventually, evolution of avalanche risk results from combined changes in hazard and vulnerability (exposure included within) and is driven by intertwined shifts in the socio-economic, environmental and climatic contexts. Over the study period, avalanche risk increased the most in Upper Maurienne since the 1950s, as more and more accommodations became exposed to an increasingly strong hazard. Before 1950, exposure was quite moderate but hazard was already strong due to favourable topographic and climatic coditions (Figure 3.6). By contrast, hazard

in the Guil valley arguably slightly decreased due to the strong increase in forest protection in and around avalanche paths. This, combined with the more limited development of settlements within avalanche prone terrain from 1860 to 2017, means that avalanche risk in the Guil valley may have slightly decreased, with strong local variations from one avalanche path to another as function of local reforestation and urbanisation trends (Figure 3.6). Finally, in Valloire, the likely slight increase in snow avalanche hazard downslope had arguably little consequences, since no noticeable increase in exposed elements occurred at the same time. Hence, avalanche risk from 1860 to 2017 may have remained more or less stationary with no particular decreasing/increasing trend (Figure 3.6).

One may argue that construction of technical protection measures such as dams reduce vulnerability and/or exposure of buildings (Fuchs et al., 2017) but such structures may fail against extreme avalanches such as those that occurred during winter 1998/1999 (Rapin and Ancey, 2000). For this reason, defense structures are not considered in land use planning in France (DGPR, 2015). However, it is clear that, locally, their existence may decrease the risk. For instance, recent construction of new defense structures may have partially compensated the increase in exposure of new buildings, notably in the Upper Maurienne (Zgheib et al., 2020). We did not include this effect in our work because it would have implied refined small-scale modeling of defense structure impact on avalanche dynamics, a computational burden incompatible with our our large-scale study. However, given the rather low number of defence structures in our study areas, we believe that this limitation is of no effect on the first-order trends we highlight.

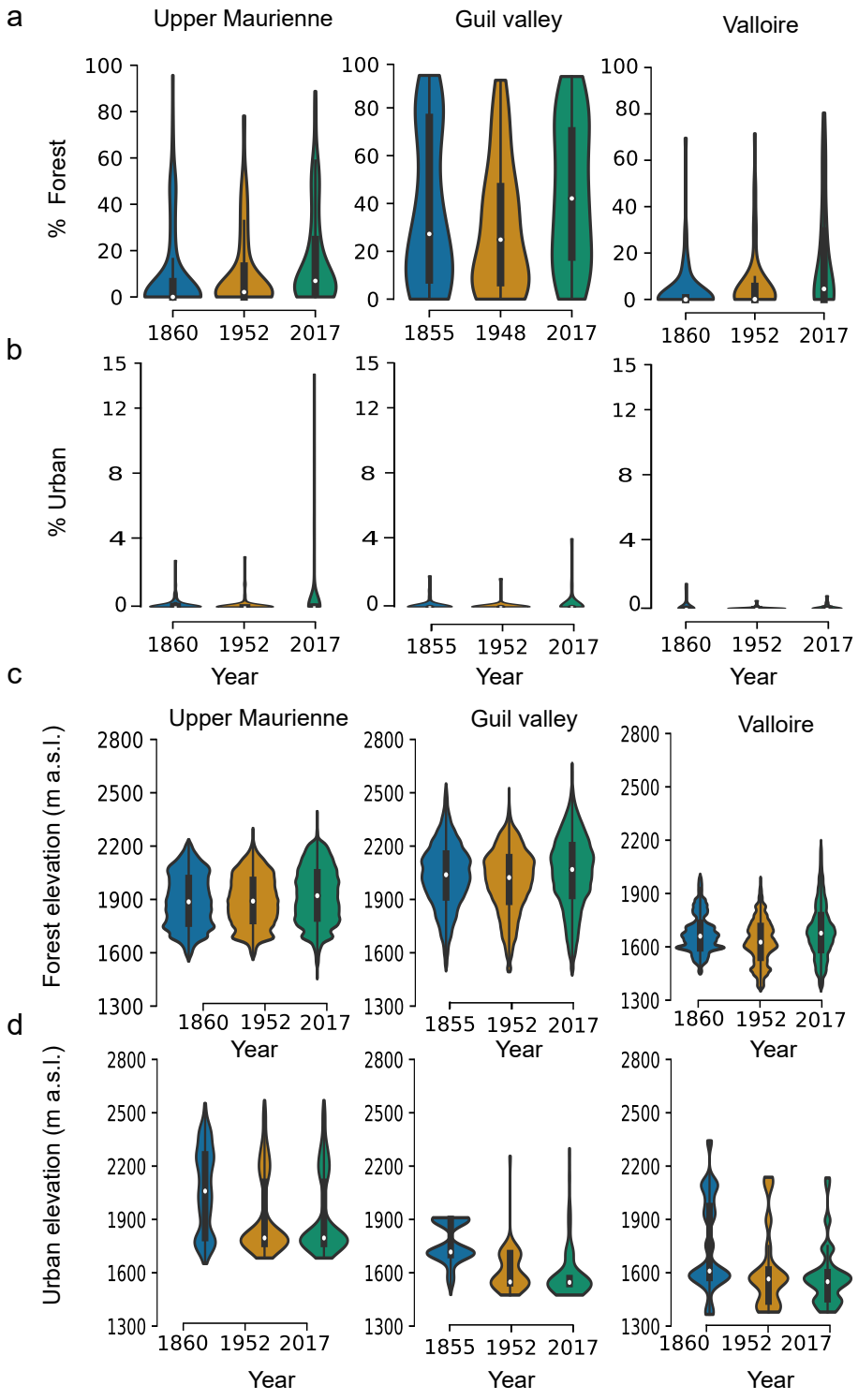

Figure 3.4: Violin plots showing the kernel smoothed probability distribution of the data in the three study areas at the considered dates. A box plot is included within each violin plot, providing the mean, the interquartile range and the 95% confidence interval for the data. The following parameters, collected within the extension of avalanche paths from the EPA record, are represented: a) percentage of forests b) percentage of urban areas c) elevation of forest pixels d) elevation of urban pixels.

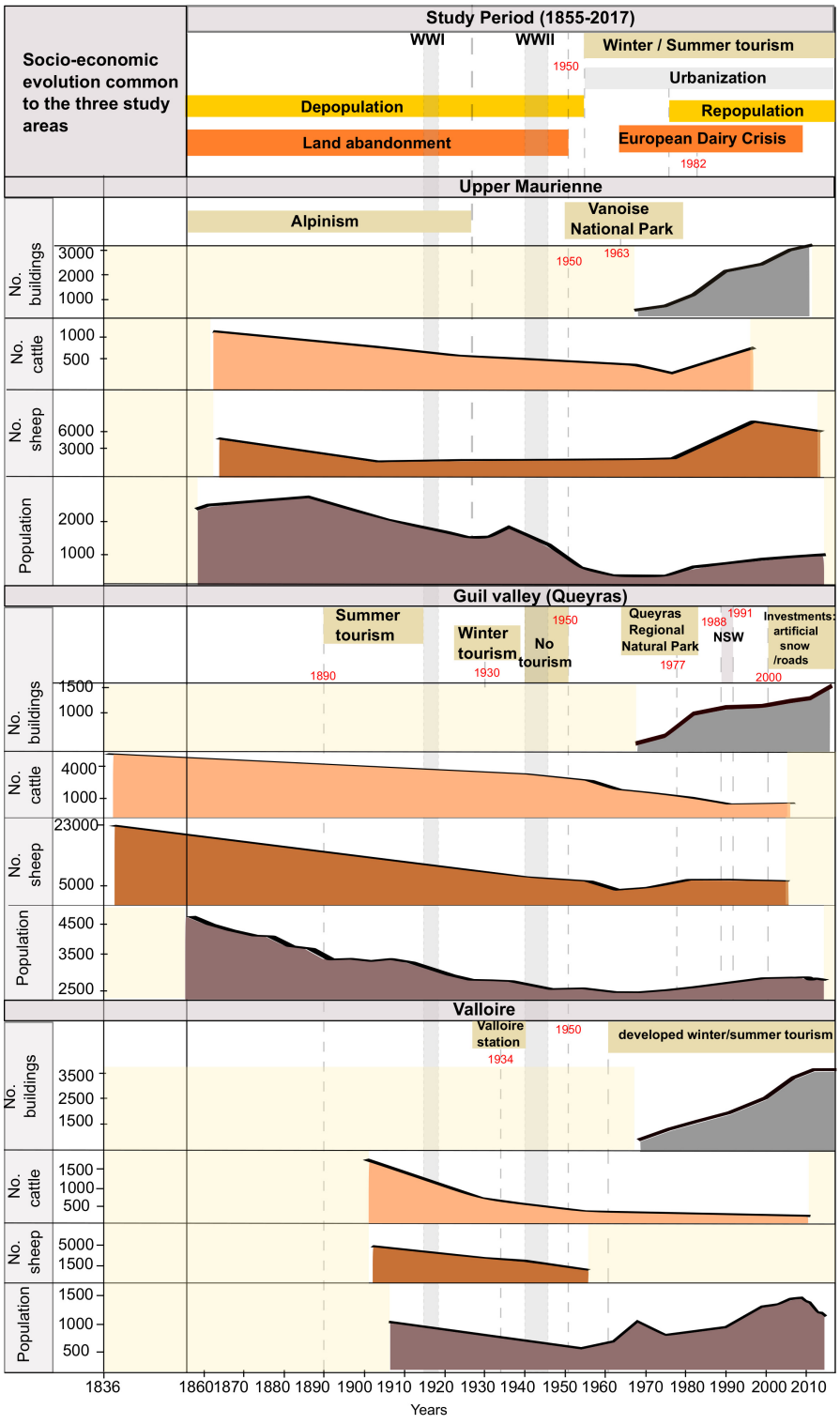

Figure 3.5: Diachronic evolution of the socio-environmental context in the Upper Maurienne, Guil valley and Valloire from 1855 until 2017. The term NSW in the figure stands for 'No Snow Winter' and refers to winters with very low snowfall making the ski industry not economically viable. For the Guil valley, the evolution of the number of cattle and sheep is inferred at the scale of the entire Queyras massif (Figure 3.1 b) since no information per municipality was available, □ refers to periods with no available data. Data sources: Population: EHESS, INSEE, Agro-pastoral: Drogue (1950); Rambaud and Vincienne (1964); Jail (1969); Digard (1974); Jail (1977); Perret et al. (1992); Vincent (2007), the pastoral inquiries and agricultural census.

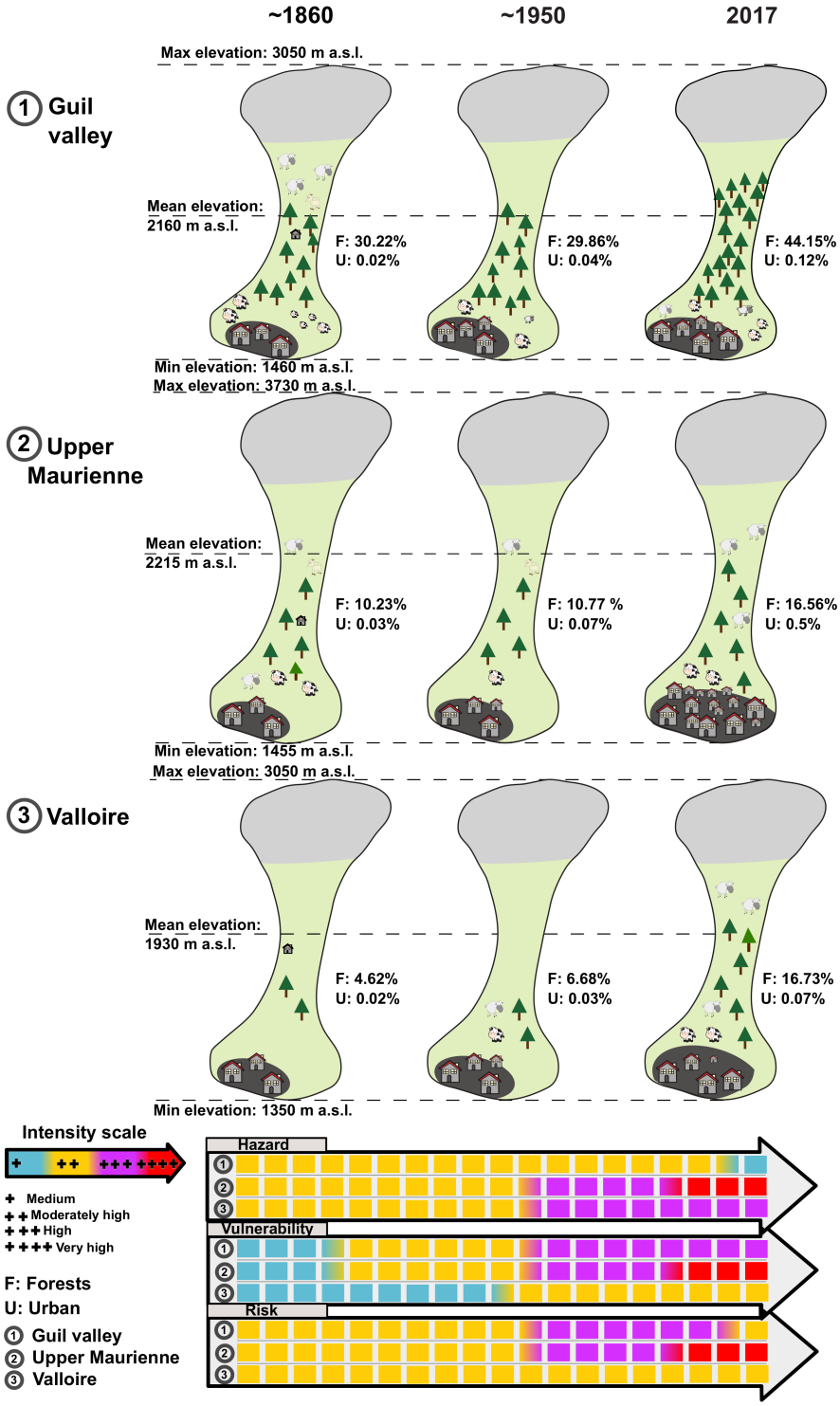

Figure 3.6: Co-evolution of land cover, avalanche risk and its component from 1860 to 2017 in the Upper Maurienne valley, Guil valley and Valloire. For each period, this qualitative model sums-up changes in land-cover and in the different components of avalanche risk to settlements.

3.4 Conclusion and outlooks

In this work, as an answer to the need of integrated studies addressing the different components of avalanche risk changes altogether, we assessed the co-evolution of land cover, the socio-economic system and climatic variables in avalanche prone terrain in three upper valleys of the French Alps: the Upper Maurienne, the Guil valley and Valloire from 1860 to 2017. Land cover change analysis involved identification of different land cover classes, creation of land cover maps originating from historical maps and aerial photographs, spatial and thematic homogenization to enhance inter-comparability and bias correction, which resulted in complete series of comparable landscape matrices. Subsequent analysis of a comprehensive corpus of data related to climate conditions, avalanche hazard changes and socio-economic indicators provided inference of the evolution of avalanche risk to settlements. This eventually allowed building a qualitative model highlighting changes in land cover and in the different components of avalanche risk to settlements in the Upper Maurienne, Guil valley and Valloire, demonstrating that some trends are common to all three study areas but also that strong local peculiarities exist.

Notably, the study shows that, from 1860 to 2017, avalanche risk in the Upper Maurienne increased, as avalanche hazard increased and the number of exposed elements surged following the development of tourism sector whereas, alternatively, in the Guil valley, avalanche risk may have locally decreased following a decline in snow avalanche hazard in heavily reforested paths. Eventually, in Valloire, avalanche risk remained rather stationary, since exposure to snow avalanches was and remains relatively low compared with the Upper Maurienne and the Guil valley. This clearly demonstrates that, even if common large scale drivers such as climate warming, afforestation and land abandonment and socio-economic transitions are unambiguous, local dynamics play a crucial role in avalanche risk evolution. More widely, our results help understanding the intertwined complex patterns resulting in mountain risks changing faster than ever and very differently from one location to another (Hock et al., 2020).

Due to its integrative nature and rather large spatial scale, our study retains numerous uncertainties related to the different data and methods employed. For instance, land cover change analysis is subject to several uncertainties linked to the classification and change detection phase. However, our methodology limits both errors via homogenization of the spatial and thematic information across data sources (Petit and Lambin, 2001; Zgheib et al., 2020), so that, notably, the overall trajectory of the evolution of elements at risk (category : Urban) and reforestation (category : Forest) should be considered as reliable. Also, i) definition of avalanche prone terrain as a 50 m buffer beyond the current limit of avalanche paths in the local avalanche map, ii) analysis of climate and avalanche hazard changes based on reanalyses and model-based homogenized trends, and iii) not considering defense structures in hazard assessment are clear sources of uncertainty. However, we believe the local avalanche map and inventory and the physical and statistical modelling techniques that were employed to be reliable enough to grasp the evolution of hazard and its snow and weather drivers in the three study areas with a level of accuracy sufficient for the purpose of our large scale, partially qualitative, study.

In the future, with ongoing climate warming, changes in avalanche activity will be exacerbated (Castebrunet et al., 2014; Stoffel and Corona, 2018; Hock et al., 2020). Provided upward exposure trends continues, further increase in avalanche risk in many high mountain areas is likely (Hock et al., 2020). By delivering reliable estimates of local evolution and its main drivers,

our approach should contribute to the development of effective adaptation strategies. To this end, however, future expansion of our partially qualitative methodology towards a fully quantitative risk assessment framework is desirable. This would imply the numerical analysis of vulnerability in all its dimensions (physical, social, economic, etc.) and probabilistic-numerical avalanche modelling (Eckert et al., 2010c) within an explicit non-stationary framework including the impact of defense structures and forests on avalanche dynamics. Resulting risk estimates would take into account climate, environmental and socio-economic trends (Farvacque et al., 2019; Peduzzi, 2019), providing i) risk values at different temporal horizons and ii) how different land use planning strategies affects the future of risk. Ultimately, designing future successful disaster risk reduction strategies fulfilling stakeholders needs would become possible.

3.5 Appendix

3.5.1 Appendix A: Land cover data

Table 3.2: Maps and aerial photographs used to document the evolution of land cover in the study areas. IGN is the French National Geographical Institute

Type	Year	Scale/resolution	Source	Study Area
Historical maps	1860	1/40000	IGN	Upper Maurienne,Valloire
Historical maps	1855	1/40000	IGN	Guil Valley
Historical maps	1952	1/50000	IGN	Upper Maurienne, Guil Valley
Historical maps	1958	1/50000	IGN	Valloire
Aerial photos	1952	0.5m	IGN	Upper Maurienne, Valloire
Aerial photos	1948	0.5m	IGN	Guil Valley
	2017	1.5m	IGN	Upper Maurienne, Valloire, Guil Valley

3.5.2 Appendix B: Correction of the bias between historical maps and aerial photographs

To calculate the bias, let 1952 be the pivot year, for which both aerial photographs and historical maps are available.

First let S_k be the surface area corresponding to land cover type k:

$$S_k = P_k \times S_0, \tag{3.1}$$

where S_0 is the total surface of the study area and P_k is the fraction of land cover type k. Knowing that $\sum P_k = 1$ and $\sum S_k = S_0$ we can calculate the relative error ε_k per land cover class using the 1952 aerial photography as reference as follows:

$$\varepsilon_k = \frac{S_0 P_{km} - S_0 P_{kp}}{S_0 P_{kp}} = \frac{P_{km} - P_{kp}}{P_{kp}}, \tag{3.2}$$

leading

$$P_{kp} = \frac{P_{km}}{\varepsilon_k + 1}, \tag{3.3}$$

where P_{km} is the fraction of k resulting from the 1952 historical map and P_{kp} is the fraction of k recorded from the analysis of the 1952 aerial photos.

Since all the land cover data, generated from historical maps, were already homogenized to a comparable resolution following the methodology suggested by Petit and Lambin (2001), we can assume that the relative error derived for the pivot year applies to the previous years. Thus we can create virtual landscape matrices that potentially represent the landscape composition as if it was analysed from aerial photographs all over the study period.
Let S_{kp}' be the virtual area corresponding to land cover type k knowing that only the area digitized from the map is available :

$$S_{kp}' = \frac{P_{km}}{\varepsilon_k + 1} \times S_0. \tag{3.4}$$

Thus, P_{kp}', that represents the potential fraction of land cover k as if it was generated from an aerial photos, is :

$$P_{kp}' = \frac{S_{kp}'}{\sum S_{kp}'} = \frac{S_0 \frac{P_{km}}{\varepsilon_k+1}}{\sum S_0 \frac{P_{km}}{\varepsilon_k+1}} = \frac{\frac{P_{km}}{\varepsilon_k+1}}{\sum \frac{P_{km}}{\varepsilon_k+1}}. \tag{3.5}$$

Chapter 4

Diachronic quantitative snow avalanche risk assessment as a function of forest cover changes

---

This chapter present the article entitled "Diachronic quantitative snow avalanche risk assessment as function of forest cover changes." in preperation. The following authors contributed to the work: Florie Giacona, Anne-Marie Granet-Abisset, Samuel Morin and Nicolas Eckert.

Abstract: Mountain forests are a cost effective nature-based solution to reduce risks due to natural hazards. Forests prevent snow avalanche initiation and decelerate flowing avalanches, thus reducing runout distances and impact pressures. However, these effects are rarely taken into account within quantitative avalanche risk assessment, a surprising fact in light of the strong reforestation that occurred in the European Alps over the last ∼150-200 years. In this work, we propose a holistic avalanche risk analysis methodology to evaluate to which extent the probability of exceedance of runout distances, impact pressures and ultimately avalanche risk estimates for various types of building-like elements at risk are affected by forest cover changes. Results on a typical case study of the French Alps show that, from a completely deforested to a completely forested path, avalanche risk for a building located downslope decreases by 53-99%, depending on how forest cover is accounted for in avalanche statistical-dynamical modelling. Forest cover data inferred from old maps and photographs demonstrate that a 20-60% risk reduction actually occurred between 1825 and 2017 at the site because of the local afforestation dynamics, with significant modulations according to the considered building technology. In addition to ascertaining the protective role of forests against snow avalanche hazard, these results: i) highlight the potential of combining nature-based solutions with traditional structural measures to reduce risk to acceptable levels at reasonable costs, ii) open the door to the quantification of avalanche risk changes on the long range as function of changes in all its hazard, vulnerability and exposure drivers.

Keywords: Snow avalanches, statistical-dynamical modelling, quantitative risk assessment, socio-environmental changes, forests, nature-based protection

Contents

4.1 Introduction

Over the years, classical structural protection measures against natural hazards (e.g. dams, or additionally reinforced walls) have been increasingly criticized due to their negative environmental and aesthetic impact and, sometimes, their potential to increase exposure to risk (Delage, 2003; Moos et al., 2018). Some studies even consider that traditional protection structures, sometimes denoted as grey approaches, are unable to adapt to changes in hazards driven by climate change (Poratelli et al., 2020b; Kumar et al., 2020). These arguments, in addition to the large construction and maintenance costs of structural protection measures have turned the focus towards more sustainable cost effective ecosystem-based solutions for disaster risk reduction (Eco-DRR, also known as nature-based solutions).

In mountain areas, the most well known example of Eco-DRR solutions are forests, protecting people and their assets mostly against gravity-driven natural hazards (Brang et al., 2001, 2006). The protective role of forest stands against, e.g. rockfalls (Dupire et al., 2016) and snow avalanches (Bebi et al., 2009), is of a great importance in Alpine regions, preventing human deaths and destruction of buildings and infrastructures (Getzner et al., 2017). In the case of snow avalanches, the most common function of forests is preventing large slab initiation by stabilizing the snowpack in release areas (Salm, 1978; De Quervain, 1978; Gubler and Rychetnik, 1991; Viglietti et al., 2010; Teich et al., 2012a) but they also have the capacity to decelerate flowing avalanches (Anderson and McClung, 2012; Takeuchi et al., 2018). Their protective potential is directly linked to forest structural parameters, e.g. the stem density for small-medium avalanches (Teich et al., 2012a, 2014), and the distance traveled before penetrating into the forest for large avalanches triggered above the timberline (McClung, 2003; Takeuchi et al., 2011; Teich et al., 2012a).

Forest-avalanche interactions is an old topic in snow avalanche modelling. In earliest studies, friction was locally increased within the model to mimic the decelerating impact of forests on avalanche runout distances (Salm, 1978; Gubler and Rychetnik, 1991; Bartelt and Stöckli, 2001; Takeuchi et al., 2011). In such so-called frictional approaches, avalanche models often use a Voellmy friction law that considers the total friction as the sum of a dry-Coulomb coefficient μ and a turbulent term depending on the squared velocity and on the inverse of a coefficient ξ (Voellmy, 1955). μ generally varies within the $0.1-0.7$ range, and is often thought to summarize snow properties (Salm et al., 1990). ξ generally varies within the $1000-10{,}000\ m/s^2$ range for forest-free terrain, and aims at representing the roughness of the path potentially related to land cover properties (Salm et al., 1990; Ancey et al., 2003). This explains why, in frictional approaches, more often than not, ξ is lowered to 400 m/s^2 in forests. This leads to an increase of the velocity dependent friction that some authors related to the entrainment of heavy trees and stems by the flow (Bartelt and Stöckli, 2001). However, some research also considered a concomitant slight increase in μ with a $\Delta\mu$ ranging between $+0.02$ and $+0.05$ from forest-free to forested terrain (Gruber and Bartelt, 2007; Christen et al., 2010). More recently, as an alternative to frictional approaches, Feistl et al. (2014) proposed the detrainment approach in which the forest-avalanche interaction is modeled through a single parameter detrainment function. This approach accounts for the braking effect of forests on avalanche flows, and is thought to be suitable to simulate small to medium avalanches using 3D models (Feistl et al., 2014).

From a different perspective, research that aimed at better mitigating avalanche risk historically focused on the sole hazard component of the risk, and mostly using deterministic approaches relying on physics (Harbitz et al., 1998). However, even the best numerical avalanche model cannot, without further probabilistic and vulnerability considerations, evaluate the risk levels and related uncertainties that are required, e.g., for land use planning and the design of defense structures. As a consequence, dealing with snow avalanche risk has recently changed from sole hazard prevention to risk management, which includes explicit consideration of vulnerability and exposure (Bründl et al., 2009). Early implementations relied on simple scenarios representing extreme avalanches (Fuchs et al., 2004), but, quickly, the newly developed extreme-value based and/or statistical-dynamical models representing the full variability of avalanche events likely to occur where adopted (Keylock et al., 1999; Barbolini et al., 2004b; Cappabianca et al., 2008; Eckert et al., 2008a, 2009; Favier et al., 2014b, 2016). This was clearly a step towards more integrated avalanche risk mitigation solutions potentially accounting, e.g., for acceptability thresholds (Arnalds et al., 2004) and/or cost–benefit constraints faced by stakeholders. However, to our knowledge, few studies so far have tried to take into account the protective effects of forests within quantitative avalanche risk assessments, and when this was attempted, only with simple statistical relations (Grêt-Regamey and Straub, 2006) or scenarios (Teich and Bebi, 2009) for the hazard model only. By contrast, comprehensive combinations of numerical probabilistic hazard models taking into account changes in land cover, elements at risk and their vulnerability have already been achieved, e.g., for rockfall risk (Moos et al., 2018; Farvacque et al., 2019) and it is a rather common strategy (although still difficult to properly achieve) for flood risk (Rogger et al., 2017; Bathurst et al., 2020).

The latter point is especially surprising in light of the strong reforestation that occurred in the European Alps (and numerous other mountain areas) over the last $\sim$ 150-200 years (Mather et al., 1999; Bebi et al., 2017). This time frame roughly corresponds to the classical 100-300 year reference periods that define legal thresholds in land-use planning (Eckert et al., 2018). This pleads for a dynamical assessment of the impact of reforestation on avalanche risk accounting for potentially quick changes in forest extension and structure. Already existing examples provide insights about how reforestation can affect avalanche risk. Giacona et al. (2018) demonstrated that, in medium-high mountains, interactions between avalanche activity, forest stands, social practices and climate result in strong temporal modulations of mountain landscapes and avalanche risk. García-Hernández et al. (2017) highlighted strong decrease in snow avalanche damage in the Asturian massif (Spain) linked to reforestation following the end of industrial activities. Similarly, Mainieri et al. (2020) and Zgheib et al. (in revision) showed a decrease in avalanche hazard and risk, respectively, in the Queyras massif (France), mostly due to agricultural abandonment. However, in these different studies, the diachronic methodology used to assess avalanche risk changes was rather qualitative, which is not enough to supply decision makers with diagnoses that are immediately usable.

On this basis, in this paper, we i) include forest cover changes within an avalanche risk assessment approach and ii) demonstrate on a typical case study of the French Alps how deeply changes in forest cover that occurred over the 1825-2017 period may have affected avalanche hazard and subsequent risk estimates for various types of building-like elements at risk. To that end, the Bayesian statistical-dynamical model of Eckert et al. (2010c) is expanded to account for multiple release areas within the same path and it is calibrated using on-site data. The

local distribution of avalanche hazard is then tuned according to observed changes in the forest fraction (the latter being defined as the aerial percentage of the terrain covered by forests within the extension of the avalanche path). This is achieved by i) evaluating forest cover changes within the case study extension from a combination of aerial photographs and ancient maps (Zgheib et al., 2020) and relating these changes to the friction coefficients μ and ξ of the Voellmy friction law. The resulting diachronic hazard distributions are then combined with fragility curves for different types of reinforced concrete (RC) buildings (Favier et al., 2014b), so as to produce first ever avalanche risk estimates that account for land cover changes in a comprehensive way. Note, however, that our aim is neither the in-depth modeling of the forest-avalanche interaction, nor of the damage due to avalanches for concrete, which would require more advanced modelling techniques than those we use. Instead, we develop a holistic risk assessment methodology relaying on a rather simple frictional-like approach for avalanche-forest interactions and on a large set of fragility curves evaluated under quasi-static assumptions. This is arguably enough to grasp the on-site evolution of avalanche risk for buildings and to show how the protective effect of forests and building technology may combine to limit the risk, which may ultimately allow the proper implementation of efficient grey-green protection measures against snow avalanches.

4.2 Case-study

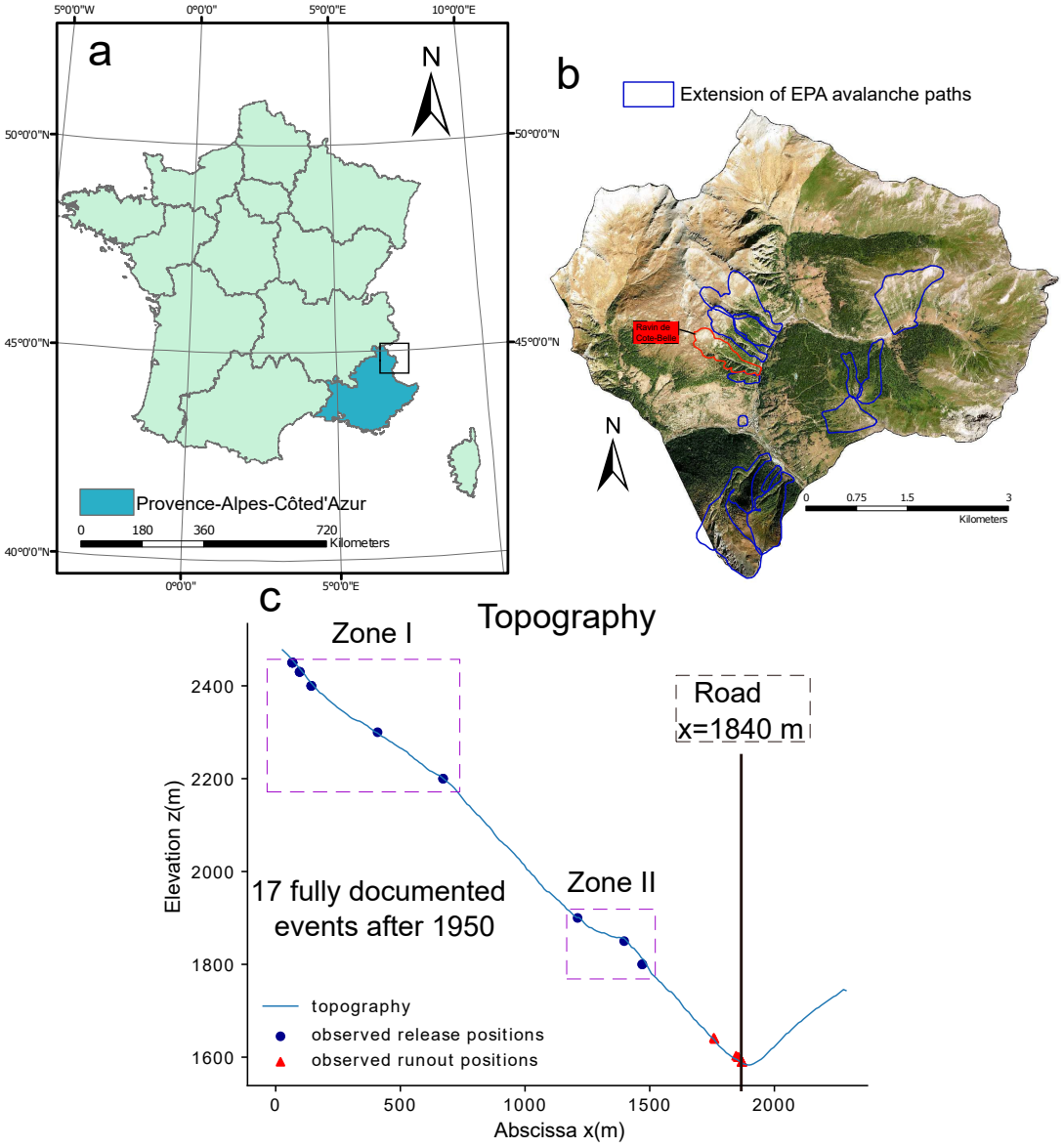

Figure 4.1: Case-study: Ravin de Côte-Belle avalanche path. a) Location within the French Alps, municipality of Abriès, Queyras massif, b) Extension of avalanche paths from the EPA record, the Ravin de Côte-Belle avalanche path is highlighted in red and c) 2-D topography with historical data from the EPA record (the 17 fully documented events that occurred after 1950), and avalanche release zones I and II. Within the analysis, the road position at x=1840 m is taken as the location of a potential new building, so as to assess how risk to settlements has evolved as function of forest cover changes.

Our study site, the Ravin de Côte-Belle path (44°48' N, 6°55' E), is located in the Hautes Alpes department (Provence-Alpes-Côte d'Azur region) in the French Alps (Figure 4.1a), on the

northern slopes of the municipality of Abriès (Queyras massif) (Figure 4.1b). Snow avalanches are mostly triggered from two distinct well localized release zones: Zone I between 2500 and 2200 m a.s.l, and Zone II between 1900 and 1800 m a.s.l (Figure 4.2a,b). Most of the avalanches stop in the runout zone around 1600 m a.s.l. The departmental road D411 linking le Roux village to Abriès cuts the runout area at the abscissa x= 1840 m (Figure 4.1c). Within the analysis, this position is taken as the location of a potential new building, so as to assess how risk to settlements has evolved as function of forest cover extension within the path extension.

Winter climate in the Queyras massif is cold, with relatively low precipitation in comparison to the rest of the French Alps (Durand et al., 2009a,b). However, local avalanche activity is significant (Corona et al., 2013; de Bouchard d'Aubeterre et al., 2019), notably during "easterly returns", i.e. atmospheric flows coming from the Mediterranean Sea that are responsible of heavy snowfall in the the eastern part of the French Alps, leading to marked avalanche cycles (Eckert et al., 2010b). As a consequence, the Ravin de Côte-Belle path is well documented in the French Avalanche Permanent Survey (referred to as EPA: Enquête Permanante des Avalanches (Bourova et al., 2016)), with 21 avalanches recorded between 1934 and 2018.

For the calibration of the avalanche statistical-dynamical model, all the 21 events from the EPA record were used to evaluate local avalanche occurrence frequency. By contrast, only 17 events that occurred between 1950 and 2017 were sufficiently documented (release elevation, runout elevation, snow deposit), to be used for the calibration of the magnitude component of the model, 13 released from Zone I and 4 released from zone II. Meteorological conditions corresponding to the dates at which the events occurred were added, notably snow depths at the elevation of the starting zones. These were taken from available reanalyses provided by the Safran-CROCUS model chain (Vernay et al., 2019).

Land cover changes from 1825 to 2017 within the the Ravin de Côte-Belle were assessed using available historical maps and aerial photographs (Table 4.2, Appendix A) following the optimal combination approach proposed by Zgheib et al. (2020). Historical maps of 1825 were georeferenced, and forest extensions were manually digitized. Regarding aerial photographs, pre-processed images were obtained for 2017 and 1948, whereas an orthorectification had to be applied to the 1980 image, and forest cover was digitized manually. For each date, the forest fraction, i.e. the aerial percentage of the terrain covered by forests within the extension of the avalanche path, could then be evaluated, as well as the more comprehensive elevation distribution of forest pixels. It is clear that the forest fraction in the Ravin de Côte-Belle path increased all over the study period, and at accelerated pace over the last decades, from 0.16 in 1825 to 0.24 in 1948, 0.35 in 1980 and to 0.46 in 2017 (Figure 4.2a). In more details, afforestation from 1825 to 2017 occurred mostly at high elevations of the path, between 2000 and 2200 m a.s.l (Figure 4.2b,c,d,e). In 2017, the forest reached the highest avalanche release area (Zone I), and completely covered the lower avalanche release area identified (Zone II).

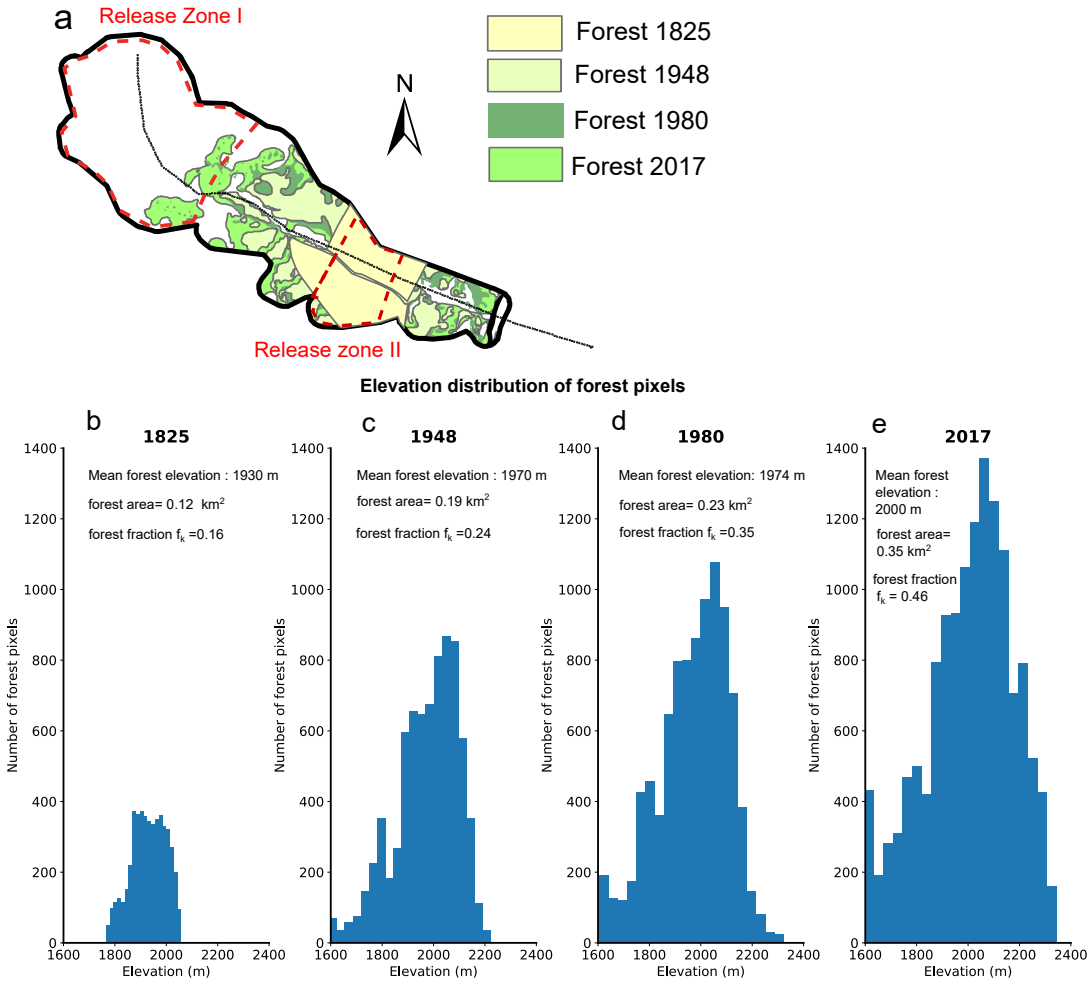

Figure 4.2: Forest cover evolution at Ravin de Côte Belle avalanche path. a) Release zones I and II and diachronic map of forest cover extensions in 1825, 1948, 1980 and 2017. Elevation distribution of forest pixels in b) 1825 (forest fraction $f_k = 0.16$), c) 1948 (forest fraction $f_k = 0.24$), d) 1980 (forest fraction $f_k = 0.35$) and e) 2017 (forest fraction $f_k = 0.46$). Pixel size is 0.5x0.5 m^2.

4.3 Methodology

4.3.1 A Bayesian statistical-dynamical model expanded to multiple release areas

The Bayesian statistical-dynamical model used in this study was developed by Eckert et al. (2010c). According to Naaim et al. (2004), it is based on the depth-averaged Saint Venant equations solved along a curvilinear profile $z = f(x)$, where z is elevation and x is the horizontal distance measured from the top of the avalanche path. Within the model, the following Saint Venant mass and momentum conservation laws represent a one dimensional flow on the curvilinear profile solved using a finite volume scheme (Naaim, 1998). To facilitate the specification

of the input conditions corresponding to each avalanche simulation and to reduce computation times, snow incorporation and deposition are ignored:

$$\frac{\partial h}{\partial t} + \frac{\partial (hv)}{\partial x} = 0, \tag{4.1}$$

$$\frac{\partial (hv)}{\partial t} + \frac{\partial (hv^2 + g\frac{h^2}{2})}{\partial x} = h(gsin\phi - F), \tag{4.2}$$

where v is the flow velocity, h is the flow depth, ϕ is the local slope, t is the time and F is the total friction.

The total friction F considered is the classical Voellmy friction law (Voellmy, 1955):

$$F = \mu gcos\phi + \frac{g}{\xi h} v^2. \tag{4.3}$$

Total friction is thus the sum of a dry-Coulomb coefficient μ and a turbulent term depending on the squared velocity and on the inverse of a coefficient ξ (Voellmy, 1955).

The full stochastic model representing the variability of avalanche events at the study site is noted $p(y, a|\theta_M, \lambda)$. Avalanche magnitude y is a random vector including all the correlated multivariate quantitative characteristics that vary from one event to another, namely runout distance, velocity and pressure profiles, or snow volume. Avalanche frequency a is a scalar discrete random variable corresponding to the number of avalanches recorded each winter. Avalanche magnitude and frequency are classically modeled as two independent random processes so that their joint distribution writes as a product and related parameters can be inferred separately (Eckert et al., 2010c):

$$p(y, a|\theta_M, \lambda) = p(y|\theta_M)p(a|\lambda). \tag{4.4}$$

Avalanche frequency is modeled as a Poisson distributed process, with a scalar parameter $\theta_F = \lambda$ representing the mean annual avalanche number i.e. $a|\lambda \sim P(\lambda)$, necessary for the computation of return periods. The magnitude model specified below is more complex, with thirteen parameters $\theta_M = (\alpha_1, \alpha_2, \beta_1, \beta_2, p, b_1, b_2, \sigma_h, c, d, e, \sigma, \xi)$. Also, the magnitude model evaluates, for each avalanche, the latent friction μ and the computed runout distance x_{stop}.

The studied path is characterized by the presence of two distinct starting zones: Zone I between 2500 and 2200 m a.s.l and Zone II between 1900 and 1800 m a.s.l (Figure 4.2a,b). To include this information into the analysis, rather than by the original single Beta distribution (Eckert et al., 2010c), we model x_{start} as a Binomial mixture of two Beta distributions. This could be easily, in the future, generalized to even more complex cases using a multinomial mixture (e.g., Lavigne et al. (2012)):

$$\begin{aligned} &x_{start_i} = P(x_{start_i} \in [x_{min_1}, x_{max_1}]).x_{start_1} + (1 - P(x_{start_i} \in [x_{min_2}, x_{max_2}])).x_{start_2}, \\ &P(x_{start_i} \in [x_{min_1}, x_{max_1}]) \sim B(p) \end{aligned} \tag{4.5}$$

Since normalization is a requirement when dealing with the Beta distribution, normalized release abscissas are calculated and considered in the model as follows:

$$\begin{aligned} x_{start_{norm_1}} &= \frac{x_{start_1} - x_{min_1}}{x_{max_1} - x_{min_1}} \mathbb{1}(x_{start_1} \in [x_{min_1}, x_{max_1}]) \sim Beta(\alpha_1, \beta_1), \\ x_{start_{norm_2}} &= \frac{x_{start_2} - x_{min_2}}{x_{max_2} - x_{min_2}} \mathbb{1}(x_{start_2} \in [x_{min_2}, x_{max_2}]) \sim Beta(\alpha_2, \beta_2), \end{aligned} \tag{4.6}$$

where x_{min_1}, x_{max_1}, x_{min_2} and x_{max_2} are the minimal and maximal abscissas delimiting release zones I and Zone II estimated for the case study using topographical thresholds, and α_1, α_2, β_1 and β_2 the parameters of the corresponding Beta distributions.

The mean release depth h_{start} is assumed to be Gamma-distributed with parameters b_1 and b_2 reflecting its dependency on release abscissa and a constant dispersion around the mean σ_h (Eckert et al., 2010c). Here and in what follows the conditioning by x_{min_1}, x_{min_2}, x_{max_1} and x_{max_2} is dropped for simplicity:

$$h_{start}|b_1, b_2, \sigma_h, x_{start} \sim Gamma(\frac{1}{\sigma_{h^2}}(b_1 + b_2 x_{start_{norm}})^2, \frac{1}{\sigma_{h^2}}(b_1 + b_2 x_{start_{norm}})), \tag{4.7}$$

where $x_{start_{norm}} = \frac{x_{start} - x_{min_1}}{x_{max_2} - x_{min_1}}$ is the normalized release abscissa evaluated all over the different release areas.

Given the normalized release abscissa $x_{start_{norm}}$ and the mean release depth h_{start}, the friction coefficient μ is modeled as a latent variable describing the random effects from one avalanche to another and it is assumed normally distributed (Eckert et al., 2010c):

$$\mu|c, d, e, \sigma, x_{start}, h_{start} \sim N(c + d x_{start_{norm}} + e h_{start}, \sigma). \tag{4.8}$$

Parameters c, d and e represent the dependency of μ on the release abscissa and mean release depth, with a constant dispersion σ around the mean. Alternatively, the velocity dependent friction coefficient ξ is modeled as a parameter in the strict statistical sense of the term. Both ξ and μ_i, i $\in [1, n]$ where n is the data sample size of fully documente events are estimated from the data.

Small Gaussian differences between the observed runout distances $x_{stop_{data}}$ and computed runout distances x_{stop} are postulated:

$$x_{stop_{data}}|\sigma_{num}, x_{stop} \sim N(x_{stop}, \sigma_{num}). \tag{4.9}$$

These differences can result from numerical errors due to the imperfection of the propagation model, and/or from observation errors. The standard deviation of these numerical errors σ_{num} is set to 15 m to grant model identifiability.

Inference of the full model is a difficult problem which is solved by splitting it to simpler tasks. As stated before, the frequency and magnitude models are inferred separately. For the frequency model inference, all 21 avalanches events recorded since 1934 are used. For the magnitude model inference, only the n=17 fully documented events are used. Avalanche events are assumed mutually independent. This implies that the joint likelihood of all events is the product of their individual marginal likelihood.

For the frequency model, Bayesian inference is analytical. With the chosen $Gamma(a_\lambda, b_\lambda)$ prior for the parameter λ, the posterior distribution of λ remains Gamma distributed: $Gamma(a_\lambda + T_{obs}, b_\lambda + N_{obs})$, where the pair (a_λ, b_λ) represent the prior knowledge concerning the distribution of avalanche occurrences. N_{obs} is the total number of avalanches recorded on the study site (i.e. 21 events) during T_{obs} years of observation.

The parameters of the Binomial Beta mixture model of x_{start}, α_1, α_2, β_1 and β_2 are estimated using the method of moments, a frequentist approach for parameter estimation (Appendix B).

The rest of the magnitude model is inferred using Bayesian methods, resulting in the joint posterior distribution of remaining parameters and latent variables:

$$p(\theta, \mu, x_{stop}|data, \sigma_{num}) \propto \pi(\theta) \times p(h_{start}, x_{stop_{data}}|\theta, \mu, x_{start}, x_{stop}, \sigma_{num}) \times p(\mu, x_{stop}|\theta, h_{start}, x_{start}, x_{stop_{data}}, \sigma_{num}) \quad (4.10)$$

where θ= (b_1,b_2,σ_h,c,d,e,σ,ξ), $\pi(\theta)$ is the joint prior distribution for the related parameters and *data* represents all observations. Numerical computation was achieved using the Metropolis Hasting algorithm within a Markov chain Monte Carlo (MCMC) scheme detailed in Eckert et al. (2010c). Convergence was checked using several chains starting at different points of the space parameter. For each unknown a point estimate is computed from the joint posterior distribution, in addition to the posterior mean, the posterior standard deviation and the 95% credible interval (Table 4.1).

Table 4.1: Parameter estimates of the statistical dynamical model. When Bayesian inference is used, for each parameter, the marginal prior distribution used is given, as well as summary statistics of the posterior distribution (the posterior mean is retained as point estimate). The mixture model for the release position (Equation 4.5) is calibrated separately using the method of moments (Appendix B).

	Prior	Posterior mean /point estimate	SD	2.5%	97.5%
b_1	$b_1 \sim N(3,1)$	1.56	0.22	1.25	2.16
b_2	$b_2 \sim N(0,1)$	-0.54	0.27	-1.01	-0.04
σ_h	$\sigma_h \sim Gamma(5,10)$	0.59	0.23	0.31	1.2
c	$c \sim N(0.5,0.2)$	0.34	0.05	0.24	0.44
d	$d \sim N(0,0.25)$	-0.02	0.05	-0.12	0.086
e	$e \sim N(0,0.125)$	-0.02	0.015	-0.06	-0.001
σ	$\sigma \sim Gamma(1,0.03)$	0.16	0.04	0.09	0.25
ξ	$\xi \sim N(1300,100)$	2297	13.5	2275	2323
α_1		α_1=0.28			
α_2		α_2=0.02			
β_1		β_1=0.67			
β_2		β_2=0.01			
p		p=13/17			
λ	$\lambda \sim Gamma(0.01,0.001)$	0.31	0.07	0.17	0.45

4.3.2 Simulation of avalanche hazard conditional to local calibration

To evaluate avalanche hazard conditional to local calibration, 10,000 predictive simulations (Eckert et al., 2007, 2010c; Fischer et al., 2015, 2020) were performed with all parameters set to their Bayesian or frequentist point estimates (Table 4.1). In details, for each simulation, x_{start} is evaluated according to the mixture model (Equation 4.5) that allows reconstructing a Binomial mixture of two Beta distributions. Then, the normalised release abscissa injected in

the simulation model is $x_{start_{norm}} = \frac{x_{start} - x_{min1}}{x_{max_2} - x_{min_1}}$, where x_{start} is the simulated release abscissa depending on its location on the path, x_{max_2} the maximal abscissa of Zone II and x_{min_1} the minimal abscissa of Zone I. A statistical-dynamical Monte Carlo approach is necessary to obtain the full joint distribution of the outputs of the numerical avalanche model knowing the distribution of the inputs. It involves integration over the distribution of the latent friction coefficient μ and is written as follows:

$$p(y|\hat{\theta_M}) = \int p(x_{start}|\hat{\alpha_1}, \hat{\alpha_2}, \hat{\beta_1}, \hat{\beta_2}, \hat{p}) p(h_{start}|\hat{b_1}, \hat{b_2}, \hat{\sigma_h}, x_{start}) p(x_{stop}|x_{start}, h_{start}, \mu, \hat{\xi}) d\mu, \tag{4.11}$$

where "hat" classically denotes a statistical estimate. This simulation strategy leads to, for instance, the joint distribution of the input variables $(x_{start}, h_{start}, \mu|\hat{\theta_M})$ and of the output variables $p(x_{stop}, v_{xt}, h_{xt}|\hat{\theta_M})$ of the avalanche propagation model, where v_{xt} and h_{xt} represent, for each avalanche simulation, the velocity and flow depth computed for each abscissa and time step (Figure 4.3).

Subsequently, the return period $T_{x_{stop}}$ associated with the runout distance x_{stop}, is estimated by combining $\hat{\lambda}$ and the cumulative distribution function (cdf) of runout distances $\hat{F}(x_{stop}) = P(X_{stop} \leq x_{stop})$ as follows:

$$T_{x_{stop}} = \frac{1}{\hat{\lambda}(1 - \hat{F}(x_{stop}))}. \tag{4.12}$$

The inverse problem is then solved, and the runout distance quantile corresponding to the return period T is evaluated as:

$$x_{stopT} = \hat{F}^{-1}_{x_{stop}}(1 - \frac{1}{\hat{\lambda}T}). \tag{4.13}$$

A Monte Carlo confidence interval is computed for the non exceedance probability associated with a given runout distance. It allows checking if the sample size is large enough to give reliable estimates.

$$CI_\alpha = \hat{F}(x_{stop}) \pm q_{N_{\alpha c}} \sqrt{\frac{\hat{F}(x_{stop})(1 - \hat{F}(x_{stop}))}{n}}, \tag{4.14}$$

where n is the sample size (in our case 10,000) and $q_{N_{\alpha c}}$ is the quantile of the standard normal distribution corresponding to the desired confidence level α_c.

The runout return period obtained were used to extract the distribution of maximal velocities v_x^{max} (Figure 4.3f) and maximal flow depths h_x^{max} (Figure 4.3e) at abscissas corresponding to different return periods, notably 10 years.

Eventually, the distribution of impact pressures for the free surface flow is calculated by transforming velocities into pressures as follows:

$$P = C_x \frac{1}{2} \rho v^2, \tag{4.15}$$

where C_x is the dimensionless coefficient of resistance i.e. drag coefficient, ρ is the snow density and v is the flow velocity. Studies like Sovilla et al. (2008) and Naaim et al. (2008) link velocity

to pressure in a comprehensive but complex way that involve semi-empirical relations between the drag coefficient C_x and the Froude number. For simplicity, we stick here on C_x=2, an approximation usable for wide, wall like structures, and ρ= 300 kgm^{-3} all along the analysis. Associated Monte Carlo confidence intervals are computed similar to Equation 4.14.

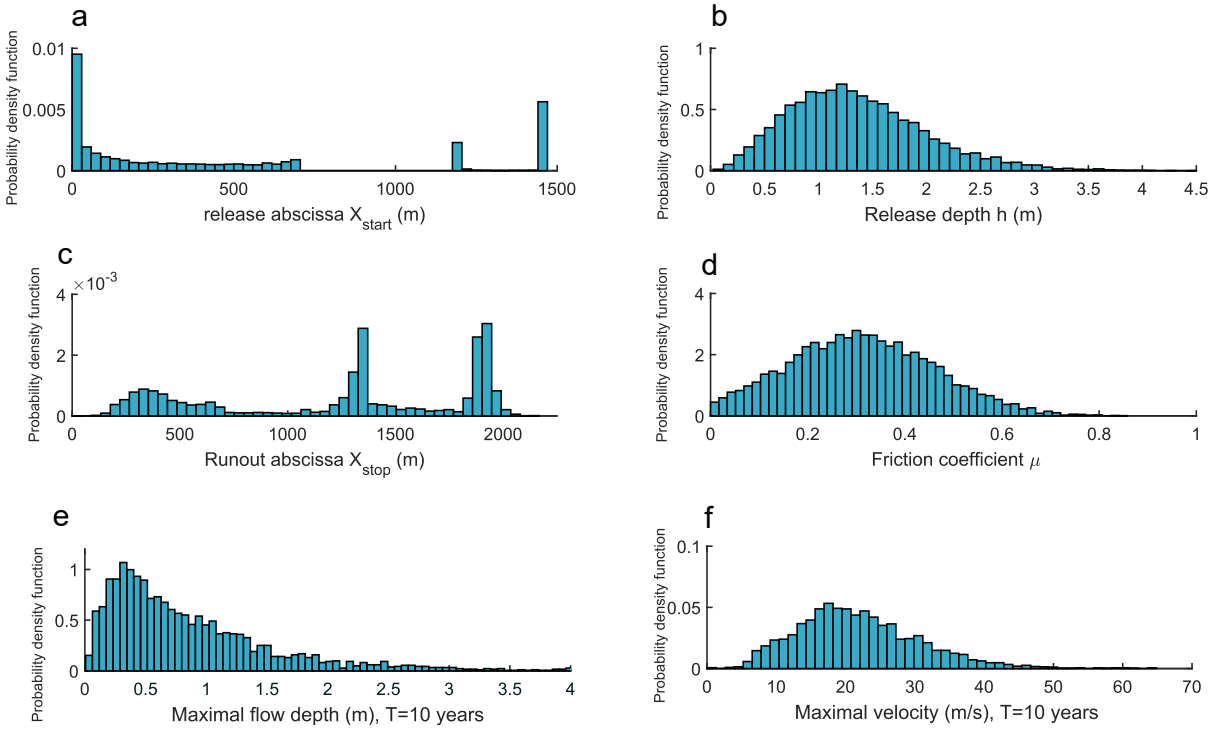

Figure 4.3: Avalanche hazard at Ravin de Côte-Belle, statistical-dynamical simulations according to local calibration and mean forest fraction f_k = 0.35 (as in 1980). Distribution of a) release abscissa, b) release depth, c) runout abscissa, d) friction coefficient μ, e) maximal flow depth at abscissa position corresponding to a return period of T=10 years, and f) maximal velocity at abscissa position corresponding to a return period of T=10 years.

4.3.3 Integration of forest cover changes within avalanche hazard assessment

The model calibrated using the methodology described in Section 4.3.1 considers avalanche events as mutually independent, i.e. the result of the calibration is independent of the order of the events (except that each event is associated to the snow depth data in the release zone that prevailed at the date at which it occurred). Therefore, it is implicitly assumed that all events have occurred for the same path configuration and forest cover. This configuration corresponds to the average forest fraction over the period during which the events used for the calibration of the magnitude model occurred, namely 1950-2018. According i) to the quasi linear increase of forest fraction between 1948 and 2017 grasped from the aerial photographs, and ii) the slightly uneven temporal distribution of avalanche events within the EPA record over the 1950-2018 period, this mean forest fraction $\bar{f}$ arguably coincides with the forest fraction digitized from the 1980 aerial photograph, namely $\bar{f}$=0.35.

Here, we seek at showing how the distribution of hazard and subsequent risk levels can be impacted by forest cover changes by introducing the forest fraction into the modelling in a robust way. Six values of f_k are considered, among which four represent the actual chronic of forest fractions digitized for the period 1825-2017 at the study site, and two extreme cases. In details, f_k values considered are 0 (no forest, deforestation), 0.16 (forest fraction in 1825), 0.24 (forest fraction in 1948), $\bar{f} = f_k$= 0.35 (equal to the forest fraction in 1980), 0.46 (forest fraction in 2017) and 1 (the path is fully covered by forests).

As explained in introduction, in frictional approaches, forest-avalanche interaction is often modeled by changing the value of ξ and slightly increasing the value of μ in the forested section of the path. However, it has been known for a long time that the runout distance is mostly controlled by the static friction coefficient μ (e.g. Dent and Lang (1980), Borstad and McClung (2009)), which has been recently confirmed by more systematic analyses by Heredia et al. (2020). Similarly, Teich et al. (2012b) showed that focusing on the turbulent friction ξ only is not enough since the effects on runout distances remain too limited. Hence, we consider that changes in land cover can affect both ξ and μ and consider the three following cases, corresponding to the different possible relations between forest fraction and friction coefficients:

Case I: It is assumed that the dependence of the friction coefficient μ on land cover, particularly forests, can be modeled by adding a term $g(f_k - \bar{f})$ that increases/decreases the mean of the distribution of the static friction coefficient μ based on the value of the forest fraction f_k relative to $\bar{f}$. This uses the fact that μ is a latent variable in our statistical-dynamical model. A linear dependency between the mean of the distribution of μ and f_k is chosen, similar to the one between the mean of μ, release abscissa and mean release depth:

$$\mu \sim N(c + dxstart_{norm} + eh + g(f_k - \bar{f}), \sigma), \tag{4.16}$$

where the parameters c, d, and remain set to their posterior estimates (Table 4.1) resulting from the model calibration. Choosing a suitable value for g is a difficult task. To this aim, we use the fact that, when the effects of the variables $xstart$ and h is neglected, minimal value of the mean of μ, obtained for $f_k = 0$, equals $c - g\bar{f}$. Physical knowledge and repeated calibrations in various avalanche terrain using deterministic or stochastic methods (Salm et al., 1990; Ancey et al., 2004; Naaim et al., 2013) indicate that classical very low values of μ are around 0.15, which eventually leads to $g \sim 0.6$. Given that this remains, however, a strong assumption we performed a sensitivity analysis with values of g spanning the full $g = 0.4 - 0.8$ range.

Case II: It is assumed that the turbulent coefficient ξ exponentially decays with an increasing forest fraction:

$$\xi = \hat{\xi} b^{(f_k - \bar{f})} \tag{4.17}$$

where $\hat{\xi}$ is the posterior estimate resulting from the calibration step. This relation uses the fact that ξ is as a parameter in the strict statistical sense of the term. It is considered that, moving from deforested to forested terrain, ξ decreases by roughly 60 % (approx. 1000 m/s^2 to 400 m/s^2) (Feistl, 2015). This corresponds to b=0.5. However, just like the previous case, the sensitivity of the results to this parameter is tested by spanning the range between b=0.2 and b=0.8. Eventually, the choice of an exponential relationship stems from the rather limited protection offered by forests against natural hazard during the primary steps of forest colonisation (Wohlgemuth et al., 2017) versus the maximum protection offered when reforestation of

the avalanche path is complete.

Case III: It is assumed that both μ and ξ depend on the forest fraction, combining the models corresponding to Cases I II. Results are analysed and discussed for g=0.6 and b=0.5.

Note that, due to the specification of cases I-III, for f_k=$\bar{f}$=0.35, friction coefficients, and, hence, results of Sect. 3.2. remain unchanged, so that no further simulation campaign is necessary. For all other forest fractions and in each case, 10,000 avalanches are simulated to reconstruct the joint distribution of model input-outputs according to Equation4.11. Subsequently, return periods, confidence intervals, and impact pressures are computed based on Equation 4.12-4.15.

4.3.4 Avalanche risk evaluation

Risk in the natural hazard field is defined as the expected damage resulting from the interaction between a damageable phenomenon and a vulnerable exposed entity. According to Eckert et al. (2012), the specific (dimensionless) avalanche risk r_z for an element at risk z is:

$$r_z = \lambda \int p(y) V_z(y) dy, \tag{4.18}$$

where $V_z(y)$ is the vulnerability of the element z to the avalanche magnitude y. Favier et al. (2014b) further shows that this generic expression can be rewritten at abscissa x_b as:

$$r_z(x_b) = \lambda \int p(P|x_b \leq x_{stop}) p(x_b \leq x_{stop}) \times V_z(P) dP. \tag{4.19}$$

Here, avalanche magnitude distribution corresponds to the joint distribution of runout distances x_{stop} and pressures P i.e. $p(P, x_{stop})$=$p(P|x_b \leq x_{stop})p(x_b \leq x_{stop})$ where $p(P|x_b \leq x_{stop})$ is the pressure distribution at abscissa x_b knowing that x_b has been reached by an avalanche and $p(x_b \leq x_{stop})$ is the probability for an element at x_b to be reached by an avalanche. To assess the evolution of avalanche risk to settlements we consider at x=1840 m a typical mountainous dwelling house. Its overall vulnerability is determined by the failure probability of its most vulnerable part, i.e. the wall facing the avalanche (Favier et al., 2014a). Within a reliability framework, Favier et al. (2014a) evaluated vulnerability curves for such typical buildings impacted by snow avalanches. This was done by modelling the response of a reinforced concrete (RC) wall impacted by a uniform dense avalanche flow under the assumption of a quasi-static loading. These curves were obtained for various building types and for different limit state definitions: the elastic limit state (ELS), the ultimate limit state (ULS), the accidental limit state (ALS) and Collapse (YLT). The elastic limit state (ELS) represent the upper limit of the elastic phase beyond which cracks begin to form and the concrete develops a non-linear behavior (Bertrand et al., 2010). At this point the structure can still carry loads and the damage is considered low. Under continuously increasing pressure, the tensile crack will grow until the concrete or the steel reach respectively the ultimate compression strain and ultimate tensile strain (Favier et al., 2014a), thus announcing the reach of the ultimate limit state (ULS) and the onset of steel yield (plastic (permanent) deformation inside the steel). The accidental limit state (ALS) is considered to ensure that the structure can withstand accidental events (statistically less likely to occur) e.g. explosions. Finally, yield lines or macro-cracks form through the member leading to the collapse of the structure (YLT: yield line theory). For more details refer

to Appendix C and Favier et al. (2014a). In this study, we consider ten building types and the four limit state definitions. This results in a large set of 40 vulnerability relations (Appendix C) providing the probability for the considered building type to surpass the considered limit state (i.e. the failure probability) when subjected to a given avalanche impact pressure. This large set allows studying in a robust way how risk to buildings varies with forest cover within the path, and, notably, how different combinations of building types and forest fractions can result in given risk levels.

4.4 Results

4.4.1 Control of runout distance and impact pressure distributions by forest fraction

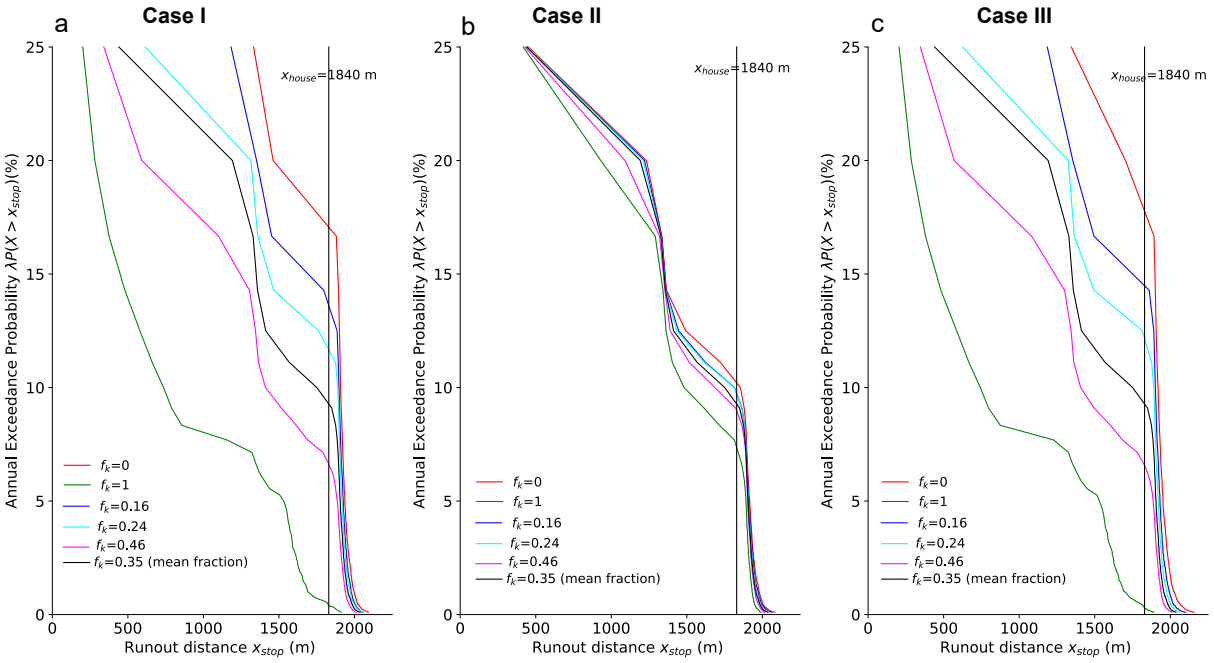

Figure 4.4: Annual exceedance probability of runout distances for : a) Case I (f_k acts only on the static friction coefficient μ), b) Case II (f_k acts only on the turbulent friction coefficient ξ) and c) Case III (f_k acts on both the static friction coefficient μ and the turbulent friction coefficient ξ). Results are shown for the six forest fractions: f_k=0 (deforestation), 0.16 (as in 1825), 0.24 (as in 1948), 0.35 (mean forest fraction, as in 1980), 0.46 (as in 2017), 1 (complete reforestation). Due to the forest fraction integration model specification (Equation 4.16-4.17), by definition, for $f_k = \bar{f}$) (as in 1980), results are the same in the three cases and correspond to those obtained conditional to local calibration.

The first part of the analysis examines the relationship between a varying forest fraction and runout distances. From the data in Figure 4.4, it is apparent that the annual probability of an avalanche exceeding the house abscissa $x_{house} = 1840m$ significantly decreases with an

increasing forest fraction. The largest variation is in case III (the forest fraction was introduced as a parameter impacting both the static friction μ and the turbulent friction ξ), followed very closely by case I (forest fraction acts on μ), whereas modification is much lower in case II (the forest fraction is linked to the velocity dependent friction ξ). Considering the two extremes situations f_k=0 (deforestation) and f_k=1 (complete reforestation), this correspond to shifts from a 17.6% annual exceedance probability (f_k=0) to 0.25% (f_k=1) (Figure 4.4c) in Case III, from 17% (f_k=0) to 0.36% (f_k=1) (Figure 4.4a) in Case I, and from 10% (f_k=0) to 7% (f_k=1) only in case II (Figure 4.4b). From a temporal point of view, focusing on changes that actually occurred within the path, for Cases I and III, the probability of an avalanche exceeding the house abscissa $x_{house} = 1840m$ decreased from 14% in 1825 (f_k=0.16) to 6% 2017 (f_k=0.46) (Figure 4.4a,c), whereas in 1980 (f_k=0.35, mean forest fraction for the study period) it was around 9%. Eventually, note that, along the path, the runout exceedance probability varies more with forest fraction for abscissas $\leqslant$ 1840 m than for abscissas $>$ 1840 m (Figure 4.4).

With the mean forest fraction corresponding to 1980 ($f_k = \bar{f} = 0.35$), the return period is 11 years for events reaching the x_{house}=1840 m abscissa. Logically given the changes observed for exceedence probabilities, Case III (Figure 4.5f) and I (Figure 4.5d), have the largest impact on the return period at $x_{house} = 1840$, whereas case II (Figure 4.5e) leads to the lowest variations. For the two extreme situations f_k=0 (deforestation) and f_k=1 (complete reforestation), T rises from 5.7 years (Case III, f_k=0) to T= 393 years (Case III, f_k=1), from 5.9 years (Case I, f_k=0) to T=273 years (Case I, f_k=1) and from T=10 years (Case II, f_k=0) to T=14 years (Case II, f_k=1) only (Figure 4.5e). From a temporal point of view, for Case I and III, events reaching X_{house} had a return period of around 7 years in 1825 which rose to 15.5 years in 2017 (Figure 4.5a,c,d,f). In general, largest variations in the runout distance -return period relationship with the forest fraction are for runout abscissas $\geq$ 1600m, namely the compete bottom of the path where the return period increases strongly with abscissa (Figure 4.5 a,b,c). All Monte Carlo confidence intervals are very small (Figure 4.5d,e,f), showing that the number of simulations performed is largely enough to highlight significant changes of runout distance distributions with forest fractions.

Figure 4.6 shows the annual probability of occurrence of pressure values at three distinct positions of the avalanche path, for all cases and forest fractions studied. The annual probability for an impact pressure $\geqslant$ 30 kpa at x_{house} varies between 5%-20% for all cases, except for complete reforestation (f_k=1) in Case I and III where it drops to nearly 0 (Figure 4.6a,d). Considering the two extreams $f_k = 0$ (deforestation) and $f_k = 1$ (complete reforestation), the annual exceedance probability at x_{hous}=1840 m $p(Pressure_{house} \geqslant 30$ kpa) varies from 16% (f_k=0) to 0.2% (f_k=1) for Case I, and from 18% (f_k=0) to 0.1% (f_k=1) for Case III (Figure 4.6 a,d). Here also, Case II has no large impact on the annual exceedance probability compared to the other two cases since $p(\text{Pressure}_{house} \geqslant 30$ kpa) varies from 9% (f_k=0) to 5% (f_k=1). From the temporal point of view, for Case I and Case III, the annual probability of impact pressures $\geqslant$ 30 kpa at x_{house} decreased from around 13% in 1825 (f_k=0.16) to 5% in 2017 (f_k=0.46) (Figure 4.6 a,d), whereas in 1980 ($f_k = \bar{f} = 0.35$) it was 7.6%. Again, 95% confidence intervals demonstrate the significance of changes according to the simulation sample size (Figure 4.6d). Regarding the location within the path, high impact pressures are more likely to occur in the propagation zone i.e. at 1000 m (Figure 4.6b), followed by the runout zone, here represented by the house abscissa x_{house} = 1840 m (Figure 4.6c) and finally in the starting zone at x=400

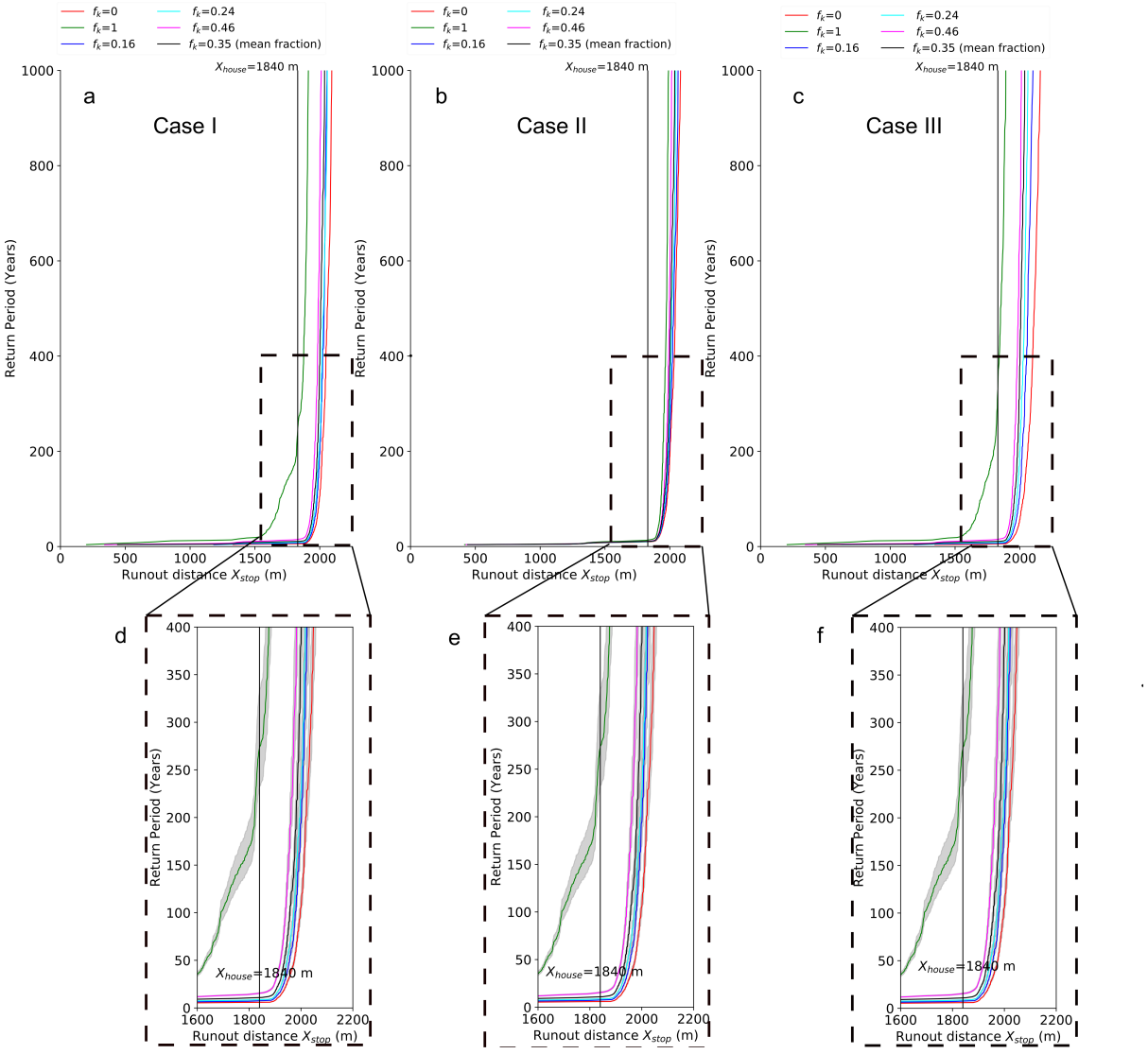

Figure 4.5: One-to-one relation between runout distances and return periods for a) Case I (f_k acts only on the static friction coefficient μ), b) Case II (f_k acts only on the turbulent friction coefficient ξ) and c) Case III (f_k acts on the static and turbulent friction coefficient μ and ξ respectively). d,e and f) Close up on the one-to-one relation between runout distances $>$ 1600 m and return periods, and the associated ■ 95% confidence intervals for the return period (Equation 4.14). Results are shown for six forest fractions: f_k=0 (deforestation), 0.16 (as in 1825), 0.24 (as in 1948), 0.35 (mean forest fraction, as in 1980), 0.46 (as in 2017), 1 (reforestation). Due to the forest fraction integration model specification (Equation 4.16-4.17), by definition, for $f_k = \bar{f}$) (as in 1980), results are the same in the three cases and correspond to those obtained conditional to local calibration.

m (Figure 4.6a). For example, in 1980 (f_k=0.35, i.e. the mean forest fraction), the annual probability of pressures exceeding 250 Kpa was 4% at x=1000, 2% at x=1840 m and 1% at x=

400 m (Figure 4.6). In general, results show that, for all three positions, the annual probability of having high pressures decreases with higher forest fractions, with Cases III and I leading to the largest changes with forest fraction (Figure 4.6).

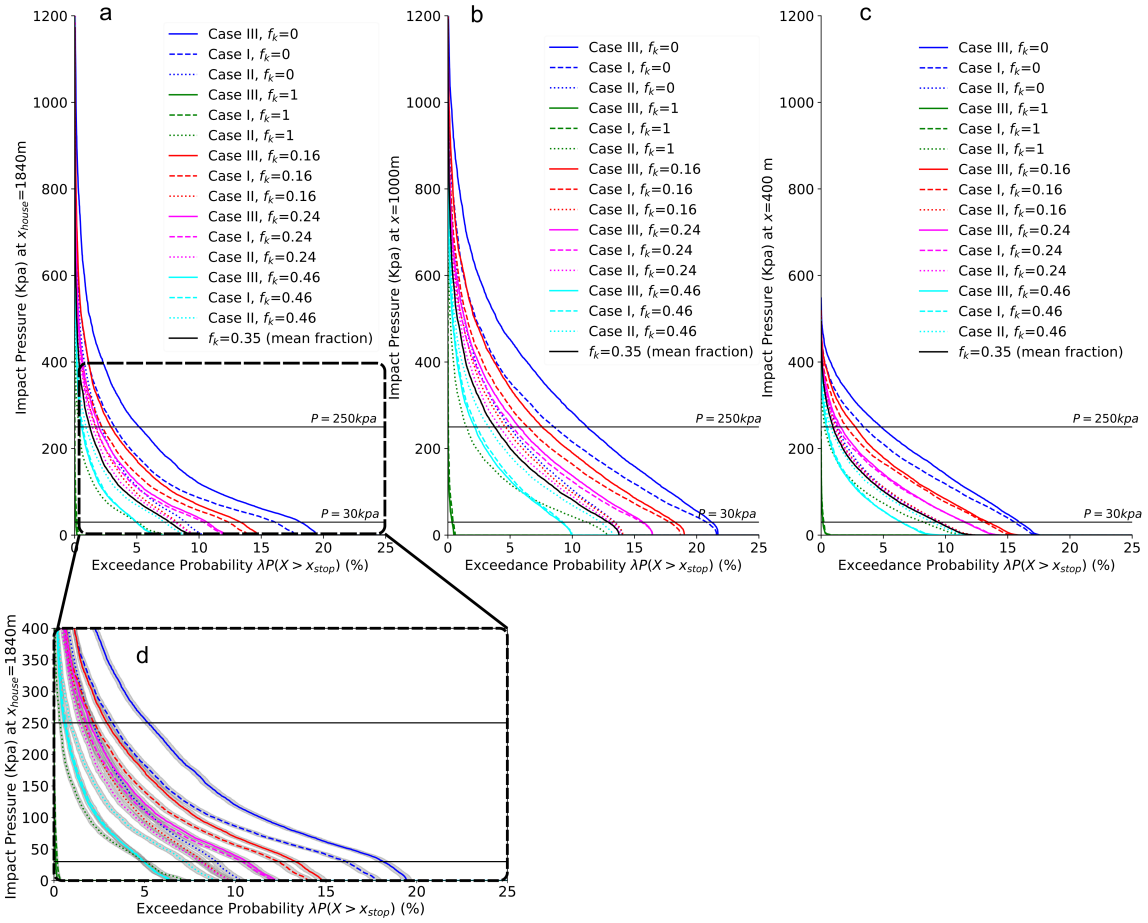

Figure 4.6: Annual exceedance probability of impact pressure modeled for the three cases I (f_k acts only on the static friction coefficient μ), II (f_k acts only on the turbulent friction coefficient ξ) and III (f_k acts on both the static and turbulent friction. Results are provided for three abscissa positions within the path: a) at x_{house} = 1840 m located in the runout zone, b) x=1000 m within the propagation zone and c) x=400 m located in Zone I (release area) (Figure 4.1d). d). Close up on the annual exceedance probability of impact pressure at x_{house} = 1840 m, and the associated ▪ 95% confidence intervals. Results are shown for the six forest fractions: f_k=0 (deforestation), 0.16 (as in 1825), 0.24 (as in 1948), 0.35 (mean forest fraction, as in 1980), 0.46 (as in 2017), 1 (complete reforestation). Due to the forest fraction integration model specification (Equation 4.16-4.17), by definition, for f_k= $\bar{f}$) (as in 1980), results are the same in the three cases and correspond to those obtained conditional to local calibration.

4.4.2 Control of risk for buildings by forest fraction

Figure 4.7 depicts the risk for the house located at x=1840 m (T=11 years in 1980, $f_k = \bar{f} = 0.35$), for all building types and the four limit sates. At this location, in 1980, avalanche risk was between 0.03 and 0.08 depending on the considered limit state and building type (Figure 4.7). Unsurprisingly given the definition of the limit states, for all building types and for a given forest fraction, the ELS (Figure 4.7a) based risk > ULS risk (Figure 4.7b) > ALS risk (Figure 4.7c) > YLT based risk (Figure 4.7d). The strongest building type is the building VIII with four clamped edges and the weakest is configuration IV i.e. one free and three simply supported edges (Figure 4.7). Overall, the weakest buildings include at least one free edge, whereas the strongest have at least two clamped and no free edges (Figure 4.7).

From the results, it is immediately clear that, for a given building type and limit state, the risk decreases with an increasing forest fraction. Yet, whereas the ELS based risk to all building types vary almost similarly with forest fraction in all cases (Figure 4.7a), for the other failure states (Figure 4.7b,c,d), risk varies according to the building type, the considered case and forest fraction in a more complex way. Considering the two extreme situations f_k=0 (deforestation) and f_k=1 (complete reforestation), Case III and I show the largest risk variations according to forest fraction changes for all limit states and building types (Figure 4.7). For example, the annual probability for a building located at x=1840 m to reach the Elastic limit state drops for Case I and III from > 0.16 (f_k=0) to 0.00 (f_k=1), but by no more than 0.03 for case II (Figure 4.7a). From a temporal point of view, between 1825 (f_k=0.16) and 2017 (f_k=0.46), the risk roughly averaged over all building types and limit states decreased by almost 60% for Case I and III and 20% for case II.

4.4.3 Sensitivity to the forest fraction integration model

Sensitivity of our results to the forest fraction integration model was investigated by varying the parameters g and b controlling the degree of impact of the forest fraction on the annual exceedance probability of runout distances (Figure 4.8) and avalanche risk for a building located at x=1840 m (T=11 years in 1980 for $f_k = \bar{f} = 0.35$) (Figure 4.9). The main result is that over the large considered variation ranges, forest fraction changes affect annual probability of exceedance of runout distances and risk for buildings in a rather similar way whatever the values chosen for g (case I) and b (Case II). Obviously, in details, results are slightly shifted when g and b are modified. For example, the higher g, the faster μ values increase with forest fraction, and the faster exceedance probabilities and ultimately risks for building decrease with forest fraction. But more importantly, both in cases I and II, exceedance probability bands for f_k=0 and f_k=1 (in green and blue respectively), never intersect each others (Figure 4.8), which suggest that the forest fraction value has a much more decisive effect on our results than the choice of given g and b value (as soon as a reasonable range is considered).

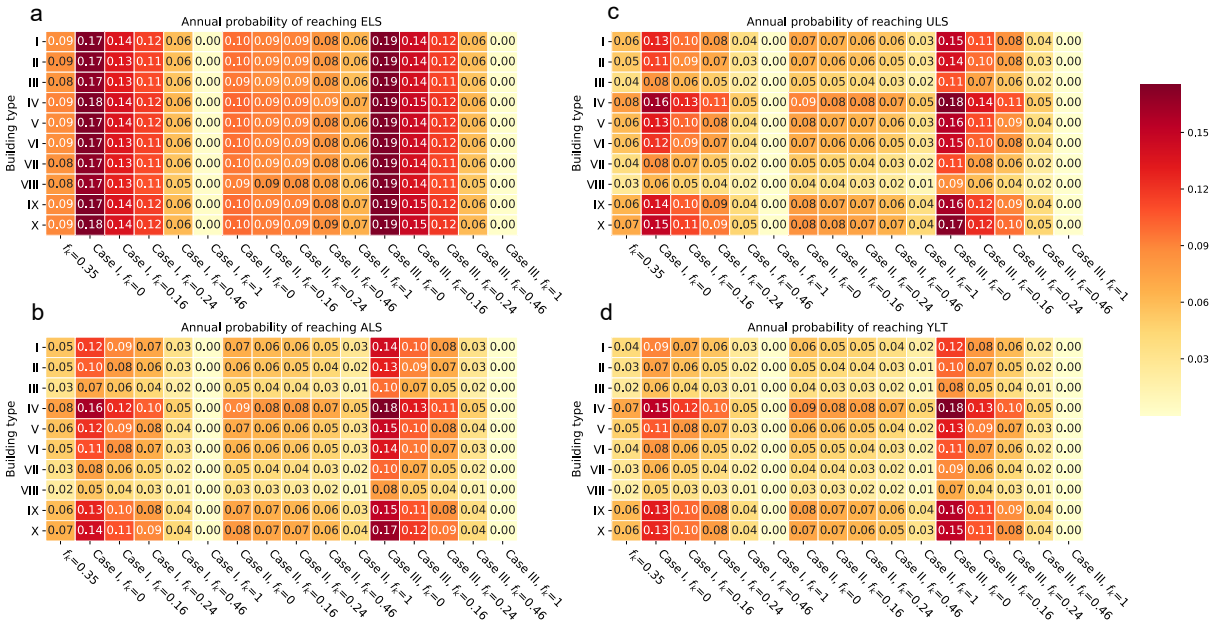

Figure 4.7: Risk i.e annual probability for a building, located at x=1840 m within the Ravin de Côte-Belle avalanche path to reach the limit state considered (Figure 4.10, Appendix C). The analysis considers ten building types (Table 4.3, Appendix C), four limit states and the three forest integration cases I (f_k acts only on the static friction coefficient μ), II (f_k acts only on the turbulent friction coefficient ξ) and III (f_k acts on both the static and turbulent friction coefficient μ and ξ respectively). All forest fractions are considered. Due to the forest fraction integration model specification (Equation 4.16-4.17), by definition, for $f_k = \bar{f}$) (as in 1980), results are the same in the three cases and correspond to those obtained conditional to local calibration.

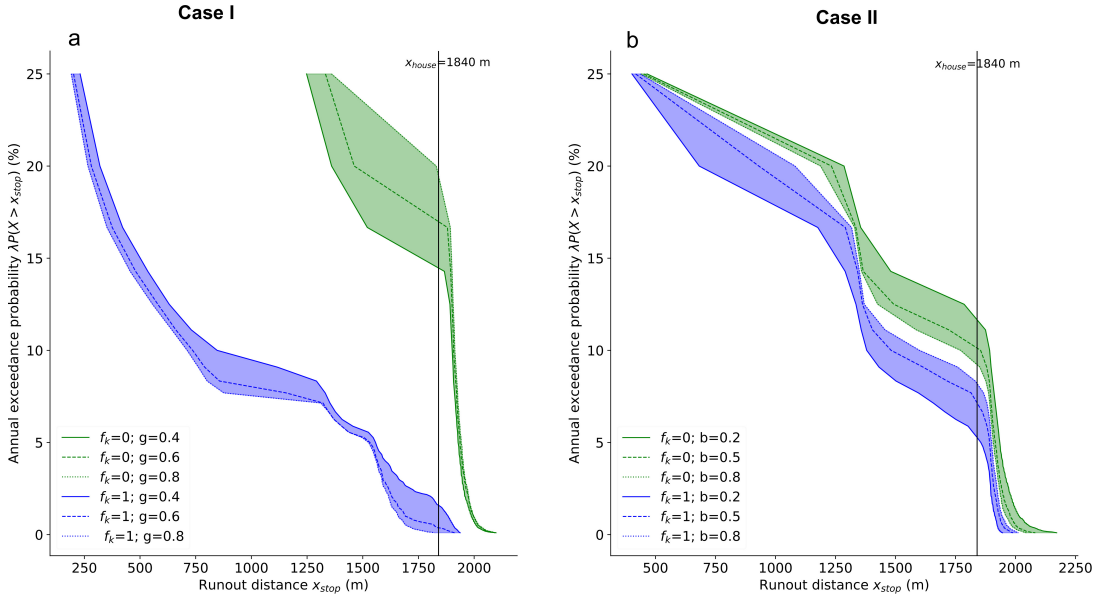

Figure 4.8: Sensitivity of the annual exceedance probability of runout distances to the forest fraction integration model in a) Case I (f_k acts only on the static friction coefficient μ) and b) Case II (f_k acts only on the turbulent friction coefficient ξ). g and b are the parameters representing the dependency of μ and ξ on the forest fraction f_k, respectively. ▫ represent the annual exceedance probability band delimited by g=0.8 and g=0.4.▫ represent the annual exceedance probability band delimited by b=0.8 and b=0.2. Only the two extreme forest fractions are considered, i.e. deforestation (f_k=0) and complete reforestation (f_k=1).

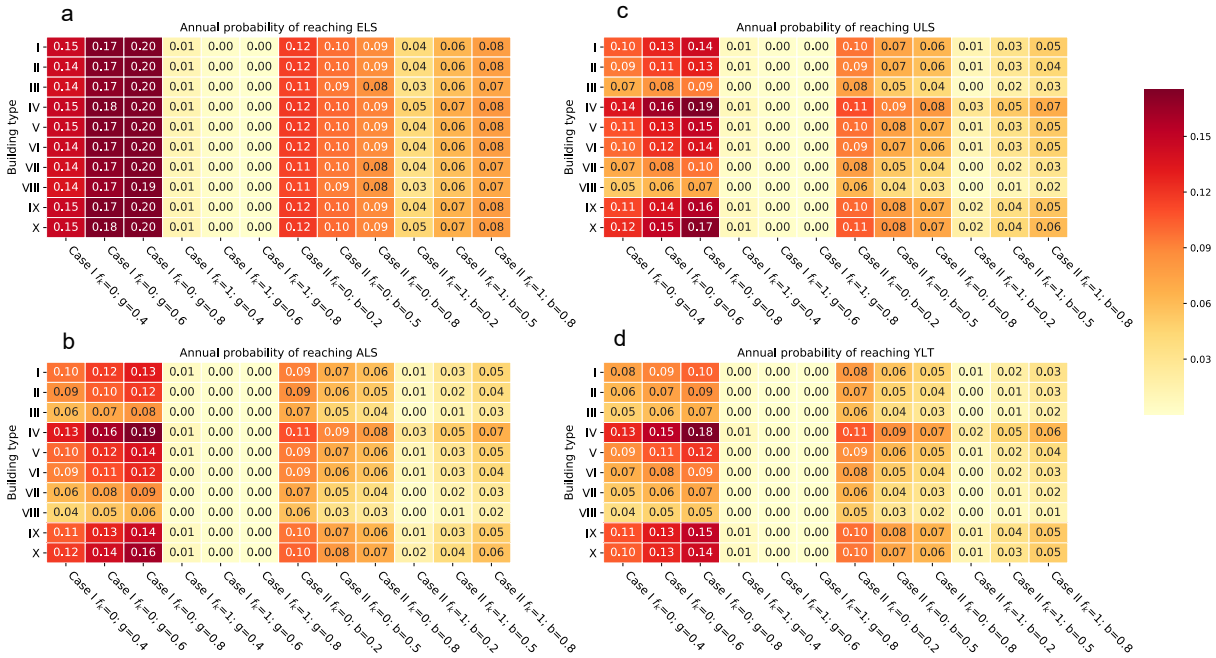

Figure 4.9: Risk sensitivity to the forest fraction integration model. Risk is the annual probability for a building located at x=1840 m within the Ravin de Côte-Belle avalanche path to reach the limit state considered. The analysis considers ten building types, four limit states, and the two forest integration cases I (f_k acts only on the static friction coefficient μ) and II (f_k acts only on the turbulent friction coefficient ξ). g and b are the parameters representing the dependency of μ and ξ coefficients on the forest fraction f_k, respectively. Only the two extreme forest fractions are considered, i.e. deforestation (f_k=0) and complete reforestation (f_k=1).

4.5 Discussion

4.5.1 Avalanche risk changes with changes in forest cover

This study aimed at assessing the impact of the changes in the forest fraction on avalanche hazard and risk to a building located at x= 1840 m in the Ravin de Côte-Belle path (Queyras massif). Unsurprisingly, our findings showed, for an increasing forest fraction, a decrease in $p(X_{stop} \geq x_{house}$= 1840 m) (increase in return period) (Figure 4.4), probability of high impact pressures at the house abscissa (Figure 4.6a) and eventually avalanche risk (Figure 4.7). All these results originated from the combined effect of the forest fraction on runout distances and velocities, i.e. increasing f_k both reduces the annual runout probability and the velocity conditional to reach, which results in decreased annual pressure probabilities, and, ultimately, lower risk levels. These results are in line with previous studies notably Teich and Bebi (2009) whom also highlighted a decrease in avalanche risk linked to the spatial variability of the forest cover. Hence, using a more systematic risk-based methodology, we confirm the importance of the protective role of forests against snow avalanches.

From a temporal perspective, we showed that the probability for a snow avalanche reaching

the building decreased by almost half between 1825 and 2017 as a result of path's afforestation (forest fraction tripled between 1825 and 2017). Consequently, avalanche risk for buildings also decreased by more than a half (Figure 4.7). This is consistent with the findings of Mainieri et al. (2020) and Zgheib et al. (in revision) regarding the evolution of hazard and risk, respectively, in the Queyras massif. These authors showed that both avalanche hazard and risk decreased sharply after 1950, linked to reforestation of the avalanche paths, the latter being a result of the socio-economic transitions (i.e. abandonment, tourism and changes in forest policies) that took place in the Queyras massif (Granet-Abisset, 1991) and the Alps in general (MacDonald et al., 2000) since around mid-nineteenth century. It is therefore likely that, in the Queyras massif, avalanche risk trends similar to the one we highlight exist in many paths that went through the same intense reforestation process. Extrapolation beyond the Queyras massif is more difficult seeing that, despite common global socio-economic and environmental transitions in the mountains of the world, local disparities are always present and they highly impact the trajectory evolution of hazard and risk (Zgheib et al., in revision). Hence, similar studies should now be conducted in other massifs to indicate to which extent our findings applies to wide mountain areas or not. Given i) the very strong decrease in risk our integrated quantitative methodology was able to identify, ii) the current lack of consideration of temporal changes in reference risk levels with land use and climate (Eckert et al., 2018), such studies would be of outermost importance for improving both safety and sustainability of mountain communities.

4.5.2 A potential for combined nature-based and structural protection measures

Avalanche risk was assessed for ten different building types and four limit states for reinforced concrete. It was quite a surprise to find that avalanche risk to all building types is relatively similar if the elastic limit state is considered as the failure mode. The latter suggest that preventing the elastic failure of the wall is independent of the building configuration, and highly controlled by a well managed protection forest. However, this is only valid for avalanches with an impact pressure $\leq$ 36 kpa i.e. the maximum impact pressure needed for the elastic failure of the wall (all configurations considered, Appendix C, Figure 4.11).

Alternatively, for large avalanches exerting higher impact pressures, building type is a decisive factor and the strongest construction type should be adopted for the avalanche facing wall. A combined forest/building configuration scenario could be also considered, where risk reduction is ensured through an array of possible combinations (Figure 4.7)

Typically, avalanche protection structures capable of withholding the flow or inducing runout shortening e.g. avalanche dams could be potentially considered through a decisional framework (Favier et al., 2016). However, considering the impressive temporal evolution of the forest cover in the avalanche path and its proven capacity to reduce risk, the aforementioned can be replaced by greener solutions. However, Ecosystem-based solutions for Disaster Risk Reduction (Eco-DRR) e.g. protective forests combined with structural avalanche protection techniques i.e. snow sheds, snow fences, snow bridges etc., are highly effective in reducing collective risk in dense areas exposed to snow avalanches (Teich and Bebi, 2009). In such case they are an effective, economically viable (Poratelli et al., 2020a) option to be considered for avalanche management.

4.5.3 Dependence of the Voellmy friction coefficients on the forest fraction

To reach our conclusions, a key step of the approach was the representation of the dependency of the Voellmy friction coefficients on the forest fraction. Notably, changing the static friction coefficient μ based on the forest fraction f_k i.e. Case I, had the largest impact on all the studied variables (runout return period, impact pressure and risk) compared to varying the friction coefficient ξ (Case II). This relates to the high sensitivity to changes in μ of runout distances in accordance with previous studies (Barbolini et al., 2000; Heredia et al., 2020). To which extent our results are direct consequences of partially subjective model characteristics is thus debatable. First argument in favor of our choices for the forest/friction dependency is that they are consistent with our statistical-dynamical model structure, i.e. addition of a fixed effect in the linear model for the variable μ and modification of the parameter ξ with an exponential dependency on f_k, as well as with physical and empirical knowledge regarding current values of μ and ξ and their variations with terrain properties. More pragmatically, the sensitivity analysis highlighted that most of the changes in the annual probability of exceedance of x_{house} and in related avalanche risk to buildings are explained by variations in the forest fraction and not by parametric choices. Thus, our results, notably the sharp risk decrease from 1825 to 2017 appear as robust. However, in the future, inclusion of b and g within the calibration of the statistical-dynamical model could be envisaged. At the cost of additional inference difficulties, this would allow a refined analysis of the relationship between the forest fraction and friction parameters, and, ultimately, avalanche risk.

4.5.4 Other pro's and con's of the modelling strategy

In addition to potentially debatable modelling assumptions, this work also suffers from a number of limitations. Notably, the proposed approach does not consider the altitudinal distribution of the forest (Figure 4.2b,c, d,e) and potential changes in its structure. Yet, depending on its position, a protection forest can either stabilize the snow and prevent avalanching (Salm, 1978; Viglietti et al., 2010) (location in the starting zone of the avalanche), or decelerate a flowing avalanche (Anderson and McClung, 2012) (location in runout or propagation zone). The latter depends on forest structural characteristics and on the magnitude of the avalanche (small, medium, large; not considered in the current study). For example, large avalanches initiating way above the timberline are though to destroy the forest with negligible deceleration (Brang et al., 2006) but noticeable lateral spread (Christen et al., 2010). This statement remains under discussion in light of studies showing that the runout distance of large avalanche can be decreased despite destruction of trees (Takeuchi et al., 2018). Our approach does not engage in this complexity. In addition, since the proposed avalanche-forest friction model does not consider altitudinal distribution of the forest, our results does not reflect the possibility that the avalanche release Zone II is potentially inactive in 2017. This is highly likely considering that in 2017 the density of forest pixels between 1800 m a.s.l and 1900 m a.s.l and above is very high compared with the previous years (Figure 4.2e). These shortcuts could potentially be relaxed in future developments.

By contrast, the novelty of the proposed integrative quantitative approach for the snow avalanche field is clear. It lays in (i) consideration of the full variability of avalanche hazard,

conditional on the temporal evolution of forest fraction in the avalanche path through comprehensive hazard statistical-dynamical modeling, (*ii*) taking into account different building types and failure states in the evaluation of risk changes. This step forward with regards to the state of the art successfully highlights the local decrease in avalanche risk for buildings according to observed changes in forest cover, features the important protective capacity of forests against snow avalanches, and points towards the potential of different forest cover/configuration of the building combinations to manage and reduce risk to the desired level.

4.6 Conclusion and further outlooks

This study proposed an innovative integrative risk analysis methodology to evaluate diachronic risk estimates that account for land cover changes within the avalanche path in a comprehensive way. First, a Bayesian statistical-dynamical model was expanded to account for multiple release areas, and then locally calibrated for the Ravin de Côte-Belle avalanche path in Abriès (Queyras massif, French Alps). Changes in the distribution of avalanche hazard were then evaluated according to the observed changes in the aerial percentage of the terrain covered by forests. Results were eventually combined with reinforced concrete fragility curves for different types of buildings and failure states. This allowed quantifying to which extent avalanche hazard and risk to buildings decreases with increasing forest fraction. Notably, between 1825 and 2017, avalanche risk in the Ravin de Côte-Belle decreased by 20%-60% depending on how forest cover is accounted for in avalanche statistical-dynamical modelling. In addition, we showed that the decrease in risk depends not only on the forest fraction but also on the construction technology used for the building in the avalanche path. This should, in the future, allow objective cost/benefit analysis of the economic viability of protection forests versus structural mitigation measures (Moos et al., 2018). It could also facilitate the set up of successful disaster risk reduction strategies that consider the building technology used, along with the type of avalanche protection (i.e. forest, structural measures or combination of the latter) to ensure the reduction of risk to acceptable level, namely intelligently combine Eco-DRR and technical protection measures in order to fulfill stakeholders needs.

Even more widely, in the future, scientists predict an increase in risks due to natural hazards in high mountain areas (Ballesteros-Cánovas et al., 2018; Hock et al., 2020). Since evolution of avalanche risk depends on the interactions between hazard, exposure and vulnerability driven by socio-economic, land cover and climatic drivers (Zgheib et al., 2020, in revision), dynamic quantitative risk assessment should become the basis of future disaster risk reduction, mitigation plans and policies. Although being arguably a first step, our approach is still far from this ambitious objective. We indeed considered only the impact of the temporal evolution of forest on risk, and through partially ad-hoc simulations. The latter limitation could be addressed, as suggested above, by calibrating the link between the forest fraction and the Voellmy friction coefficients. However, to take into account the combined effect of a changing climate and land cover on avalanche hazard, the current model should now be made more explicitly non-stationary to derive frequency-magnitude relationship changing over time in a comprehensive and realistic way. Combined with elements at risk evolving in terms of vulnerability and/or exposition as function of socio-economic transitions, this would provide crucial support to the great challenge

of adaptation.

4.7 Appendix

4.7.1 Appendix A: Data collected for mapping forest cover evolution

Table 4.2 introduces the set of aerial photographs and old maps used for the analysis of the evolution of the forest fraction in the Ravin de Côte-Belle avalanche path.

Table 4.2: Source data for mapping forest cover evolution at Ravin de Côte-Belle avalanche path from 1825 to 2017. IGN is the French National Geographical Institute

Year	Data type	Scale/ resolution	Source
1825	Cadastral map	1/1250	Cadastral service of the Hautes-Alpes department
1948	Black-and-white aerial photographs	0.5 m	IGN
1980	Black-and-white aerial photographs	0.5 m	IGN
2017	Color aerial photographs	1.5 m	IGN

4.7.2 Appendix B: Frequentist inference of the mixture model for the release position

According to the topography of the Ravin de Côte-Belle avalanche path, x_{start} is modeled as a Binomial mixture of two Beta distributions (Equation 4.5). The five parameters of the mixture, α_1, α_2, β_1, β_2 and p, are estimated using the method of moments as follows:

$$\hat{p} = P(x_{start_i} \in [x_{min_1}, x_{max_1}]) = \frac{n_1}{N} \tag{4.20}$$

where N is the total number of avalanches considered for the calibration of the magnitude model (i.e. 17 avalanches at the study site), and, among these, n_1 is the number of avalanches released from Zone I (i.e. 13 avalanches at the study site).

Inversion of the standard formula for the mean and variance of a Beta distribution as function of its parameters leads:

$$\begin{aligned}
\hat{\alpha_1} &= \bar{X_1}(\frac{\bar{X_1}(1-\bar{X_1})}{v_1} - 1) \\
\hat{\alpha_2} &= \bar{X_2}(\frac{\bar{X_2}(1-\bar{X_2})}{v_2} - 1) \\
\hat{\beta_1} &= (1-\bar{X_1})(\frac{(\bar{X_1}(1-\bar{X_1}))}{v_1} - 1) \\
\hat{\beta_2} &= (1-\bar{X_2})(\frac{(\bar{X_2}(1-\bar{X_2}))}{v_2} - 1)
\end{aligned} \tag{4.21}$$

where $\bar{X_1}$, $\bar{X_2}$, v_1, v_2 are, respectively, the empirical mean and variance of normalized release positions in Zone I and II calculated as follows:

$$\begin{aligned} \bar{X_j} &= \frac{1}{n_j}\sum_{i=1}^{n_j} X_{norm_j} \\ v_j &= \frac{1}{n_j}\sum_{i=1}^{n_j}(X_{norm_j} - \bar{X_j})^2 \end{aligned} \tag{4.22}$$

where n_j is the number of avalanches released in the specific release zone j ($n_1 = 13$ and n_2=4 at the study site).

4.7.3 Appendix C: Fragility curves for RC buildings exposed to snow avalanches

Figure 4.11 represents the fragility curves obtained by Favier et al. (2014a) using reliability analysis, considering four failure limit states of the reinforced concrete (RC) wall facing the avalanche for ten different building configurations (Table 4.3). These four limit states (q_{Elas}, q_{ULS}, q_{ALS}, q_{YLT}) are defined in the stress-displacement graph in Figure 4.10. The loading pressure is the sole avalanche magnitude variable considered.

Table 4.3: The ten RC building types considered, defined by the boundary conditions applying to the wall facing the avalanche. Each of these conditions, once a limit state is chosen, leads a specific fragility curve usable as input for risk assessment (Favier et al., 2014a).

Building type	Boundary condition
I	four simply supported edges
II	simply supported on the two large edges, clamped on the two small edges
III	simply supported on one large edge, clamped on the three other edges
IV	one free large edge , simply supported on the three other edges
V	one free large edge , clamped on the three other edges
VI	clamped on the small edge, simply supported on the three other edges
VII	simply supported side by side, clamped on the two other edges
VIII	four clamped edges
IX	One free large edge, one clamped large edge, simply supported on the two small edges
X	One free large edge, one simply supported large edge clamped on the two small edges

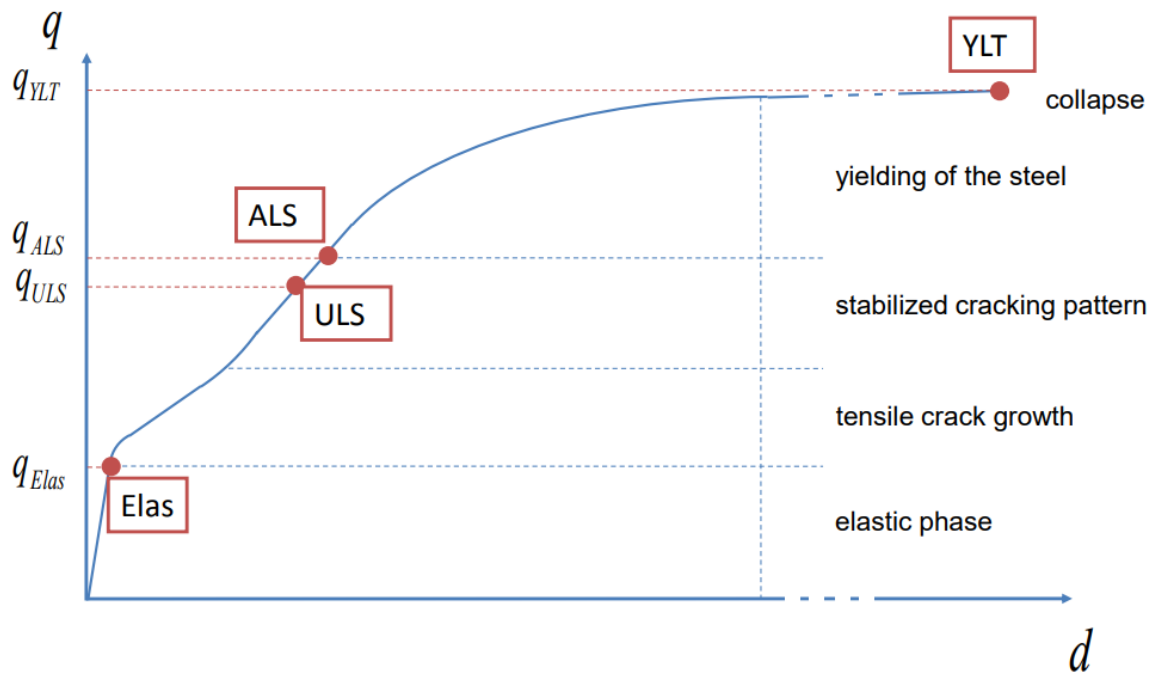

Figure 4.10: Generic stress-displacement representation of a RC wall subject to quasi-static avalanche loading, with loading pressure as the sole stress variable considered. The diagram highlights the four limit states considered: Elas (elastic limit state), ULS (ultimate limit state), ALS (accidental limit state), YLT (yield line theory, collapse of the building), each of them leading to a specific fragility curve for a given building type (Favier et al., 2014a)

.

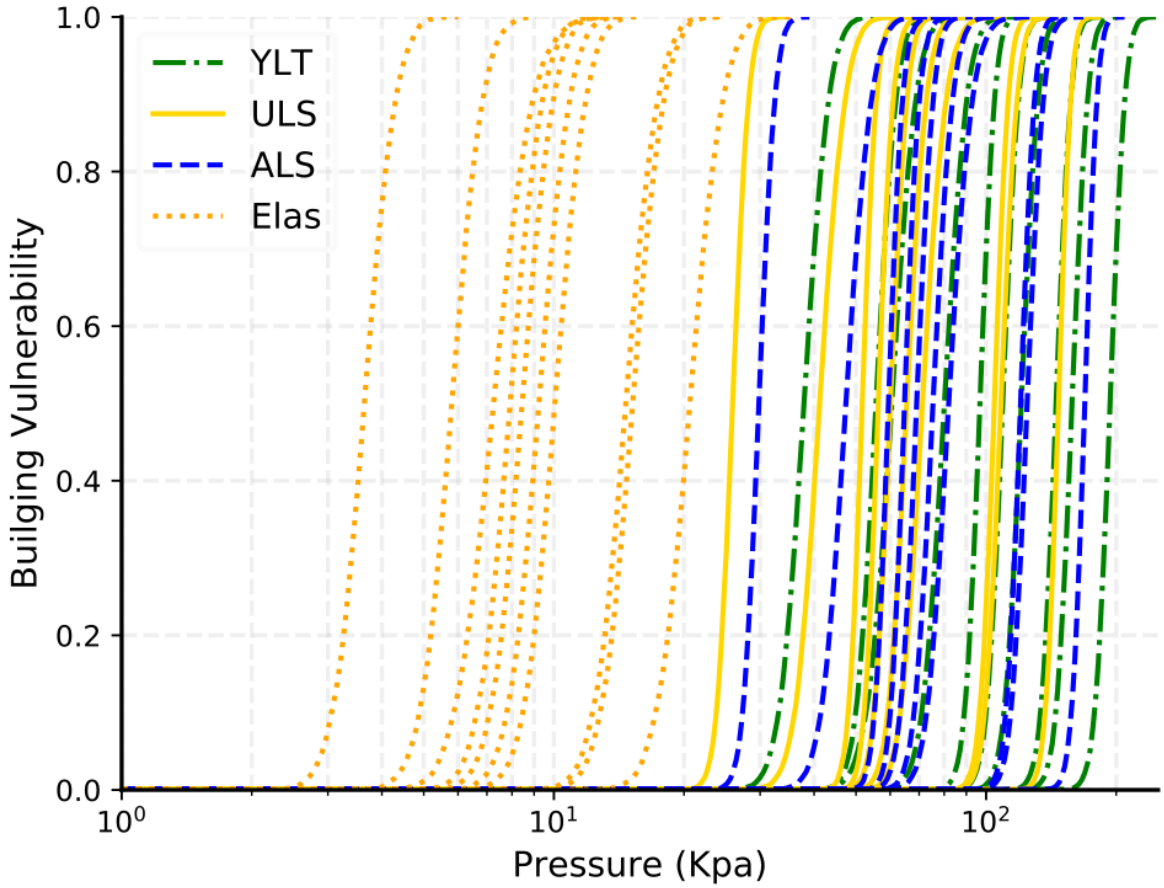

Figure 4.11: The 40 vulnerability relations for RC buildings subject to quasi-static avalanche loading considered in this study. Each of them corresponds to one of the four limit state and one of the ten boundary conditions and was obtained using reliability analysis (Favier et al., 2014a).

Chapter 5

Conclusion and perspectives

Contents

5.1 Contributions and main findings

Spatio-temporal trajectories of avalanche risk are influenced by socio-economic, climatic and land cover changes. Understanding avalanche risk changes therefore require integrative assessment techniques mobilizing interdisciplinary knowledge and expertise of various natural and social sciences. On this basis, the aims of this thesis were to (*i*) develop an integrative qualitative approach combining knowledge from natural and social sciences to assess long term changes in avalanche risk and in all its components, hazard, vulnerability and exposure, as function of changes in their socio-economic and environmental drivers, (*ii*) investigate the extent to which local socio-economic, land cover and climatic peculiarities may lead to spatial and temporal disparities in risk trajectories and (*iii*) propose the first quantitative avalanche risk estimates that take into account changes in forest cover within avalanche paths. The three objectives are addressed in three independent articles presented herein in chapter 2, 3 and 4. For each of the latter, the main conclusions are summed-up in the following sections. Finally, the thesis concludes on a series of perspectives towards a more holistic avalanche risk management. All the proposed methodologies are transferable to other natural hazards, notably in wider mountain environments, as a contribution to the elaboration of effective adaptation strategies in a context of increasing risks related to combined socio-economic and environmental transitions.

5.1.1 Holistic spatio-temporal avalanche risk analysis

A holistic risk analysis methodology is introduced in this thesis as an answer to the need (*i*) for integrated studies addressing the different components of avalanche risk and their drivers and (*ii*) studies investigating the spatial variability of risk driven by local disparities in the evolution of the social and natural systems. The methodology is applied to three regions in the French Alps: The upper Maurienne, Valloire, Guil valley.

By combining a large corpus of sources (historical maps, aerial photographs, population data, livestock inventories, snow and climate data) with advanced processing techniques, we inferred the long term evolution of avalanche hazard, vulnerability (exposure) and ultimately risk. As an important part of the analysis, land cover change was assessed from a series of historical maps and aerial photos. Before proceeding to the change detection phase a spatial homogenization was applied for the historical maps based on the Petit and Lambin (2001, 2002) methodology. This step was essential in order to compensate for scale dependency problems of landscape patterns. Thereafter, a series of comparable landscape matrices was created using a bias correction considering 1952 as the common correction year. Land cover analysis was conducted on the scale of the entire upper Maurienne area and in the vicinity of avalanche paths for the three studied areas, thus allowing the inference of avalanche risk to settlements in avalanche paths.

The novelty of the proposed holistic risk analysis methodology lies in the combination of land cover changes, historical, socio-economic and climate data, to assess long term changes in avalanche risk, their components and drivers. To our knowledge, this type of integrative modeling in the snow avalanches field has not been done before. In addition, the proposed map/photos bias assessment and landscape matrix correction is innovative and could be useful for different studies aiming at assessing long term land cover changes, particularly exposed

elements to natural hazards, using heterogeneous data. As for our results, they highlight (*i*) the dynamic nature of hazard, vulnerability and risk linked to socio-economic, land cover and climatic changes and (*ii*) the potential divergence in spatio-temporal risk trajectories linked to small disparities in the aforementioned factors controlling hazard, exposure and vulnerability. Notably, from 1860 to 2017, avalanche risk increased in the upper Maurienne valley, as a result of increased avalanche activity and a surge of the number of exposed elements following the development of the tourism sector. The reforestation that occurred following the agricultural abandonment was insufficient and had no protective effect against snow avalanches. Thus we believe that risk in the upper Maurienne increased as the vulnerability of the settlements exposed to avalanche rose. By contrast, in the Guil valley, avalanche risk locally decreased following a decline in snow avalanche hazard in heavily reforested paths. Eventually, in Valloire, avalanche risk remained rather stationary, since reforestation is incomplete and exposure to snow avalanches is low compared with the upper Maurienne and the Guil valley. This clearly demonstrates that, even if common large scale drivers such as climate warming, afforestation, land abandonment and socio-economic transitions are unambiguous, local dynamics play a crucial role in avalanche risk evolution.

5.1.2 Integrating forests in quantitative avalanche risk assessment

Quantitative risk assessment in the avalanche field mostly neglects the presence of forests in avalanche paths, and their potential effect on avalanche hazard and risk. Thus, to fill this gap, we integrate forest cover changes within an integrated avalanche risk assessment approach to demonstrate how observed changes in forest cover may have affected avalanche hazard and subsequent risk estimates for various types of building-like elements at risk. Herein, the forest fraction f_k is defined as the aerial percentage of the terrain covered by forests within the extension of the avalanche path. Six forest fractions f_k were considered in the analysis. Four of them represent real changes that occurred in the avalanche path analyzed from a combination of aerial photos and old maps for the 1825-2017 period. The other extreme cases f_k=0 (deforestation) and f_k=1 (reforestation) are also considered.

First, the Bayesian statistical-dynamical model of Eckert et al. (2010c) is expanded to account for potentially multiple release areas and is calibrated for the *Ravin de Côte Belle* avalanche path in Abriès (Queyras massif, French Alps) using the chronology of recorded events (1950-2018) acquired from the French Avalanche Permanent Survey (EPA). Then, the local distribution of avalanche hazard is evaluated according to observed changes in the forest fraction. The interaction between forests and avalanches is recognized in avalanche modeling mostly by increasing the total basal friction within the Voellmy friction law. Thus, the parameter f_k representing the forest fraction within the avalanche path was introduced in the simulation phase within three distinct cases, representing in three different scenarios the impact of the forest on the Voellmy friction coefficient μ and ξ. The resulting hazard distributions are then combined with reinforced concrete fragility curves for different types of buildings (Favier et al., 2014b), to assess the diachronic evolution of avalanche risk estimates of a building located at the bottom of the avalanche path.

Results show that the probability of exceedance of runout distances, the impact pressure at the building abscissa and ultimately avalanche risk to the building decreases with increasing

forest fraction. Moving from a forest fraction f_k=1 to f_k=0 decreased avalanche risk on average by 99% for the cases when f_k acts on the static friction parameter μ of the Voellmy law and 53% when f_k acts on the turbulent friction parameter ξ. An important part of the risk reduction occurred in the study area between 1825 and 2017 (60% (f_k acts on the static friction parameter μ) and 20% (f_k acts on the turbulent friction parameter ξ)) when the forest fraction increased from f_k= 0.16 to f_k= 0.46. In addition, and for our studied path, we showed that the decrease in risk depends not only on the forest fraction but also on the construction technology used for the building in the avalanche path. The result can be seen as a step toward successful combination of green-grey (ecosystem-based/engineering solutions) avalanche measures fulfilling the need for maximum protection under budget constraints.

5.2 Perspectives

5.2.1 Holistic qualitative risk modeling

The holistic qualitative avalanche risk analysis proposed in **chapter 2** and expanded in **chapter 3** could be further developed to address the remaining limitations of the approach. For example, the historical series of avalanche events used in the analysis, dating back to ∼1900's, could be completed using older historical information extracted from different archival sources. For instance, Giacona et al. (2017) identified ∼ 700 historical references to avalanche events in the Vosges massif dating back to the 1780. Using mathematical modeling, the aforementioned compiled series of avalanche events was homogenized (Giacona et al., submitted). This process eliminates the effect of data source heterogeneity and human influence on avalanches, keeping only the natural variability of the hazard potentially linked to climate change (Giacona et al., submitted).

In addition, performing a sensitivity analysis on the buffer size, would allow an uncertainty assessment on the number of exposed elements, and, eventually, on snow avalanche risk. As a reminder, the buffer considered in the study is 50 m beyond the current limit of avalanche paths in the local avalanche map. It was created to assess land cover change within avalanche paths.

Finally, integrating defense structures in our analysis is probably one of the most important future studies to be considered. This could allow a more refined analysis of risk evolution that takes into account mitigation efforts.

5.2.2 Toward holistic quantitative avalanche risk analysis

The quantitative avalanche risk assessment performed in **chapter 4** should be developed to include all the drivers of risk and eventually ensure the development of integrative dynamic risk measures. This work would allow the set up of effective mitigation strategies that truly considers the integrative dynamic nature of avalanche risk. For this purpose, below, is an example of a series of developments that could be done.

A better representation of the forest structure in avalanche models: Forest/ avalanche interaction and dynamics vary depending on the size of the avalanche (large, medium, small), forest structural parameters, topography and the distance traveled before penetrating into

forests. Thus, our model could be further developed to (*i*) account for specific forest parameters like stem density and (*ii*) specify the forest location in the avalanche path.

A better understanding of the link between the friction parameters and the forest fraction: The quantitative avalanche risk assessment performed in **chapter 4** considers only in the simulation phase the temporal change of the friction parameters linked to the forest fraction. A further development of the approach would include the forest fraction in the calibration phase. Each avalanche will thus have an additional parameter f_k characterizing the forest fraction within the avalanche path for the year k of the avalanche. The probabilistic models describing the link between the friction parameters μ and ξ and the forest fraction f_k are estimated using the data. From this development we expect better understanding of the effect of the forest cover on the friction parameters of the Voellmy law. Ultimately, this would advance the knowledge on the impact of the forest on avalanche propagation and allow better, more exact quantification of the evolution od avalanche risk.

Non-stationary avalanche modeling: Long term changes in snow avalanche risk result from combined changes in its environmental and social components. Thus, a version of the statistical-dynamical model of Eckert et al. (2010c) explicitly adopted for non-stationarity in avalanche dynamics could be developed. The model would consider non-stationary input/output distributions for the data. For example, the probabilistic models describing the release area, low depth and the friction parameters of the rheological law will be made time-dependent following to robust parametric forms.

5.2.3 Toward integrative quantitative risk modeling

The aforementioned proposed developments, notably the non stationary avalanche modeling, allow the generation of integrative, dynamic risk measures taking into account the simultaneous evolution of all the system components (Figure 4.1). The evolution of vulnerability could be treated through scenarios that consider the presence of protection structures in the avalanche path and a dynamically changing number of exposed elements. Ultimately, results of the complete work would show how risk has evolved in the past as function of hazard changes (linked to land cover and climate change) combined with changes in number and nature of elements at risk (buildings, people, roads, etc.) (linked mostly to socio-economic development) and the protective measures taken by the authorities (land use planning, protection structures, etc.). The latter should provide new complete insights on the evolution of society, the environment and avalanche hazard over a long period of time.

5.3 Final thoughts

Imagine a multi-stage interconnected network of macro-components, representing the social, environmental and climate sphere. Within each sphere, a set of interconnected nodes describing networked structures of individuals, groups, institutions, ecosystems, snow, wind etc., and the ties that connect them. Such network is only a simplification of the complex processes driving risk. Thus, understanding the complexity of risk dynamics begins with the an appreciation of

the processes driving its spatio-temporal trajectories. This is essential to build a more resilient social system, capable of withstanding the future threats posed by natural hazards exacerbated by climate change.

In this PhD we showed the importance of understanding these complex links, and we used the results to infer evolution of risk trajectories, that could be used as a tool for designing better mitigation strategies. However, this is just a very small part of what should be done. Understanding the subtleties of the risk process require long term commitment of a highly interdisciplinary team of researchers dedicated to develop this topic of utmost importance to the current and future societies. I personally hope that this first initiative will be followed by several others, not only for risk analysis, but in all disciplines that require the understanding of complex systems using an interdisciplinary collaboration framework.

Bibliography

R. Ackrill. *Common Agricultural Policy*, volume 9. A&C Black, 2000.

W. N. Adger. Vulnerability. *Global Environmental Change*, 16(3):268–281, 2006. ISSN 0959-3780. doi: 10.1016/j.gloenvcha.2006.02.006. URL http://www.sciencedirect.com/science/article/pii/S0959378006000422.

A. Allix. Philippe ariès, histoire des populations françaises et de leurs attitudes devant la vie depuis le xviiie siècle. *Géocarrefour*, pages 85–86, 1949. ISSN 1164-6284. URL https://www.persee.fr/doc/geoca_1164-6284_1949_num_24_1_6625.

C. Ancey. Avalanches: une approche rationnelle dans la gestion du territoire? In *L'avalanche: une catastrophe-histoire culturelle d'une représentation*, number EPFL-TALK-164635, 2009.

C. Ancey and V. Bain. Dynamics of glide avalanches and snow gliding. *Reviews of Geophysics*, 53(3):745–784, 2015. doi: 10.1002/2015RG000491. URL https://agupubs.onlinelibrary.wiley.com/doi/abs/10.1002/2015RG000491.

C. Ancey, M. Meunier, and D. Richard. Inverse problem in avalanche dynamics models. *Water Resources Research*, 39(4), 2003. doi: 10.1029/2002WR001749.

C. Ancey, C. Gervasoni, and M. Meunier. Computing extreme avalanches. *Cold Regions Science and Technology*, 39(2-3):161–180, 2004. doi: 10.1016/j.coldregions.2004.04.004.

G. Anderson and D. McClung. Snow avalanche penetration into mature forest from timber-harvested terrain. *Canadian Geotechnical Journal*, 49(4):477–484, 2012. doi: https://doi.org/10.1139/t2012-018.

L. Arcuset. Possible paths towards sustainable tourism development in a high-mountain resort. The case of Valloire. *Journal of Alpine Research/ Revue de géographie alpine*, (97-3), 2009. doi: 10.4000/rga.1048.

Arnalds, K. Jónasson, and S. Sigurðsson. Avalanche hazard zoning in iceland based on individual risk. *Annals of Glaciology*, 38:285–290, 2004. ISSN 0260-3055. doi: 10.3189/172756404781814816. URL https://www.cambridge.org/core/article/avalanche-hazard-zoning-in-iceland-based-on-individual-risk/E0EEFB91F67D6A19415B1C0CB4EEAB49.

M. Baatz. Multi resolution Segmentation: an optimum approach for high quality multi scale image segmentation. In *Beutrage zum AGIT-Symposium. Salzburg, Heidelberg, 2000*, pages 12–23, 2000.

H. P. Bader and B. Salm. On the mechanics of snow slab release. *Cold Regions Science and Technology*, 17(3):287–300, 1990. ISSN 0165-232X. doi: 10.1016/S0165-232X(05)80007-2.

D. Baldock, G. Beaufoy, F. Brouwer, and F. Godeschalk. Farming at the margins: Abandonment or redeployment of agricultural land in europe. london/the hague. *Institute for European Environmental Policy (IEEP)/Agricultural Economics Research Institute (LEI-DLO)*, 1996.

J. Ballesteros-Cánovas, D. Trappmann, J. Madrigal-González, N. Eckert, and M. Stoffel. Climate warming enhances snow avalanche risk in the Western Himalayas. *Proceedings of the National Academy of Sciences of the United States of America*, 115(13):3410–3415, 2018. doi: 10.1073/pnas.1716913115. URL https://www.scopus.com/inward/record.uri?eid=2-s2.0-85044403647&doi=10.1073%2fpnas.1716913115&partnerID=40&md5=79e9449dcb50f73d45c07001dd7ec4ee. cited By 23.

B. Barbier. Le tourisme rural montagnard. Le cas des Hautes-Alpes. *Méditerranée*, 69(4-1989): 5–7, 1989. ISSN 0025-8296. doi: 10.3406/medit.1989.2969.

M. Barbolini, U. Gruber, C. J. Keylock, M. Naaim, and F. Savi. Application of statistical and hydraulic-continuum dense-snow avalanche models to five real european sites. *Cold Regions Science and Technology*, 31(2):133–149, 2000. ISSN 0165-232X. doi: 10.1016/S0165-232X(00)00008-2.

M. Barbolini, F. Cappabianca, and R. Sailer. Empirical estimate of vulnerability relations for use in snow avalanche risk assessment. *WIT Transactions on Ecology and the Environment*, 77, 2004a. doi: 10.2495/RISK040481.

M. Barbolini, F. Cappabianca, and F. Savi. Risk assessment in avalanche-prone areas. *Annals of Glaciology*, 38:115–122, 2004b. ISSN 0260-3055. doi: 10.3189/172756404781815103.

M. L. Barker. Traditional landscape and mass tourism in the Alps. *Geographical Review*, 72(4): 395–415, 1982. doi: 10.2307/214593.

P. Bartelt and V. Stöckli. The influence of tree and branch fracture, overturning and debris entrainment on snow avalanche flow. *Annals of Glaciology*, 32:209–216, 2001. doi: 10.3189/172756401781819544.

P. Bartelt, B. Salm, and U. Gruber. Calculating dense-snow avalanche runout using a voellmy-fluid model with active/passive longitudinal straining. *Journal of Glaciology*, 45(150):242–254, 1999. ISSN 0022-1430. doi: 10.3189/S002214300000174X.

J. C. Bathurst, B. Fahey, A. Iroumé, and J. Jones. Forests and floods: using field evidence to reconcile analysis methods. *Hydrological Processes*, 2020. doi: 10.1002/hyp.13802.

G. Battipaglia, U. Büntgen, S. P. J. McCloskey, O. Blarquez, N. Denis, L. Paradis, B. Brossier, T. Fournier, and C. Carcaillet. Long-term effects of climate and land-use change on larch budmoth outbreaks in the French Alps. *Climate Research*, 62(1):1–14, 2014. doi: https://doi.org/10.3354/cr01251.

P. Bebi, D. Kulakowski, and C. Rixen. Snow avalanche disturbances in forest ecosystems—State of research and implications for management. *Forest ecology and Management*, 257(9):1883–1892, 2009. doi: https://doi.org/10.1016/j.foreco.2009.01.050.

P. Bebi, R. Seidl, R. Motta, M. Fuhr, D. Firm, F. Krumm, M. Conedera, C. Ginzler, T. Wohlgemuth, and D. Kulakowski. Changes of forest cover and disturbance regimes in the mountain forests of the Alps. *Forest Ecology and Management*, 388:43 – 56, 2017. ISSN 0378-1127. doi: https://doi.org/10.1016/j.foreco.2016.10.028. Ecology of Mountain Forest Ecosystems in Europe.

M. Beniston, D. Farinotti, M. Stoffel, L. M. Andreassen, E. Coppola, N. Eckert, A. Fantini, F. Giacona, C. Hauck, M. Huss, H. Huwald, M. Lehning, J.-I. López-Moreno, J. Magnusson, C. Marty, E. Morán-Tejéda, S. Morin, M. Naaim, A. Provenzale, A. Rabatel, D. Six, J. Stötter, U. Strasser, S. Terzago, and C. Vincent. The european mountain cryosphere: a review of its current state, trends, and future challenges. *The Cryosphere*, 12(2):759–794, Mar. 2018. ISSN 1994-0424. doi: 10.5194/tc-12-759-2018.

S. B. Bergua, M. Á. P. Piedrabuena, and J. M. Alfonso. Snow avalanches, land use changes, and atmospheric warming in landscape dynamics of the Atlantic mid-mountains (Cantabrian Range, NW Spain). *Applied Geography*, 107:38–50, 2019. doi: 10.1016/j.apgeog.2019.04.007.

C. Berlin, F. Techel, B. K. Moor, M. Zwahlen, R. M. Hasler, and S. N. C. study group. Snow avalanche deaths in Switzerland from 1995 to 2014—Results of a nation-wide linkage study. *PLoS one*, 14(12), 2019. doi: 10.1371/journal.pone.0225735.

A. Bernués, J. L. Riedel, M. A. Asensio, M. Blanco, A. Sanz, R. Revilla, and I. Casasús. An integrated approach to studying the role of grazing livestock systems in the conservation of rangelands in a protected natural park (sierra de guara, spain). *Livestock Production Science*, 96(1):75–85, 2005. ISSN 0301-6226. doi: 10.1016/j.livprodsci.2005.05.023. URL http://www.sciencedirect.com/science/article/pii/S0301622605001582.

D. Bertrand, M. Naaim, and M. Brun. Physical vulnerability of reinforced concrete buildings impacted by snow avalanches. *NHESS*, 10(7):1531–1545, July 2010. ISSN 1684-9981. doi: 10.5194/nhess-10-1531-2010. URL https://nhess.copernicus.org/articles/10/1531/2010/.

J. Birkmann. *Measuring vulnerability to promote disaster-resilient societies: Conceptual frameworks and definitions*, volume 1. 2006.

J. Birkmann. Risk. In P. T. Bobrowsky, editor, *Encyclopedia of Natural Hazards*, pages 856–862. Springer Netherlands, Dordrecht, 2013. URL 10.1007/978-1-4020-4399-4_296.

T. Blaschke. What's Wrong with Pixels? Some Recent Developments Interfacing Remote Sensing and GIS. *Zeitschrift fur Geoinformationssysteme*, 14(6):12–17, 2001.

T. Blaschke. Object based image analysis for remote sensing. *ISPRS Journal of Photogrammetry and Remote Sensing*, 65(1):2–16, Jan. 2010. ISSN 0924-2716. doi: 10.1016/j.isprsjprs.2009.06.004.

G. Bogdanov and R. Rangelova. Social impact of emigration and rural-urban migration in central and eastern europe. *Final Country Report Bulgaria, EC*, 2012.

H.-G. Bohle. Vulnerability and criticality: Perspectives from social geography. *IHDP Update*, 2:1–7, Jan. 2001.

H. Bohnenblust and C. Troxler. Risk analysis-is it a useful tool for the politician in making decisions on avalanche safety. In *Davos Symposium: Avalanche formation, movement and effects, edited by: Salm, B. and Gubler, H*, volume 162, pages 653–664, 1987.

C. Bollin, C. Cárdenas, H. Hahn, and K. S. Vatsa. Disaster risk management by communities and local governments. *Washington, DC: Inter-American Development Bank*, 2003.

M. Bonnefoy, D. Richard, L. Barral, J. Espana, and R. Gaucher. The localization map of avalanche phenomena (clpa): stakes and prospects. In *Proceedings of the 12th Congress Interpraevent*, pages 23–26, 2010.

C. P. Borstad and D. M. McClung. Sensitivity analyses in snow avalanche dynamics modeling and implications when modeling extreme events. *Can. Geotech. J.*, 46(9):1024–1033, Aug. 2009. ISSN 0008-3674. doi: 10.1139/T09-042. URL https://doi.org/10.1139/T09-042.

J. Bourcet. Le mélèze dans les Alpes internes. *biologie et forêt*, 1984.

E. Bourova, E. Maldonado, J.-B. Leroy, R. Alouani, N. Eckert, M. Bonnefoy-Demongeot, and M. Deschatres. A new web-based system to improve the monitoring of snow avalanche hazard in France. *Natural Hazards and Earth System Sciences*, 16(5):1205–1216, 2016. doi: 10.5194/nhess-16-1205-2016.

L. Bracchetti, L. Carotenuto, and A. Catorci. Land-cover changes in a remote area of central apennines (italy) and management directions. *Landscape and Urban Planning*, 104(2):157–170, 2012. ISSN 0169-2046. doi: 10.1016/j.landurbplan.2011.09.005. URL http://www.sciencedirect.com/science/article/pii/S0169204611002842.

P. Brang, W. Schönenberger, E. Ott, and B. Gardner. Forests as Protection from Natural Hazards. *The forests handbook*, 2:53–81, 2001. doi: 10.1002/9780470757079.ch3.

P. Brang, W. Schönenberger, M. Frehner, R. Schwitter, J.-J. Thormann, and B. Wasser. Management of protection forests in the European Alps: an overview. *Forest Snow and Landscape Research*, 80(1):23–44, Jan. 2006.

Y. Brugnara, S. Brönnimann, J. M. Zamuriano Carbajal, J. Schild, C. Rohr, and D. Segesser. Reanalysis sheds lights on 1916 avalanche disaster. *ECMWF Newsletter*, (151):28–34, 2017. doi: 10.21957/h9b197.

G. Brugnot. Développement des politiques forestières et naissance de la restauration des terrains de montagne. *Annales des Ponts et Chaussées*, 2002(103):23–30, July 2002. ISSN 0152-9668. doi: 0.1016/S0152-9668(02)80031-6.

E. Brun, E. Martin, V. Simon, C. Gendre, and C. Coleou. An energy and mass model of snow cover suitable for operational avalanche forecasting. *Journal of Glaciology*, 35(121):333–342, 1989. doi: 10.3189/S0022143000009254.

M. Bründl, H. E. Romang, N. Bischof, and C. M. Rheinberger. The risk concept and its application in natural hazard risk management in switzerland. *Natural Hazards and Earth System Sciences*, 9(3):801, 2009.

L. Bruzzone and S. B. Serpico. An iterative technique for the detection of land-cover transitions in multitemporal remote-sensing images. *IEEE transactions on geoscience and remote sensing*, 35(4):858–867, 1997. doi: 10.1109/36.602528.

M. Bründl, M. McAlpin, U. Gruber, and S. Fuchs. Application of the marginal cost-approach and cost-benefit analysis to measures for avalanche risk reduction–a case study from davos, switzerland. *RISK21-Coping with Risks due to Natural Hazards in the 21st Century*, pages 155–168, 2006.

M. Bründl, H. E. Romang, N. Bischof, and C. M. Rheinberger. The risk concept and its application in natural hazard risk management in Switzerland. *Natural Hazards and Earth System Sciences*, 9(3):801, 2009. doi: 10.5194/nhess-9-801-2009.

M. Bründl, S. Margreth, J. F. Shroder, W. Haeberli, and C. Whiteman. *Chapter 9 - Integrative Risk Management: The Example of Snow Avalanches*, chapter 9, pages 263–301. Academic Press, Boston, Jan. 2015. doi: 10.1016/B978-0-12-394849-6.00009-3.

O. Buser and H. Frutiger. Observed maximum run-out distance of snow avalanches and the determination of the friction coefficients and . *Journal of Glaciology*, 26(94):121–130, 1980. ISSN 0022-1430. doi: 10.3189/S0022143000010662.

W. Bätzing, M. Perlik, and M. Dekleva. Urbanization and depopulation in the alps. *Mountain Research and Development*, 16(4):335–350, 1996. ISSN 02764741, 19947151. doi: 10.2307/3673985. URL http://www.jstor.org/stable/3673985.

F. Cappabianca, M. Barbolini, and L. Natale. Snow avalanche risk assessment and mapping: A new method based on a combination of statistical analysis, avalanche dynamics simulation and empirically-based vulnerability relations integrated in a gis platform. *Cold Regions Science and Technology*, 54(3):193–205, 2008. ISSN 0165-232X. doi: 10.1016/j.coldregions.2008.06.005. URL http://www.sciencedirect.com/science/article/pii/S0165232X08000980.

O. D. Cardona. The need for rethinking the concepts of vulnerability and risk from a holistic perspective: a necessary review and criticism for effective risk management. *Mapping vulnerability: Disasters, development and people*, 17:37–51, 2004.

H. Castebrunet, N. Eckert, and G. Giraud. Snow and weather climatic control on snow avalanche occurrence fluctuations over 50 yr in the French Alps. 2012. doi: 10.5194/cp-8-855-2012.

H. Castebrunet, N. Eckert, G. Giraud, Y. Durand, and S. Morin. Projected changes of snow conditions and avalanche activity in a warming climate: The French Alps over the 2020-2050 and 2070-2100 periods. *Cryosphere*, 8(5):1673–1697, 2014. doi: 10.5194/tc-8-1673-2014.

CCE. Informations internes sur l'agriculture: Essai d'appréciation des conditions d'application et des résultats d'une politique de réforme en agriculture dans des régions agricoles difficiles. Technical report, Commission Des Communautés Européennes, May 1975.

R. Chambers. Editorial introduction: Vulnerability, coping and policy. *IDS Bulletin*, 20(2):1–7, 1989. doi: 10.1111/j.1759-5436.1989.mp20002001.x.

S. Chauchard, F. Beilhe, N. Denis, and C. Carcaillet. An increase in the upper tree-limit of silver fir (Abiesalba Mill.) in the Alps since the mid-20th century: A land-use change phenomenon. *Forest Ecology and Management*, 259(8):1406–1415, Mar. 2010. ISSN 0378-1127. doi: https://doi.org/10.1016/j.foreco.2010.01.009.

M. Christen, P. Bartelt, and J. Kowalski. Back calculation of the In den Arelen avalanche with RAMMS: interpretation of model results. *Annals of Glaciology*, 51(54):161–168, 2010. doi: 10.3189/172756410791386553.

H. Conway and C. F. Raymond. Snow stability during rain. *Journal of Glaciology*, 39(133):635–642, 1993. ISSN 0022-1430. doi: 10.3189/S0022143000016531. URL https://www.cambridge.org/core/article/snow-stability-during-rain/245B493A27E9D9E131D11FD5DF2525B1.

C. Corona, J. L. Saez, M. Stoffel, G. Rovéra, J.-L. Edouard, and F. Berger. Seven centuries of avalanche activity at Echalp (Queyras massif, southern French Alps) as inferred from tree rings. *The Holocene*, 23(2):292–304, 2013. doi: 10.1177/0959683612460784.

S. A. O. Cousins. Analysis of land-cover transitions based on 17th and 18th century cadastral maps and aerial photographs. *Landscape Ecology*, 16(1):41–54, 2001. ISSN 1572-9761. doi: 10.1023/A:1008108704358. URL https://doi.org/10.1023/A:1008108704358.

A. Darwish, K. Leukert, and W. Reinhardt. Image segmentation for the purpose of object-based classification. In *Geoscience and Remote Sensing Symposium, 2003. IGARSS'03. Proceedings. 2003 IEEE International*, volume 3, pages 2039–2041. Ieee, 2003. doi: 10.1109/IGARSS.2003.1294332.

G. de Bouchard d'Aubeterre, A. Favillier, R. Mainieri, J. L. Saez, N. Eckert, M. Saulnier, J.-L. Peiry, M. Stoffel, and C. Corona. Tree-ring reconstruction of snow avalanche activity: Does avalanche path selection matter? *Science of the total environment*, 684:496–508, 2019.

M. De Quervain. Problems of avalanche research. In *Symposium at Davos 1965—Scientific Aspects of Snow and Ice Avalanches*, number 69, pages 1–8. IAHS Publishing, 1965.

M. De Quervain. Wald und lawinen. In *Proceedings of the IUFRO Seminar Mountain Forests and Avalanches, Davos, Switzerland*, pages 219–231, 1978.

M. Debussche, J. Lepart, and A. Dervieux. Mediterranean landscape changes: evidence from old postcards. *Global ecology and biogeography*, 8(1):3–15, 1999.

P. Delage. Risk in civil engineering: from natural to man-made hazards. In *France–Standford Conference on "Risk issues in contemporary science and engineering", Standford*, 2003.

J. D. Dent and T. E. Lang. Modeling of snow flow. *Journal of Glaciology*, 26(94):131–140, 1980. ISSN 0022-1430. doi: 10.3189/S0022143000010674. URL https://www.cambridge.org/core/article/modeling-of-snow-flow/44679562E6DF11062F0C8B01DFBBA934.

DGPR. *Guide Méthodologique: Plan de Prévention des Risques Naturels, Avalanches*. Ministère de l'écologie, du développement durable, et de l'énergie, 2015.

J.-P. Digard. La vie pastorale à Bonneval-sur-Arc (Haute-Maurienne). *Le Monde alpin et rhodanien. Revue régionale d'ethnologie*, 2(2):7–57, 1974.

D. Drogue. Les ovins dans les Alpes françaises. Répartition et évolution récentes du cheptel autochtone. *Revue de géographie alpine*, 38(4):633–678, 1950.

S. Dupire, F. Bourrier, J.-M. Monnet, S. Bigot, L. Borgniet, F. Berger, and T. Curt. The protective effect of forests against rockfalls across the French Alps: Influence of forest diversity. *Forest Ecology and Management*, 382:269–279, 2016. doi: 10.1016/j.foreco.2016.10.020.

Y. Durand, G. Giraud, E. Brun, L. Mérindol, and E. Martin. A computer-based system simulating snowpack structures as a tool for regional avalanche forecasting. *Journal of Glaciology*, 45(151):469–484, 1999. ISSN 0022-1430. doi: 10.3189/s0022143000001337.

Y. Durand, G. Giraud, M. Laternser, P. Etchevers, L. Mérindol, and B. Lesaffre. Reanalysis of 47 years of climate in the French Alps (1958–2005): climatology and trends for snow cover. *Journal of applied meteorology and climatology*, 48(12):2487–2512, 2009a. doi: 10.1175/2009JAMC1810.1.

Y. Durand, M. Laternser, G. Giraud, P. Etchevers, B. Lesaffre, and L. Mérindol. Reanalysis of 44 yr of climate in the French Alps (1958–2002): methodology, model validation, climatology, and trends for air temperature and precipitation. *Journal of Applied Meteorology and Climatology*, 48(3):429–449, 2009b. doi: 10.1175/2008JAMC1808.1.

N. Eckert, E. Parent, and D. Richard. Revisiting statistical–topographical methods for avalanche predetermination: Bayesian modelling for runout distance predictive distribution. *Cold Regions Science and Technology*, 49(1):88–107, 2007.

N. Eckert, É. Parent, T. Faug, and M. Naaim. Optimal design under uncertainty of a passive defense structure against snow avalanches: from a general bayesian framework to a simple analytical model. *Natural Hazards and Earth System Sciences*, 8(5):1067–1081, 2008a.

N. Eckert, E. Parent, M. Naaim, and D. Richard. Bayesian stochastic modelling for avalanche predetermination: From a general system framework to return period computations. *Stochastic Environmental Research and Risk Assessment*, 22(2):185–206, 2008b. doi: 10.1007/s00477-007-0107-4.

N. Eckert, E. Parent, T. Faug, and M. Naaim. Bayesian optimal design of an avalanche dam using a multivariate numerical avalanche model. *Stochastic Environmental Research and Risk Assessment*, 23(8):1123–1141, 2009. doi: 10.1007/s00477-008-0287-6.

N. Eckert, H. Baya, and M. Deschatres. Assessing the Response of Snow Avalanche Runout Altitudes to Climate Fluctuations Using Hierarchical Modeling: Application to 61 Winters of Data in France. *Journal of Climate*, 23(12):3157, June 2010a. ISSN 08948755. doi: 10.1175/2010JCLI3312.1.

N. Eckert, C. Coleou, H. Castebrunet, M. Deschatres, G. Giraud, and J. Gaume. Cross-comparison of meteorological and avalanche data for characterising avalanche cycles: the example of december 2008 in the eastern part of the french alps. *Cold Regions Science and Technology*, 64(2):119–136, 2010b. doi: 10.1016/j.coldregions.2010.08.009.

N. Eckert, M. Naaim, and E. Parent. Long-term avalanche hazard assessment with a bayesian depth-averaged propagation model. *Journal of Glaciology*, 56(198):563–586, 2010c. doi: 10.3189/002214310793146331.

N. Eckert, E. Parent, R. Kies, and H. Baya. A spatio-temporal modelling framework for assessing the fluctuations of avalanche occurrence resulting from climate change: application to 60 years of data in the northern French Alps. *Climatic Change*, 101(3-4):515–553, Aug. 2010d. ISSN 01650009. doi: 10.1007/s10584-009-9718-8.

N. Eckert, C. J. Keylock, D. Bertrand, E. Parent, T. Faug, P. Favier, and M. Naaim. Quantitative risk and optimal design approaches in the snow avalanche field: Review and extensions. *Cold Regions Science and Technology*, 79:1–19, 2012. doi: 10.1016/j.coldregions.2012.03.003.

N. Eckert, C. J. Keylock, H. Castebrunet, A. Lavigne, and M. Naaim. Temporal trends in avalanche activity in the French Alps and subregions: from occurrences and runout altitudes to unsteady return periods. *Journal of Glaciology*, 59(213):93–114, 2013. ISSN 0022-1430. doi: 10.3189/2013jog12j091.

N. Eckert, M. Naaim, F. Giacona, P. Favier, A. Lavigne, D. Richard, F. Bourrier, and E. Parent. Reflexions on the basis of legal zoning for recurrent mountain risks [repenser les fondements du zonage règlementaire des risques en montagne]. *Houille Blanche*, (2):38–67, 2018. doi: 10.1051/lhb/2018019.

J.-B. Estachy. Crisis management. Mont Maudit avalanche july 12, 2012, 2014. URL https://www.recercat.cat/bitstream/handle/2072/237454/PresentacionPGHMJBEstachy.pdf?sequence=1.

P. Estienne. Les avalanches des 20 et 21 janvier 1951 dans les Alpes Suisses, Autrichiennes et Italiennes. *Revue de Géographie Alpine*, pages 381–392, 1951. ISSN 0035-1121. doi: 10.3406/rga.1951.4402.

A. Falcucci, L. Maiorano, and L. Boitani. Changes in land-use/land-cover patterns in Italy and their implications for biodiversity conservation. *Landscape ecology*, 22(4):617–631, 2007. ISSN 1572-9761. doi: https://doi.org/10.1007/s10980-006-9056-4.

D. Faranda. An attempt to explain recent trends in european snowfall extremes. *Weather and Climate Dynamics Discussions*, pages 1–20, 2019. doi: 10.5194/wcd-2019-15.

M. Farvacque, J. Lopez-Saez, C. Corona, D. Toe, F. Bourrier, and N. Eckert. How is rockfall risk impacted by land-use and land-cover changes? Insights from the French Alps. *Global and Planetary Change*, 174:138–152, 2019. doi: 10.1016/j.gloplacha.2019.01.009.

P. Favier, D. Bertrand, N. Eckert, and M. Naaim. A reliability assessment of physical vulnerability of reinforced concrete walls loaded by snow avalanches. *Natural Hazards and Earth System Sciences*, 14(3):689–704, 2014a. doi: 10.5194/nhess-14-689-2014.

P. Favier, N. Eckert, D. Bertrand, and M. Naaim. Sensitivity of avalanche risk to vulnerability relations. *Cold Regions Science and Technology*, 108:163–177, 2014b. doi: 10.1016/j.coldregions.2014.08.009.

P. Favier, N. Eckert, T. Faug, D. Bertrand, and M. Naaim. Avalanche risk evaluation and protective dam optimal design using extreme value statistics. *Journal of Glaciology*, 62(234): 725–749, 2016. doi: 10.1017/jog.2016.64.

C. Favre, A. Grel, E. Granier, R. Cosserat-Mangeot, J. Bachacou, and J. L. Dupouey. Digitalisation des cartes anciennes. *Manuel pour la vectorisation de l'usage des sols et le géoréférencement des minutes*, 1(40,000):54, 2013.

T. Feistl. *Vegetation effects on avalanche dynamics.* PhD thesis, Technische Universität München, 2015.

T. Feistl, P. Bebi, M. Teich, Y. Bühler, M. Christen, K. Thuro, and P. Bartelt. Observations and modeling of the braking effect of forests on small and medium avalanches. *J. Glaciol*, 60 (219):124–138, 2014. doi: https://doi.org/10.3189/2014JoG12J05.

A. Fekete and B. Montz. *Vulnerability*, chapter 3, page 14–31. Cambridge University Press, 2018.

C. B. Field, V. Barros, T. F. Stocker, and Q. Dahe. *Managing the risks of extreme events and disasters to advance climate change adaptation: special report of the intergovernmental panel on climate change.* Cambridge University Press, 2012.

J.-T. Fischer, A. Kofler, W. Fellin, M. Granig, and K. Kleemayr. Multivariate parameter optimization for computational snow avalanche simulation. *Journal of Glaciology*, 61(229): 875–888, 2015.

J.-T. Fischer, A. Kofler, A. Huber, W. Fellin, M. Mergili, and M. Oberguggenberger. Bayesian inference in snow avalanche simulation with r.avaflow, 2020. ISSN 2076-3263.

J. Folliasson. Mouvement de la population en Maurienne au XIXe siècle. (Extrait des Annales de l'Université de Grenoble, t. XXVIII, 1916.). *Revue de Géographie Alpine*, 4(1):1–187, 1916. ISSN 0249-6178. doi: 10.3406/rga.1916.4854.

L. Fontaine. Montagnes et migrations de travail.un essai de comparaison globale (xve-xxe siècles). *Revue d'histoire moderne & contemporaine*, 52-2(2):26–48, 2005. doi: 10.3917/rhmc.522.0026.

B. Frigo, P. Bartelt, B. Chiaia, I. Chiambretti, and M. Maggioni. A reverse dynamical investigation of the catastrophic wood-snow avalanche of 18 january 2017 at rigopiano, gran sasso national park, italy. *International Journal of Disaster Risk Science*, 2020. ISSN 2192-6395. doi: 10.1007/s13753-020-00306-6. URL https://doi.org/10.1007/s13753-020-00306-6.

S. Fuchs and M. Bründl. Damage Potential and Losses Resulting from Snow Avalanches in Settlements of the Canton of Grisons, Switzerland. *Natural Hazards*, 34(1):53–69, Jan. 2005. ISSN 1573-0840. doi: 10.1007/s11069-004-0784-y.

S. Fuchs and M. Keiler. Variability of natural hazard risk in the european alps: evidence from damage potential exposed to snow avalanche. chapter 13, pages 267–279. CRC Press and Taylor & Francis, Jan. 2008. doi: 10.1201/9781420058635.ch13.

S. Fuchs and T. Thaler. *Vulnerability and resilience to natural hazards*. Cambridge University Press, 2018.

S. Fuchs, M. Bründl, and J. Stötter. Development of avalanche risk between 1950 and 2000 in the Municipality of Davos, Switzerland. *Natural Hazards and Earth System Sciences*, 4(2): 263–275, 2004.

S. Fuchs, M. Keiler, A. Zischg, and M. Bründl. The long-term development of avalanche risk in settlements considering the temporal variability of damage potential. *Natural Hazards and Earth System Science*, 5(6):893–901, 2005. doi: 10.5194/nhess-5-893-2005.

S. Fuchs, M. Thöni, M. C. McAlpin, U. Gruber, and M. Bründl. Avalanche hazard mitigation strategies assessed by cost effectiveness analyses and cost benefit analyses—evidence from davos, switzerland. *Natural Hazards*, 41(1):113–129, 2007. doi: 10.1007/s11069-006-9031-z.

S. Fuchs, C. Kuhlicke, and V. Meyer. Editorial for the special issue: vulnerability to natural hazards—the challenge of integration. *Natural Hazards*, 58(2):609–619, 2011. doi: 10.1007/s11069-011-9825-5.

S. Fuchs, M. Keiler, S. Sokratov, and A. Shnyparkov. Spatiotemporal dynamics: the need for an innovative approach in mountain hazard risk management. *Natural Hazards*, 68(3): 1217–1241, Sept. 2013. ISSN 1573-0840. doi: 10.1007/s11069-012-0508-7.

S. Fuchs, M. Keiler, and A. P. Zischg. A spatiotemporal multi-hazard exposure assessment based on property data. *Natural Hazards and Earth System Sciences*, 15(9):2127–2142, 2015. doi: 10.5194/nhess-15-2127-2015.

S. Fuchs, V. Röthlisberger, T. Thaler, A. Zischg, and M. Keiler. Natural Hazard Management from a Coevolutionary Perspective: Exposure and Policy Response in the European Alps. *Annals of the American Association of Geographers*, 107(2):382–392, Mar. 2017. ISSN 2469-4452. doi: 10.1080/24694452.2016.1235494.

S. Fuchs, M. Keiler, R. Ortlepp, R. Schinke, and M. Papathoma-Köhle. Recent advances in vulnerability assessment for the built environment exposed to torrential hazards: Challenges and the way forward. *Journal of Hydrology*, 575:587–595, Aug. 2019. ISSN 0022-1694. doi: 10.1016/j.jhydrol.2019.05.067.

P. Föhn, M. Stoffel, and P. Bartelt. Formation and forecasting of large (catastrophic) new snow avalanches. In *Proceedings of the 2002 International Snow Science Workshop*, volume 29, pages 141–148, 2002. URL https://arc.lib.montana.edu/snow-science/item/822.

C. García-Hernández, J. Ruiz-Fernández, C. Sánchez-Posada, S. Pereira, M. Oliva, and G. Vieira. Reforestation and land use change as drivers for a decrease of avalanche damage in mid-latitude mountains (NW Spain). *Global and Planetary Change*, 153:35–50, June 2017. ISSN 0921-8181. doi: https://doi.org/10.1016/j.gloplacha.2017.05.001.

P. García-Llamas, I. R. Geijzendorffer, A. P. García-Nieto, L. Calvo, S. Suárez-Seoane, and W. Cramer. Impact of land cover change on ecosystem service supply in mountain systems: a case study in the Cantabrian Mountains (NW of Spain). *Regional Environmental Change*, Sep 2018. ISSN 1436-378X. doi: 10.1007/s10113-018-1419-2.

J. M. García-Ruiz and N. Lana-Renault. Hydrological and erosive consequences of farmland abandonment in europe, with special reference to the mediterranean region - a review. *Agriculture, Ecosystems Environment*, 140(3):317–338, 2011. ISSN 0167-8809. doi: 10.1016/j.agee.2011.01.003. URL http://www.sciencedirect.com/science/article/pii/S0167880911000041.

J. M. García-Ruiz, T. Lasanta, P. Ruiz-Flano, L. Ortigosa, S. White, C. González, and C. Martí. Land-use changes and sustainable development in mountain areas: a case study in the spanish pyrenees. *Landscape Ecology*, 11(5):267–277, 1996. ISSN 1572-9761. doi: 10.1007/BF02059854. URL https://doi.org/10.1007/BF02059854.

M. Gartzia, C. L. Alados, and F. Pérez-Cabello. Assessment of the effects of biophysical and anthropogenic factors on woody plant encroachment in dense and sparse mountain grasslands based on remote sensing data. *Progress in Physical Geography: Earth and Environment*, 38 (2):201–217, Dec. 2014. ISSN 0309-1333. doi: 10.1177/0309133314524429.

C. Gauchon. Les hivers sans neige et l'économie des sports d'hiver: un phénomène récurrent, une problématique toujours renouvelée, 2009.

J. Gaume and B. Reuter. Assessing snow instability in skier-triggered snow slab avalanches by combining failure initiation and crack propagation. *Cold Regions Science and Technology*, 144:6–15, 2017. ISSN 0165-232X. doi: 10.1016/j.coldregions.2017.05.011. URL http://www.sciencedirect.com/science/article/pii/S0165232X17300460.

J. Gehrig-Fasel, A. Guisan, and N. E. Zimmermann. Tree line shifts in the Swiss Alps: Climate change or land abandonment? *Journal of Vegetation Science*, 18(4):571–582, Jan. 2007. ISSN 1100-9233. doi: 10.1111/j.1654-1103.2007.tb02571.x.

M. Gellrich, P. Baur, B. Koch, and N. E. Zimmermann. Agricultural land abandonment and natural forest re-growth in the Swiss mountains: A spatially explicit economic analysis. *Agriculture, Ecosystems & Environment*, 118(1):93 – 108, 2007. ISSN 0167-8809. doi: https://doi.org/10.1016/j.agee.2006.05.001.

M. Getzner, G. Gutheil-Knopp-Kirchwald, E. Kreimer, H. Kirchmeir, and M. Huber. Gravitational natural hazards: Valuing the protective function of Alpine forests. *Forest Policy and Economics*, 80:150–159, July 2017. ISSN 1389-9341. doi: 10.1016/j.forpol.2017.03.015.

F. Gex. *Les Morts de la guerre en Savoie (1914-1918). Préface par M. le comte L éon Costa de Beauregard, président de l'Association savoyarde des anciens combattants / F. Gex.* Librairie Dardel, 1922. doi: ark:/12148/bpt6k6576205z.

F. Giacona, N. Eckert, and B. Martin. A 240-year history of avalanche risk in the Vosges Mountains based on non-conventional (re) sources. *Natural Hazards & Earth System Sciences*, 17(6), 2017. doi: 10.5194/nhess-17-887-2017.

F. Giacona, N. Eckert, R. Mainieri, B. Martin, C. Corona, J. Lopez-Saez, J.-M. Monnet, M. Naaim, and M. Stoffel. Avalanche activity and socio-environmental changes leave strong footprints in forested landscapes: a case study in the Vosges medium-high mountain range. *Annals of Glaciology*, page 1–23, 2018. doi: 10.1017/aog.2018.26.

F. Giacona, B. Martin, N. Eckert, and J. Desarthe. Une méthodologie de la modélisation en géohistoire: de la chronologie (spatialisée) des événements au fonctionnement du système par la mise en correspondance spatiale et temporelle. *Physio-Géo. Géographie physique et environnement*, (Volume 14):171–199, 2019. doi: 10.4000/physio-geo.9186.

F. Giacona, N. Eckert, C. Corona, R. Mainieri, S. Morin, B. Martin, M. Stoffel, and M. Naim. Avalanches at low elevations already deliquesced by the Early Twentieth Century Warming . submitted.

A.-M. Granet-Abisset. *La route réinventée. Quelques éléments sur les migrations des Queyrassins au siècle dernier*, volume 19. Persée-Portail des revues scientifiques en SHS, 1991.

U. Gruber and P. Bartelt. Snow avalanche hazard modelling of large areas using shallow water numerical methods and gis. *Environmental Modelling & Software*, 22(10):1472 – 1481, 2007. ISSN 1364-8152. doi: https://doi.org/10.1016/j.envsoft.2007.01.001.

U. Gruber and S. Margreth. Winter 1999: a valuable test of the avalanche-hazard mapping procedure in Switzerland. *Annals of Glaciology*, 32:328–332, 2001. ISSN 0260-3055. doi: 10.3189/172756401781819238.

A. Grêt-Regamey and D. Straub. Spatially explicit avalanche risk assessment linking bayesian networks to a gis. *NHESS*, 6(6):911–926, Oct. 2006. ISSN 1684-9981. doi: 10.5194/nhess-6-911-2006. URL https://nhess.copernicus.org/articles/6/911/2006/.

H. Gubler. Artificial release of avalanches by explosives. *Journal of Glaciology*, 19(81):419–429, 1977. doi: 10.3189/S0022143000029440.

H. Gubler and J. Rychetnik. Effects of forests near the timberline on avalanche formation. In *Symposium at Vienna*, pages 19–37, 1991. doi: 10.1.1.841.5352.

C. B. Harbitz, D. Issler, and C. J. Keylock. Conclusions from a recent survey of avalanche computational models. In *Proceedings of the anniversary conference*, volume 25, pages 128–135, 1998.

J. Hendrikx and I. Owens. Modified avalanche risk equations to account for waiting traffic on avalanche prone roads. *Cold Regions Science and Technology*, 51(2):214–218, 2008. ISSN 0165-232X. doi: 10.1016/j.coldregions.2007.04.011. URL http://www.sciencedirect.com/science/article/pii/S0165232X07000882.

J. Hendrikx, I. Owens, W. Carran, and A. Carran. Avalanche risk evaluation with practical suggestions for risk minimization: a case study of the milford road, new zealand. In *Proceedings of the International Snow Science Workshop, Telluride, Colorado, USA*, volume 557567, pages 757–767, 2006.

M. B. Heredia, C. Prieur, and N. Eckert. Nonparametric estimation of aggregated sobol'indices: application to a depth averaged snow avalanche model. 2020.

J. Heumader. The catastrophic avalanche disasters of Galtür and Valzur on the 23 and 24 of February 1999 in the Paznaun Valley/Tyrol. In *Proceedings of the international workshop hazard mapping in avalanching areas. St. Christoph, Austria*, pages 179–185, 2000.

R. Hock, G. Rasul, C. Adler, S. Cáceres, Y. Gruber, M. Hirabayashi, et al. Chapter 2: high mountain areas. *IPCC Special Report on Ocean and Cryosphere in a Changing Climate, http://report. ipcc. ch/srocc/pdf/SROCC_FinalDraft_ Chapter2. pdf*, 2020.

P. Höller. Avalanche hazards and mitigation in Austria: a review. *Natural Hazards*, 43(1): 81–101, Oct. 2007. ISSN 1573-0840. doi: 10.1007/s11069-007-9109-2.

E. J. Hopfinger. Snow avalanche motion and related phenomena. *Annual Review of Fluid Mechanics*, 15(1):47–76, 1983. doi: 10.1146/annurev.fl.15.010183.000403.

T. E. Idowu, R. M. Waswa, K. Lasisi, M. Nyadawa, and V. Okumu. Object-based land use/land cover change detection of a coastal city using multi-source imagery: a case study of lagos, nigeria. *South African Journal of Geomatics*, 9(2):136–148, 2020. doi: 10.4314/sajg.v9i2.10.

INSEE. Séries historiques sur la population et le logement en 2016. Technical report, Institut national de la statistique et des études économiques, 2016. URL www.insee.fr.

INSEE. Tourisme en 2017, statistiques sur les hébergements touristiques. Technical report, Institut national de la statistique et des études économiques, 2017. URL www.insee.fr.

Intergraph. *ERDAS Imagine*, 2015.

C. C. IPCC. Synthesis report. contribution of working groups i. *ii and iii to the fifth assessment report of the intergovernmental panel on climate change*, 138, 2014.

M. Jail. La Haute-Maurienne. Recherches sur l'évolution et les problèmes d'une cellule montagnarde intra-alpine. *Revue de Géographie Alpine*, pages 85–146, 1969. ISSN 0035-1121. doi: https://doi.org/10.3406/rga.1969.3392.

M. Jail. Note sur l'hiver remarquable 1969-1970 dans les Alpes françaises. *Revue de Géographie Alpine*, 58(3):505–513, 1970. ISSN 0035-1121. doi: https://doi.org/10.3406/rga.1970.3495.

M. Jail. Tourisme et emplois récents en haute Maurienne : exemples de Bonneval-sur-Arc, Lanslevillard et Bessans. *Revue de Géographie Alpine*, pages 554–560, 1973. ISSN 0035-1121. doi: https://doi.org/10.3406/rga.1973.1347.

M. Jail. *Haute Maurienne, pays du diable?* Éditions Allier, 1977.

K. Jónasson, S. Þ. Sigurðsson, and Þ. Arnalds. Estimation of avalanche risk. 1999. doi: 10.1.1.368.4993.

B. Jongman, P. J. Ward, and J. C. J. H. Aerts. Global exposure to river and coastal flooding: Long term trends and changes. *Global Environmental Change*, 22(4):823–835, 2012. ISSN 0959-3780. doi: 10.1016/j.gloenvcha.2012.07.004. URL http://www.sciencedirect.com/science/article/pii/S0959378012000830.

J. S. Kargel, G. J. Leonard, D. H. Shugar, U. K. Haritashya, A. Bevington, E. J. Fielding, K. Fujita, M. Geertsema, E. S. Miles, and J. Steiner. Geomorphic and geologic controls of geohazards induced by Nepal's 2015 Gorkha earthquake. *Science*, 351(6269):aac8353, 2016. doi: 10.1126/science.aac835.

P. E. Kauppi, J. H. Ausubel, J. Fang, A. S. Mather, R. A. Sedjo, and P. E. Waggoner. Returning forests analyzed with the forest identity. *Proc Natl Acad Sci USA*, 103(46):17574, Nov. 2006. doi: 10.1073/pnas.0608343103.

M. Keiler, A. Zischg, S. Fuchs, M. Hama, and J. Stötter. Avalanche related damage potential-changes of persons and mobile values since the mid-twentieth century, case study Galtür. *Natural Hazards and Earth System Science*, 5(1):49–58, 2005. doi: 1684-9981/nhess/2005-5-49.

M. Keiler, R. Sailer, P. Jörg, C. Weber, S. Fuchs, A. Zischg, and S. Sauermoser. Avalanche risk assessment : a multi-temporal approach, results from Galtür, Austria. *NHESS*, 6(4):637–651, July 2006. ISSN 1684-9981. doi: 10.5194/nhess-6-637-2006.

C. J. Keylock. An alternative form for the statistical distribution of extreme avalanche runout distances. *Cold Regions Science and Technology*, 42(3):185–193, 2005. ISSN 0165-232X. doi: 10.1016/j.coldregions.2005.01.004. URL http://www.sciencedirect.com/science/article/pii/S0165232X05000236.

C. J. Keylock and M. Barbolini. Snow avalanche impact pressure - vulnerability relations for use in risk assessment. *Canadian Geotechnical Journal*, 38(2):227–238, 2001. doi: 10.1139/t00-100. URL https://cdnsciencepub.com/doi/abs/10.1139/t00-100.

C. J. Keylock, D. M. McClung, and M. M. Magnússon. Avalanche risk mapping by simulation. *Journal of Glaciology*, 45(150):303–314, 1999. doi: 10.3189/S0022143000001805.

R. J. T. Klein, G. F. Midglev, B. L. Preston, M. Alam, F. G. H. Berkhout, K. Dow, and M. R. Shaw. Climate change 2014: Impacts, adaptation, and vulnerability. *Intergovernmental Panel on Climate Change. Part A: Global and Sectoral Aspects; Field, CB, Barros, VR, Dokken, DJ, Mach, KJ, Mastrandrea, MD, Bilir, TE, Chatterjee, M., Ebi, KL, Estrada, YO, Genova, RC, et al., Eds*, 2014.

C. Körner. The use of 'altitude'in ecological research. *Trends in ecology & evolution*, 22(11): 569–574, 2007.

P. Kumar, S. E. Debele, J. Sahani, L. Aragão, F. Barisani, B. Basu, E. Bucchignani, N. Charizopoulos, S. Di Sabatino, A. Domeneghetti, A. S. Edo, L. Finér, G. Gallotti, S. Juch, L. S. Leo, M. Loupis, S. B. Mickovski, D. Panga, I. Pavlova, F. Pilla, A. L. Prats, F. G. Renaud, M. Rutzinger, A. S. Basu, M. A. R. Shah, K. Soini, M. Stefanopoulou, E. Toth, L. Ukonmaanaho, S. Vranic, and T. Zieher. Towards an operationalisation of nature-based solutions for natural hazards. *Science of The Total Environment*, 731:138855, 2020. ISSN 0048-9697. doi: 10.1016/j.scitotenv.2020.138855. URL http://www.sciencedirect.com/science/article/pii/S004896972032372X.

M. Kummu, H. de Moel, G. Salvucci, D. Viviroli, P. J. Ward, and O. Varis. Over the hills and further away from coast: global geospatial patterns of human and environment over the 20th-21st centuries. *Environmental Research Letters*, 11(3):034010, 2016. ISSN 1748-9326. doi: 10.1088/1748-9326/11/3/034010. URL http://dx.doi.org/10.1088/1748-9326/11/3/034010.

T. Lasanta, J. Arnáez, N. Pascual, P. Ruiz-Flaño, M. P. Errea, and N. Lana-Renault. Space-time process and drivers of land abandonment in europe. *CATENA*, 149:810–823, 2017. ISSN 0341-8162. doi: 10.1016/j.catena.2016.02.024. URL http://www.sciencedirect.com/science/article/pii/S0341816216300777.

T. Lasanta-Martínez, S. M. Vicente-Serrano, and J. M. Cuadrat-Prats. Mountain mediterranean landscape evolution caused by the abandonment of traditional primary activities: a study of the spanish central pyrenees. *Applied Geography*, 25(1):47–65, 2005. ISSN 0143-6228. doi: 10.1016/j.apgeog.2004.11.001. URL http://www.sciencedirect.com/science/article/pii/S0143622804000414.

T. Lasanta Martínez, O. Beltrán, and I. Vaccaro. Socioeconomic and territorial impact of the ski industry in the spanish pyrenees: mountain development and leisure induced urbanization. *Pirineos*, 168:103–128, 2013. doi: 10.3989/Pirineos.2013.168006.

M. Laternser and M. Schneebeli. Temporal trend and spatial distribution of avalanche activity during the last 50 years in Switzerland. *Natural Hazards*, 27(3):201–230, 2002. doi: 0.1023/A:1020327312719.

A. Lavigne. *Modélisation statistique régionale de l'activité avalancheuse*. PhD thesis, PhD thesis, AgroParisTech, 2013.

A. Lavigne, L. Bel, E. Parent, and N. Eckert. A model for spatio-temporal clustering using multinomial probit regression: application to avalanche counts. *Environmetrics*, 23(6):522–534, 2012. doi: 10.1002/env.2167.

A. Lavigne, N. Eckert, L. Bel, and E. Parent. Adding expert contributions to the spatiotemporal modelling of avalanche activity under different climatic influences. *Journal of the Royal Statistical Society: Series C Applied Statistics*, 64(4):651–671, 2015. doi: 10.1111/rssc.12095.

F. Leone, A. Colas, Y. Garcin, N. Eckert, V. Jomelli, and M. Gherardi. The snow avalanches risk on Alpine roads network. Assessment of impacts and mapping of accessibility loss. *Journal of Alpine Research/ Revue de géographie alpine*, (102-4), 2014. doi: 10.4000/rga.2501.

X. Li and A. G. O. Yeh. Principal component analysis of stacked multi-temporal images for the monitoring of rapid urban expansion in the pearl river delta. *International Journal of Remote Sensing*, 19(8):1501–1518, Jan. 1998. ISSN 0143-1161. doi: 10.1080/014311698215315.

Y. Li, M. Zhao, S. Motesharrei, Q. Mu, E. Kalnay, and S. Li. Local cooling and warming effects of forests based on satellite observations. *Nature Communications*, 6(1):6603, Mar. 2015. ISSN 2041-1723. URL https://doi.org/10.1038/ncomms7603.

K. Lied and K. Bakkehøi. Empirical calculations of snow-avalanche run-out distance based on topographic parameters. *Journal of Glaciology*, 26(94):165–177, 1980. ISSN 0022-1430. doi: 10.3189/S0022143000010704.

W. Linder. *Digital Photogrammetry A Practical Course*. Springer Berlin Heidelberg, Belgium, Europe, 4 edition, 2016. ISBN 978-3-662-50462-8. doi: 10.1007/978-3-662-50463-5.

M. Loiseau, C. Bonvalet, and C. Dutreuilh. The impact of the 1948 housing law on residential trajectories in the Paris region. *Population*, 60:301–315, 2005. doi: 10.3917/popu.503.0351.

J. I. López-Moreno, S. Goyette, S. Vicente-Serrano, and M. Beniston. Effects of climate change on the intensity and frequency of heavy snowfall events in the Pyrenees. *Climatic Change*, 105(3-4):489–508, 2011.

J. Loup. Bibliographie des Alpes Françaises pour 1970. *Revue de Géographie Alpine*, pages 401–423, 1971. ISSN 0035-1121. doi: rga_0035-1121_1971_num_59_3_1241. URL https://www.persee.fr/doc/rga_0035-1121_1971_num_59_3_1241.

D. Lu, P. Mausel, E. Brondízio, and E. Moran. Change detection techniques. *International Journal of Remote Sensing*, 25(12):2365–2401, June 2004. ISSN 0143-1161. doi: 10.1080/0143116031000139863.

E. R. Lutz and K. W. Birkeland. Spatial patterns of surface hoar properties and incoming radiation on an inclined forest opening. *Journal of Glaciology*, 57(202):355–366, 2011. ISSN 0022-1430. doi: 10.3189/002214311796405843.

J. I. López-Moreno, J. M. Soubeyroux, S. Gascoin, E. Alonso-Gonzalez, N. Durán-Gómez, M. Lafaysse, M. Vernay, C. Carmagnola, and S. Morin. Long-term trends (1958–2017) in snow cover duration and depth in the pyrenees. *International Journal of Climatology*, n/a (n/a), 2020. doi: 10.1002/joc.6571. URL https://rmets.onlinelibrary.wiley.com/doi/abs/10.1002/joc.6571.

L. Ma, M. Li, X. Ma, L. Cheng, P. Du, and Y. Liu. A review of supervised object-based land-cover image classification. *ISPRS Journal of Photogrammetry and Remote Sensing*, 130: 277–293, Aug. 2017. ISSN 0924-2716. doi: 10.1016/j.isprsjprs.2017.06.001.

D. MacDonald, J. Crabtree, G. Wiesinger, T. Dax, N. Stamou, P. Fleury, J. G. Lazpita, and A. Gibon. Agricultural abandonment in mountain areas of Europe: Environmental consequences and policy response. *Journal of Environmental Management*, 59(1):47 – 69, 2000. ISSN 0301-4797. doi: https://doi.org/10.1006/jema.1999.0335.

M. Maggioni, M. Freppaz, M. Christen, P. Bartelt, and E. Zanini. Back-calculation of small avalanches with the 2d avalanche dynamics model ramms: four events artificially triggered at the seehore test site in aosta valley (nw-italy). In *Proceedings of the International Snow Science Workshop, 16–21 September 2012, Anchorage, Alaska*, 2012.

R. Mainieri, A. Favillier, J. Lopez-Saez, N. Eckert, T. Zgheib, P. Morel, M. Saulnier, J.-L. Peiry, M. Stoffel, and C. Corona. Impacts of land-cover changes on snow avalanche activity in the French Alps. *Anthropocene*, page 100244, 2020. doi: 10.1016/j.ancene.2020.100244.

F. Malandra, A. Vitali, C. Urbinati, P. J. Weisberg, and M. Garbarino. Patterns and drivers of forest landscape change in the Apennines range, Italy. *Regional Environmental Change*, 19 (7):1973–1985, Oct. 2019. ISSN 1436-378X. doi: 10.1007/s10113-019-01531-6.

G. P. Malanson and D. R. Butler. Effects of terrain on excessive travel distance by snow avalanches. *Northwest Science*, 66:77–85, 1992.

M. Malavasi, M. L. Carranza, D. Moravec, and M. Cutini. Reforestation dynamics after land abandonment: a trajectory analysis in mediterranean mountain landscapes. *Regional Environmental Change*, 18(8):2459–2469, 2018. ISSN 1436-378X. doi: 10.1007/s10113-018-1368-9. URL https://doi.org/10.1007/s10113-018-1368-9.

S. Margreth, L. Stoffel, and C. Wilhelm. Winter opening of high alpine pass roads–analysis and case studies from the swiss alps. *Cold Regions Science and Technology*, 37(3):467–482, 2003. ISSN 0165-232X. doi: 10.1016/S0165-232X(03)00085-5. URL http://www.sciencedirect.com/science/article/pii/S0165232X03000855.

T. Marke, F. Hanzer, M. Olefs, and U. Strasser. Simulation of past changes in the austrian snow cover 1948–2009. *Journal of Hydrometeorology*, 19(10):1529–1545, 2018. doi: 10.1175/JHM-D-17-0245.1. URL https://doi.org/10.1175/JHM-D-17-0245.1.

A. Marnezy. Les stations de ski de la Haute-Maurienne: un exemple original d'aménagement touristique. *Revue de géographie alpine*, 67(3):281–307, 1979. doi: 10.3406/rga.1979.2174.

A. S. Mather and C. L. Needle. The forest transition: a theoretical basis. *Area*, 30(2):117–124, 1998. doi: 10.1111/j.1475-4762.1998.tb00055.x.

A. S. Mather, J. Fairbairn, and C. L. Needle. The course and drivers of the forest transition: The case of France. *Journal of Rural Studies*, 15(1):65–90, Jan. 1999. ISSN 0743-0167. doi: 10.1016/S0743-0167(98)00023-0.

M. Matiu, A. Crespi, G. Bertoldi, C. M. Carmagnola, C. Marty, S. Morin, W. Schöner, D. Cat Berro, G. Chiogna, L. De Gregorio, S. Kotlarski, B. Majone, G. Resch, S. Terzago, M. Valt, W. Beozzo, P. Cianfarra, I. Gouttevin, G. Marcolini, C. Notarnicola, M. Petitta,

S. C. Scherrer, U. Strasser, M. Winkler, M. Zebisch, A. Cicogna, R. Cremonini, A. Debernardi, M. Faletto, M. Gaddo, L. Giovannini, L. Mercalli, J.-M. Soubeyroux, A. Sušnik, A. Trenti, S. Urbani, and V. Weilguni. Observed snow depth trends in the european alps 1971 to 2019. *The Cryosphere Discussion*, 2020:1–50, Oct. 2020. ISSN 1994-0440. doi: 10.5194/tc-2020-289. URL https://tc.copernicus.org/preprints/tc-2020-289/.

I. Mauz. Regional Development and the French National Parks: The Case of the Vanoise National Park. *Protected Areas and Regional Development in Europe Towards a New Model for the 21st Century*, pages 115–128, 2007.

D. McClung and P. A. Schaerer. *The avalanche handbook*. The Mountaineers Books, 2006.

D. M. McClung. Magnitude and frequency of avalanches in relation to terrain and forest cover. *Arctic, Antarctic, and Alpine Research*, 35(1):82–90, 2003. doi: https://doi.org/10.1657/1523-0430(2003)035[0082:MAFOAI]2.0.CO;2.

H. E. Megerle. Tourismus und Siedlungsentwicklung in den französischen Alpen, 2018.

R. Millere. *La Guerre 1939-1945 En Haute Maurienne*, volume 31. Societe D'histoire Et D'archeologie De Maurienne, 1997. ISBN 1244 - 5584. doi: ark:/12148/bpt6k9608514h.

C. Moos, P. Bebi, M. Schwarz, M. Stoffel, K. Sudmeier-Rieux, and L. Dorren. Ecosystem-based disaster risk reduction in mountains. *Earth-Science Reviews*, 177:497–513, 2018. ISSN 0012-8252. doi: 10.1016/j.earscirev.2017.12.011. URL http://www.sciencedirect.com/science/article/pii/S0012825217303446.

J. L. Morgan, S. E. Gergel, and N. C. Coops. Aerial Photography: A Rapidly Evolving Tool for Ecological Management. *BioScience*, 60(1):47–59, 2010. ISSN 15253244. doi: 10.1525/bio.2010.60.1.9.

A. Mottet, S. Ladet, N. Coqué, and A. Gibon. Agricultural land-use change and its drivers in mountain landscapes: A case study in the Pyrenees. *Agriculture, Ecosystems & Environment*, 114(2):296 – 310, 2006. ISSN 0167-8809. doi: https://doi.org/10.1016/j.agee.2005.11.017.

M. Naaim. *Contribution to snow drift and avalanches flows modelling*. PhD thesis, Habilitation thesis, University Joseph Fourier, Grenoble, France, 1998.

M. Naaim, F. Naaim-Bouvet, T. Faug, and A. Bouchet. Dense snow avalanche modeling: flow, erosion, deposition and obstacle effects. *Cold regions science and technology*, 39(2-3):193–204, 2004.

M. Naaim, T. Faug, E. Thibert, N. Eckert, G. Chambon, F. Naaim, and H. Bellot. Snow avalanche pressure on obstacles. In *Proceedings Whistler 2008 International Snow Science Workshop September 21-27, 2008*, page 740, 2008.

M. Naaim, Y. Durand, N. Eckert, and G. Chambon. Dense avalanche friction coefficients: influence of physical properties of snow. *Journal of Glaciology*, 59(216):771–782, 2013. doi: 10.3189/2013JoG12J205.

M. Naaim, N. Eckert, G. Giraud, T. Faug, G. Chambon, F. Naaim-Bouvet, and D. Richard. Impact du réchauffement climatique sur l'activité avalancheuse et multiplication des avalanches humides dans les Alpes françaises. *La Houille Blanche*, (6):12–20, 2016. doi: 0.1051/lhb/2016055.

H. Onde. Les mouvements de la population en Maurienne et en Tarentaise. *Revue de Géographie Alpine*, 2:487–567, 1942. ISSN 0035-1121. doi: 10.3406/rga.1942.4354.

P. A. O'Gorman. Contrasting responses of mean and extreme snowfall to climate change. *Nature*, 512(7515):416–418, 2014.

C. Pairaudeau. *Travaux scientifiques du Parc National de la Vanoise*. Parc National de la Vanoise, 1983.

D. Paprotny, O. Morales-Nápoles, and S. N. Jonkman. Hanze: a pan-european database of exposure to natural hazards and damaging historical floods since 1870. *ESSD*, 10(1):565–581, Mar. 2018. ISSN 1866-3516. doi: 10.5194/essd-10-565-2018. URL https://essd.copernicus.org/articles/10/565/2018/.

L. Pearson and M. Pelling. The un sendai framework for disaster risk reduction 2015–2030: Negotiation process and prospects for science and practice. *Journal of Extreme Events*, 2 (01):1571001, 2015.

P. Peduzzi. The disaster risk, global change, and sustainability nexus. *Sustainability*, 11(4):957, 2019. doi: 10.3390/su11040957.

R. Pelorosso, A. Leone, and L. Boccia. Land cover and land use change in the Italian central Apennines: A comparison of assessment methods. *Applied Geography*, 29(1):35–48, 2009.

M. Perlik, P. Messerli, and W. Bätzing. Towns in the Alps. Urbanization Processes, Economic Structure, and Demarcation of European Functional Urban Areas (EFUAs) in the Alps. *Mountain Research and Development*, 21(3):243–252, 10, 2001. doi: 10.1659/0276-4741(2001)021[0243:TITA]2.0.CO;2.

J. Perret, D. Malavieille, C. Micheels, N. pignard Marthod, E. Perret, and N. Bertrand. Le Queyras: Diagnostic socio-'economique. resreport 248, CEMAGREF, 1992.

C. C. Petit and E. F. Lambin. Integration of multi-source remote sensing data for land cover change detection. *International Journal of Geographical Information Science*, 15(8):785–803, 2001. doi: 10.1080/13658810110074483.

C. C. Petit and E. F. Lambin. Impact of data integration technique on historical land-use/land-cover change: comparing historical maps with remote sensing data in the Belgian Ardennes. *Landscape Ecology*, 17(2):117–132, 2002.

C. Pielmeier, F. Techel, C. Marty, and T. Stucki. Wet snow avalanche activity in the Swiss Alps–trend analysis for mid-winter season. In *Proceedings of the International Snow Science Workshop, Grenoble and Chamonix*, pages 1240–1246, 2013.

E. Podolskiy, K. Izumi, V. Suchkov, and N. Eckert. Physical and societal statistics for a century of snow-avalanche hazards on Sakhalin and the Kuril Islands (1910-2010). *Journal of Glaciology*, 60(221):409–430, 2014. doi: 10.3189/2014JoG13J143.

E. A. Podolskiy, K. Nishimura, O. Abe, and P. A. Chernous. Earthquake-induced snow avalanches: I. historical case studies. *Journal of Glaciology*, 56(197):431–446, 2010. doi: 10.3189/002214310792447815.

F. Poratelli, C. Accastello, M. Freppaz, and F. Brun. Integrated grey-green management of avalanche risk: Economic and ecologic evidences from the western italian alps. *International Journal of Disaster Risk Reduction*, 46:101502, 2020a. ISSN 2212-4209. doi: 10.1016/j.ijdrr.2020.101502. URL http://www.sciencedirect.com/science/article/pii/S2212420919313020.

F. Poratelli, S. Cocuccioni, C. Accastello, S. Steger, S. Schneiderbauer, and F. Brun. State-of-the-art on ecosystem-based solutions for disaster risk reduction: The case of gravity-driven natural hazards in the alpine region. *International Journal of Disaster Risk Reduction*, 51:101929, 2020b. ISSN 2212-4209. doi: 10.1016/j.ijdrr.2020.101929. URL http://www.sciencedirect.com/science/article/pii/S221242092031431X.

PPR. Plan de Prévention des risques Naturels Prévisibles,Lanslevillard. Technical report, Direction départementale de l'agriculture et de la forêt, service rtm, Mar. 2004.

PPR. Plan de Prévention des risques Naturels Prévisibles,Bonneval Sur Arc. Technical report, Direction départementale de l'agriculture et de la forêt, service RTM, 2011.

J. Prieur. *Valloire la vallée d'or*, volume L'Histoire en Savoie of *numéro spécial été 1989*. Société Savoisienne d'Histoire et d'Archéologie, 1989.

P. Rambaud and M. Vincienne. *Les transformations d'une société rurale. — La Maurienne (1561-1962)*. Armand Colin,Paris, 1964.

F. Rapin and C. Ancey. Occurrence conditions of two catastrophic avalanches at Chamonix, France. International Snow Science Workshop, Big Sky. *Montana, USA*, 2000.

Raynal. Histoire de la population de la commune de Bessan (Hérault) (1851-1937). *Journal de la société statistique de Paris*, 87:286–291, 1946. URL http://www.numdam.org/item/JSFS_1946__87__286_0/.

K. Riitters, R. V. O'Neill, C. T. Hunsaker, J. Wickham, D. H. Yankee, S. Timmins, K. Jones, and B. L. Jackson. *A Factor Analysis of Landscape Pattern and Structure Metric*, volume 10. Feb. 1995.

Z. Roca. *Second home tourism in Europe : lifestyle issues and policy responses*. Ashgate, Farnham, 2013.

M. Rogger, M. Agnoletti, A. Alaoui, J. Bathurst, G. Bodner, M. Borga, V. Chaplot, F. Gallart, G. Glatzel, J. Hall, et al. Land use change impacts on floods at the catchment scale:

Challenges and opportunities for future research. *Water resources research*, 53(7):5209–5219, 2017.

B. Romano and F. Zullo. Landscape change in the european mountain areas. settlement of the alps: evolution and trajectories. *ri-vista*, 14(1), June 2016. doi: 10.13128/RV-18268. URL https://oaj.fupress.net/index.php/ri-vista/article/view/2740.

M. Rousselot, Y. Durand, G. Giraud, L. Merindol, and L. Daniel. Analysis and forecast of extreme new-snow avalanches: a numerical study of the avalanche cycles of February 1999 in France. *Journal of Glaciology*, 56(199):758–770, 2010. doi: 10.3189/002214310794457308.

G. N. Rutherford, P. Bebi, P. J. Edwards, and N. E. Zimmermann. Assessing land-use statistics to model land cover change in a mountainous landscape in the European Alps. *Ecological modelling*, 212(3-4):460–471, 2008.

B. Salm. Snow forces on forest plants. In *Proc. Seminar on Mountain Forests and Avalanches, Davos, Switzerland*, pages 157–181, 1978.

B. Salm, A. Burkard, and H. U. Gubler. Calcul des avalanches: une méthode pour le praticien avec des exemples (transl. christophe ancey). Technical report, l'Institut fédéral pour l'étude de la neige et des avalanches. (SLF report No. 47), 1990.

A. San Roman Sanz, C. Fernandez, F. Mouillot, L. Ferrat, D. Istria, and V. Pasqualini. Long-term forest dynamics and land-use abandonment in the mediterranean mountains, corsica, france. *Ecology and Society*, 18(2), 2013. ISSN 17083087. URL http://www.jstor.org/stable/26269315.

P. Schaerer and D. McClung. *The avalanche handbook*. The Mountaineers Books, 2006. ISBN 978-0898868098.

M. Schneebeli and P. Bebi. Snow and avalanche control. *Encyclopedia of Forest Sciences.*, pages 397–402, 2004.

M. Schneebeli, M. Laternser, and W. Ammann. Destructive snow avalanches and climate change in the Swiss Alps. *Eclogae Geologicae Helvetiae*, 90(3):457–461, 1997.

J. Schweizer. Review of dry snow slab avalanche release. *Cold Regions Science and Technology*, 30(1-3):43–57, 1999. doi: 10.1016/S0165-232X(99)00025-7.

J. Schweizer. Snow avalanches. *Water Resources IMPACT*, 6(1):12–18, 2004. ISSN 15223175. URL http://www.jstor.org/stable/wateresoimpa.6.1.0012.

J. Schweizer and M. Lütschg. Characteristics of human-triggered avalanches. *Cold Regions Science and Technology*, 33(2-3):147–162, 2001. doi: 10.1016/S0165-232X(01)00037-4.

J. Schweizer, J. Bruce Jamieson, and M. Schneebeli. Snow avalanche formation. *Reviews of Geophysics*, 41(4), 2003. doi: 10.1029/2002RG000123.

J. Schweizer, P. Bartelt, A. van Herwijnen, J. F. Shroder, W. Haeberli, and C. Whiteman. Chapter 12 - snow avalanches. In *Snow and Ice-Related Hazards, Risks and Disasters*, pages 395–436. Academic Press, Boston, Jan. 2015. doi: 10.1016/B978-0-12-394849-6.00012-3.

W. Schöner, R. Koch, C. Matulla, C. Marty, and A.-M. Tilg. Spatiotemporal patterns of snow depth within the Swiss-Austrian Alps for the past half century (1961 to 2012) and linkages to climate change. *International Journal of Climatology*, 39(3):1589–1603, 2019. doi: 10.1002/joc.5902.

P. Serra, X. Pons, and D. Saurí. Post-classification change detection with data from different sensors: Some accuracy considerations. *International Journal of Remote Sensing*, 24(16): 3311–3340, Jan. 2003. ISSN 0143-1161. doi: 10.1080/0143116021000021189.

S. Simioni, J. Dual, and J. Schweizer. Snowpack response to directed gas explosions on level ground. *Cold Regions Science and Technology*, 144:73–88, 2017. ISSN 0165-232X. doi: 10.1016/j.coldregions.2017.09.012. URL http://www.sciencedirect.com/science/article/pii/S0165232X17301465.

R. Sluiter and S. M. de Jong. Spatial patterns of mediterranean land abandonment and related land cover transitions. *Landscape Ecology*, 22(4):559–576, 2007. ISSN 1572-9761. doi: 10.1007/s10980-006-9049-3. URL https://doi.org/10.1007/s10980-006-9049-3.

A. S. Soloviev, A. V. Kalach, D. B. Desyatov, and L. V. Rossihina. Information model of the impact of avalanche snow masses on the elements of the landscape infrastructure. *Journal of Physics: Conference Series*, 1202:012015, 2019. ISSN 1742-6596. doi: 10.1088/1742-6596/1202/1/012015. URL http://dx.doi.org/10.1088/1742-6596/1202/1/012015.

B. Sovilla, M. Schaer, M. Kern, and P. Bartelt. Impact pressures and flow regimes in dense snow avalanches observed at the Vallée de la Sionne test site. *Journal of Geophysical Research: Earth Surface*, 113(F1), 2008. doi: 10.3189/002214310793146287.

B. Sovilla, M. Kern, and M. Schaer. Slow drag in wet-snow avalanche flow. *Journal of Glaciology*, 56(198):587–592, 2010. ISSN 0022-1430. doi: 10.3189/002214310793146287. URL https://www.cambridge.org/core/article/slow-drag-in-wetsnow-avalanche-flow/673C131462DFF8E9124F1330016B031B.

D. Statuto, G. Cillis, and P. Picuno. Using Historical Maps within a GIS to Analyze Two Centuries of Rural Landscape Changes in Southern Italy. *Land*, 6(3), 2017. ISSN 2073-445X. doi: 10.3390/land6030065.

W. Steinkogler, B. Sovilla, and M. Lehning. Influence of snow cover properties on avalanche dynamics. *Cold Regions Science and Technology*, 97:121–131, 2014. doi: 10.1016/j.coldregions.2013.10.002.

M. Stoffel and C. Corona. Future winters glimpsed in the alps. *Nature Geoscience*, 11(7): 458–460, 2018. doi: 10.1038/s41561-018-0177-6.

D. Strijker. Marginal lands in Europe—causes of decline. *Basic and Applied Ecology*, 6(2): 99 – 106, 2005. ISSN 1439-1791. doi: https://doi.org/10.1016/j.baae.2005.01.001. URL http://www.sciencedirect.com/science/article/pii/S1439179105000022.

C. Sulzlée. Historique des méthodes de construction des ouvrages de protection contre les avalanches. *Revue Forestière Française*, 1950.

F. Taillefumier and H. Piégay. Contemporary land use changes in prealpine mediterranean mountains: a multivariate gis-based approach applied to two municipalities in the southern french prealps. *CATENA*, 51(3):267–296, 2003. ISSN 0341-8162. doi: 10.1016/S0341-8162(02)00168-6. URL http://www.sciencedirect.com/science/article/pii/S0341816202001686.

Y. Takeuchi, H. Torita, K. Nishimura, and H. Hirashima. Study of a large-scale dry slab avalanche and the extent of damage to a cedar forest in the Makunosawa valley, Myoko, Japan. *Annals of Glaciology*, 52(58):119–128, 2011. doi: 10.3189/172756411797252059.

Y. Takeuchi, K. Nishimura, and A. Patra. Observations and numerical simulations of the braking effect of forests on large-scale avalanches. *Annals of Glaciology*, pages 1–9, Nov. 2018. doi: https://doi.org/10.1017/aog.2018.22.

E. Tasser, J. Walde, U. Tappeiner, A. Teutsch, and W. Noggler. Land-use changes and natural reforestation in the Eastern Central Alps. *Agriculture, Ecosystems & Environment*, 118(1): 115 – 129, 2007. ISSN 0167-8809. doi: https://doi.org/10.1016/j.agee.2006.05.004.

F. Techel, F. Jarry, G. Kronthaler, S. Mitterer, P. Nairz, M. Pavšek, M. Valt, and G. Darms. Avalanche fatalities in the european alps: long-term trends and statistics. *Geographica Helvetica*, 71(2):147–159, 2016. ISSN 0016-7312. doi: 10.5194/gh-71-147-2016. URL https://doi.org/10.5167/uzh-128875.

M. Teich and P. Bebi. Evaluating the benefit of avalanche protection forest with gis-based risk analyses–a case study in switzerland. *Forest Ecology and Management*, 257(9):1910–1919, Apr. 2009. ISSN 0378-1127. doi: 10.1016/j.foreco.2009.01.046.

M. Teich, P. Bartelt, A. Grêt-Regamey, and P. Bebi. Snow Avalanches in Forested Terrain: Influence of Forest Parameters, Topography, and Avalanche Characteristics on Runout Distance. *Arctic, Antarctic, and Alpine Research*, 44(4):509–519, Nov. 2012a. ISSN 1523-0430. doi: 10.1657/1938-4246-44.4.509. URL https://doi.org/10.1657/1938-4246-44.4.509.

M. Teich, I. Vasella, P. Bartelt, P. Bebi, T. Feistl, and A. Grêt-Regamey. Avalanche simulations in forested terrain: A framework towards a bayesian probabilistic model calibration. pages 628–632, Sept. 2012b.

M. Teich, J.-T. Fischer, T. Feistl, P. Bebi, M. Christen, and A. Grêt-Regamey. Computational snow avalanche simulation in forested terrain. *NHESS*, 14(8):2233–2248, Aug. 2014. ISSN 1684-9981. doi: 10.5194/nhess-14-2233-2014.

B. L. Turner, R. E. Kasperson, P. A. Matson, J. J. McCarthy, R. W. Corell, L. Christensen, N. Eckley, J. X. Kasperson, A. Luers, and M. L. Martello. A framework for vulnerability analysis in sustainability science. *Proceedings of the national academy of sciences*, 100(14): 8074–8079, 2003. doi: 10.1073/pnas.1231335100.

M. G. Turner, R. V. O'Neill, R. H. Gardner, and B. T. Milne. Effects of changing spatial scale on the analysis of landscape pattern. *Landscape ecology*, 3(3-4):153–162, 1989.

UNESCO. Avalanche atlas illustrated international avalanche classification. *UNESCO, International Institute for Educational Planning, Paris, France*, page 265, 1981.

UN/ISDR. *Living with risk: a global review of disaster reduction initiatives*, volume 1. United Nations/ International Strategy for Disaster Reduction United Nations Publications, 2004.

C. J. Van Westen. Remote sensing and gis for natural hazards assessment and disaster risk management. *Treatise on geomorphology*, 3:259–298, 2013.

J. Vandenhove. *Le Queyras: villages et hameaux*. Office d'information et de promotion du tourisme en Queyras, Maison du Queyras, 1984.

A. Velli, A. Pirola, and C. Ferrari. Evaluating landscape changes using vegetation and land-use maps: an integrated approach. *Landscape Research*, 0(0):1–14, 2018. doi: 10.1080/01426397.2018.1513128.

K. Verheyen, B. Bossuyt, M. Hermy, and G. Tack. The land use history (1278–1990) of a mixed hardwood forest in western belgium and its relationship with chemical soil characteristics. *Journal of Biogeography*, 26(5):1115–1128, 1999. doi: 10.1046/j.1365-2699.1999.00340.x. URL https://onlinelibrary.wiley.com/doi/abs/10.1046/j.1365-2699.1999.00340.x.

M. Vernay, M. Lafaysse, P. Hagenmuller, R. Nheili, D. Verfaillie, and S. Morin. The s2m meteorological and snow cover reanalysis in the french mountainous areas (1958–present), 2019.

D. Viglietti, S. Letey, R. Motta, M. Maggioni, and M. Freppaz. Snow avalanche release in forest ecosystems: A case study in the Aosta Valley Region (NW-Italy). *Cold Regions Science and Technology*, 64(2):167 – 173, 2010. ISSN 0165-232X. doi: https://doi.org/10.1016/j.coldregions.2010.08.007. International Snow Science Workshop 2009 Davos.

J. C. Villagrán De León. Vulnerability–A Conceptual and Methodological Review, Source 04/2006, United Nations University. *Institute for Environment and Human Security, Bonn*, 2006.

M. Vincent. Eleveurs de moutons et bergers entre Crau et Queyras. Evolution du pastoralisme méditeranéen sous l'effet des politiques de l'agri-environnement et du loup. 2007.

A. Voellmy. Über die zerstörungskraft von lawinen, sonderdruck aus dem 73. *Jahrgang, Schweizerische Bauzeitung, W. Jegher & A. Ostertag, Zürich*, pages 1–25, 1955.

M. Watts and H.-G. Bohle. The space of vulnerability: The causal structure of hunger and famine. *Progress in Human Geography - PROG HUM GEOGR*, 17:43–67, Mar. 1993. doi: 10.1177/030913259301700103.

S. W. M. Weis, V. N. Agostini, L. M. Roth, B. Gilmer, S. R. Schill, J. E. Knowles, and R. Blyther. Assessing vulnerability: an integrated approach for mapping adaptive capacity, sensitivity, and exposure. *Climatic Change*, 136(3):615–629, 2016. doi: 10.1007/s10584-016-1642-0.

C. Wilhelm, T. Wiesinger, M. Bründl, and W. Ammann. The avalanche winter 1999 in Switzerland-an overview. In *Proceedings International Snow Science Workshop*, volume 16. Citeseer, 2000.

T. Wohlgemuth, R. Schwitter, P. Bebi, F. Sutter, and P. Brang. Post-windthrow management in protection forests of the swiss alps. *European Journal of Forest Research*, 136(5):1029–1040, 2017. ISSN 1612-4677. doi: 10.1007/s10342-017-1031-x. URL https://doi.org/10.1007/s10342-017-1031-x.

J. Wu. Effects of changing scale on landscape pattern analysis: scaling relations. *Landscape ecology*, 19(2):125–138, 2004.

T. Zgheib, F. Giacona, A.-M. Granet-Abisset, S. Morin, and N. Eckert. Impact of land cover on avalanche hazard: how forest cover changes affect return periods and dynamical characteristics simulated by a statistical-numerical avalanche model. In *EGU General Assembly 2020, Online*, number EGU2020-165, 2019. doi: 10.5194/egusphere-egu2020-165,2019.

T. Zgheib, F. Giacona, A.-M. Granet-Abisset, S. Morin, and N. Eckert. One and a half century of avalanche risk to settlements in the upper maurienne valley inferred from land cover and socio-environmental changes. *Global Environmental Change*, 65:102–149, 2020. ISSN 0959-3780. doi: 10.1016/j.gloenvcha.2020.102149.

T. Zgheib, F. Giacona, A.-M. Granet-Abisset, S. Morin, A. Lavigne, and N. Eckert. Spatio-temporal variability of avalanche risk in the French Alps. in revision.